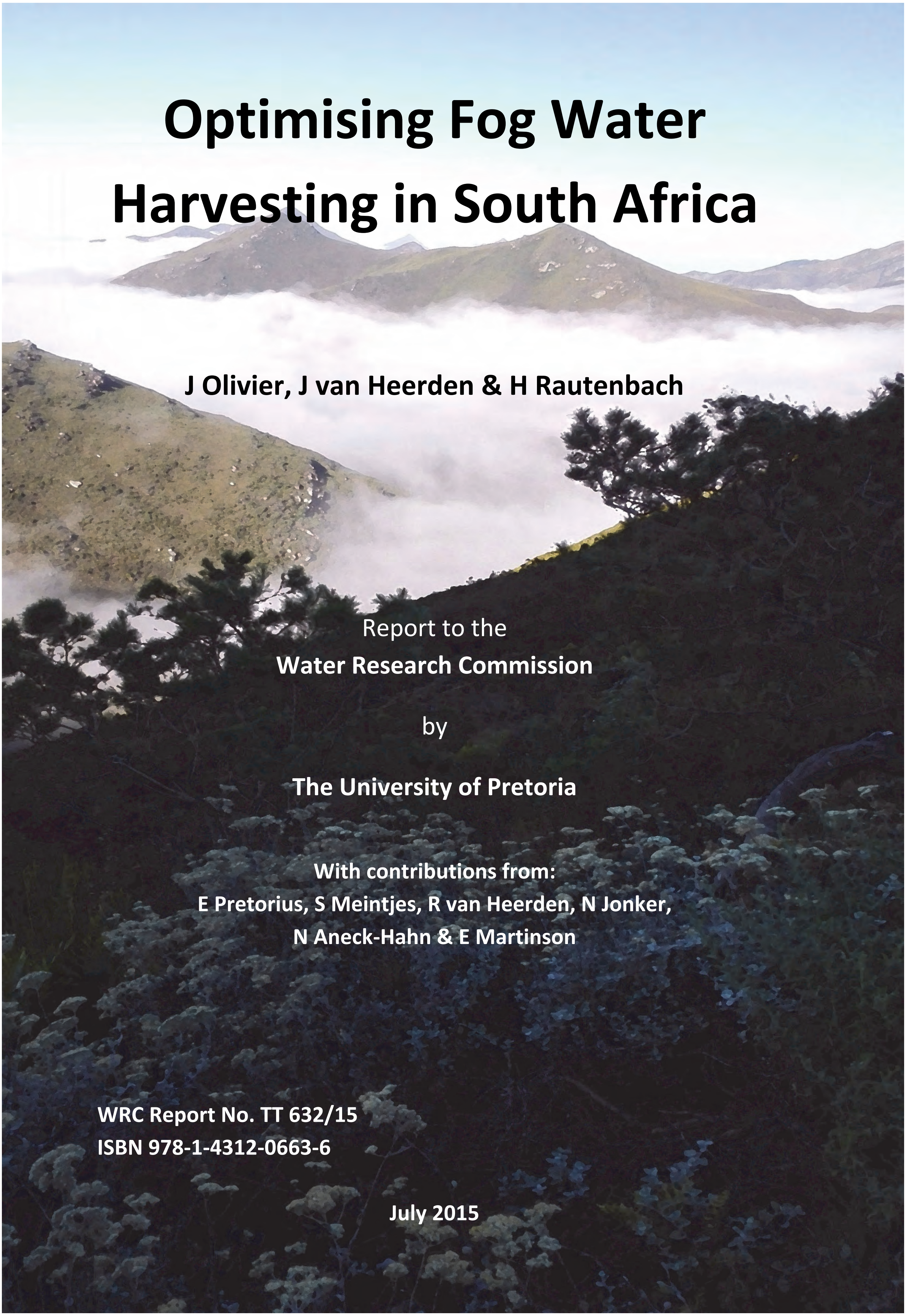

Optimising Fog Water Harvesting in South Africa

J Olivier, J van Heerden & H Rautenbach

Report to the

Water Research Commission

by

The University of Pretoria

With contributions from:

E Pretorius, S Meintjes, R van Heerden, N Jonker,

N Aneck-Hahn & E Martinson

WRC Report No. TT 632/15

ISBN 978-1-4312-0663-6

July 2015

Obtainable from
Water Research Commission
Private Bag X03
Gezina, 0031
South Africa

orders@wrc.org.za or download from www.wrc.org.za

The publication of this report emanates from a project entitled *Optimising Fog Water Harvesting in South Africa* (WRC Project No. K5/2059).

EXECUTIVE SUMMARY

Fog forms the main source of water for plants and animals in many arid regions of the world. It is only relatively recently that fog water has been collected for domestic consumption. Such projects are now being researched and implemented in many countries throughout the world. In South Africa too, research has been ongoing since 1995 to determine whether fog water harvesting would be feasible, and if so, where the optimal sites for such endeavours would be located and how much water could be collected. Preliminary research indicated that fog water collection (FWC) could be viable in the mountainous regions of the country and along the West Coast where fog occurred frequently. To test these findings, two large operational FWC systems were erected – one at Tshanowa School in the Soutpansberg mountains in Limpopo Province and the other at Lepelfontein on the West Coast. Both systems consisted of a 70 m^2 collecting screen composed of nets made from a locally produced material commonly called shade cloth. These nets were attached to 6 m high vertical poles and gutters suspended to their lower ends. During rainy or foggy conditions droplets intercepted by the nets coalesced and trickled down towards the gutters. From there the water was channelled to a filter and eventually to storage tanks. The results proved to be promising. However, a number of problems were experienced when erecting similar systems in other parts of the country. These involved structural failure of the systems, fraying and tearing of the nets, problems during on-site construction of the systems and, on the West Coast, low fog water collection rates due to near-windless conditions. One of the most serious shortcomings was the lack of an accurate and affordable commercial device that could measure low and intermittent water collection rates. The aim of the current study was to optimise fog water collection. The project had three objectives, namely to understand the physical and chemical complexities of fog and its formation, to optimise the fog harvesting process and to develop novel products that could improve on existing fog water measuring devices as well as optimise the fog net design in terms of structural stability and fog water yield.

Two sites were selected for experimentation. These were on the farms Swallows Nest in the Zondachsberg Mountains near Avontuur in the Western Cape and Steenbokfontein near Lamberts Bay on the West Coast. They are located at 33.74˚S; 23.18˚E; alt. 1 040 m AMSL and 32.17˚S; 18.33˚E; alt. 74 m, respectively. These sites are on opposite sides of the country, at nearly the same latitude but with vastly different altitudes. Both sites receive fog frequently, are easily accessible and have a high degree of security.

Various FWC system designs were tested. These included a triangular system composed of three 3 m by 10 m FWC panels arranged in the shape of an equilateral triangle (referred to as the triangular system) erected at both experimental sites. It was assumed that such a design would be more robust than the conventional flat structures and that such an arrangement of nets would be able to collect water, irrespective of the direction of fog-bearing winds. These systems were erected at the Avontuur site during 2011 and the Lamberts Bay site during 2012. Since there was a possibility that the nets could shield each other and reduce the amount of water collected, three open systems consisting of two nets each, orientated at 60˚, 90˚ and 120˚ to each other, were erected at Avontuur. Various modifications were introduced to solve problems with on- and off-site construction. The installation of Mike Cotton System loggers allowed for remote access of data through a GPRS signal, thus enabling real-time monitoring and regular (1 hourly) archiving of data.

The results showed that the triangular structure was indeed very strong and sturdy, withstanding severe storms and gale force winds. However, water collection rates were very low. Over the 35 month study period, the triangular system at Avontuur collected more than 53 000 litres of water. Highest yields were obtained during the summer months. Net 1 facing south into the prevailing fog-bearing winds collected significantly more water than nets facing NE and NW. On average, however, the triangular system recorded only 0.56 $\ell.m^{-2}.day^{-1}$. The 60˚ open zig-zag system by contrast, was considerably more efficient with a water collection rate of 2.7 $\ell.m^{-2}.day^{-1}$. The triangular system at Lamberts Bay fared much worse than at Avontuur, with only 0.08 $\ell.m^{-2}.day^{-1}$ being recorded. Here again, the south-facing net of the triangular system was more effective than the others. It is surmised that this is due to the S-SW onshore winds arising from the circulation around the South Atlantic Anticyclone, coastal lows, sea breezes and the rain following the passing of a cold front.

Research was also conducted to test the water collection efficiency of twelve different materials. These included a number of locally and imported materials ranging from 40 and 80% shade cloth (local), materials obtained from MIT in the USA, from Denkendorf in Germany and the Rachel net that is used in many countries. The materials obtained from Denkendorf in Germany proved to be the most efficient water fog water collectors, collecting more than double the volume of water than the locally produced shade cloth. These nets had a 3-D structure and could effectively trap water droplets from fog and rain. The material used for fog water collection in most other countries, i.e. the Rachel net, fared second- best. Materials which trapped and retained water (and became wet in the process) proved to be the least suitable for fog water harvesting.

During the course of this project, a novel device was developed to measure FWC rates. This low flow meter (LFM) was based on a conventional tipping bucket, but was designed to measure low (1 $\ell.hr^{-1}$) and intermittent flows from large collecting surfaces. Low flow meters were tested at the Avontuur and Lamberts Bay sites for more than three years and have shown to be efficient and reliable. Another novel device was designed, constructed and erected in an attempt to maximise fog water collection during near-windless conditions. This device, referred to as the Whirly, consists of a freely rotating central axis to which three fog water collection panels are attached. Small gutters are attached to the lower ends of the panels. During conditions with a RH of ≥98% and wind speeds of ≤ 4 $m.s^{-1}$, a battery operated motor switches on causing the Whirly to rotate slowly. As soon as the RH drops below 95% and/or the wind speed increases, the system is automatically switched off and ceases rotating. The battery is charged by means of a solar panel. Toward the end of 2014, a scaled-up version of the Whirly was constructed and erected at the Lamberts Bay site. The Whirly was much more effective than the triangular system in that it recorded an average of 0.27 $\ell.m^{-2}.day^{-1}$. This is still very low and, due to its small collecting surface area (1.38 m^2), the actual volume of water collected was negligible.

Analysis of the characteristics of fog and rain events at the experimental sites revealed that at Lamberts Bay on the arid West Coast, fog contributes 33% of the volume of water collected on the FWC system whereas at Avontuur, this amounts to only 20%. During the 2013 period, fog occurred one day out of every three (111 out of the 335-day study period). This is in agreement with long term annual fog day frequency of 110 days for Cape Columbine. The frequency of fog occurrence at Avontuur was relatively higher with 63% of the days recording fog. The rain day frequencies at the two sites were 108 and 86 days, respectively. Nevertheless, the actual rainfall at Avontuur was more than double that received at Lamberts Bay. At both sites, fog occurred more frequently during the months with low rainfall. As expected, fog occurred most frequently during the cooler evening and early morning hours, peaking between 06:00 and 08:00 at Lamberts Bay while at Avontuur, two peaks were recorded – the major one occurred before 09:00 and another, around 19:00 to 20:00. The latter may be due to a local heat-induced low pressure system that develops over the Little Karroo over the area during the afternoon.

Numerous factors affect the water harvesting potential of FWC systems. Geographic factors appear to be the most important of these, especially altitude, since this influences both the liquid water content (LWC) of the air and the wind speed. This factor might explain up to 98% of the variation in water collection. However, topographic factors such as aspect, steepness of slope and the presence of large topographic obstructions in the vicinity of a site may impact on water harvesting potential. The most suitable sites have high elevation and are located on seaward-facing terrain so as to be exposed to moisture-laden winds. The LWC content of the air and wind speeds are the most important climatic controls with the latter controlling the volume of moist air passing through the nets. Highest water collection occurs during rain-events.

The type of material used as fog collectors and the design of the system can thus influence the amount of water collected. Fortunately these can be controlled and water harvesting potential increased using appropriate design and materials.

The quality of the water collected at the two experimental sites was extremely good and suitable for human and animal consumption. The pH was near neutral (6.6 at Avontuur and 6.9 at Lamberts Bay) with the dominant cations being Na^{+} and Ca^{2+} at the West Coast site and Na^{+} at Avontuur. Chlorine formed the dominant anion at both sites. Surprisingly, the concentration of the major cations in the Lamberts Bay samples were higher than would be expected from a solely maritime origin. This applies especially to the Ca and K ions, where more than 90% originate from sources other than maritime. A relatively greater proportion of the Cl and Mg ions originate from the ocean but with some enrichment from other sources. It is interesting to note that the sea salt fraction of Ca, Mg, K and Cl aerosols in the Avontuur water samples exceed that at Lamberts Bay. At first glance, this appears to be contrary to expectation in view of the greater distance from the sea of Avontuur in comparison to that of the Lamberts Bay site. However, it must be kept in mind that the fog occurring at Avontuur originates from maritime air from the Southern Indian Ocean which is forced to ascend the escarpment by onshore breezes. As at Lamberts Bay, the Ca aerosol component in water collected at Avontuur, probably arises from dust.

A preliminary environmental impact assessment was conducted at the Avontuur site during 2012 and 2014. The results indicated that there might be an impact on soil and biota during the construction phase of a FWCS. However, these were only of a temporary nature. Comparison of the biota in the vicinity of the structures at the Avontuur site showed that the vegetation was almost fully re-established within a season or two. It is also possible that the micro-climate was disturbed immediately downwind of the structures. Preliminary observations (using only one set of instruments on the windward side of the FWCS and one placed a few meters behind the south-facing net) indicated that the net had a slight buffering effect on wind speeds. This effect increased with the speed of incident winds and decreased with the degree of wetness of the nets. There was some indication of the development of a weak low behind the net, causing a slight deflection in wind direction. Previous research conducted on the effect of vertical structures indicated that such effects decrease over distance.

In order to facilitate decision-making, it was important to investigate how fog frequencies could be influenced by climate change. Since sufficient fog water collection potential is very site-specific, a technique using a fine resolution topography field with forced topographic ascent by onshore synoptic winds determined for individual topographic points was developed to identify the most likely condition for fog formation. Appropriate criteria were applied to projected synoptic wind patterns, and projections of fog frequency changes were obtained for the Avontuur experimental site. It was found that fog frequencies at the Avontuur experimental site might decrease by approximately 10% in future, provided that the projected climate change will occur. The topographic technique developed is not only of value for climate change projections at each available topography point in South Africa, but also to identify suitable fog water collection sites along the South African escarpment under current synoptic scale wind conditions.

An overview of the research conducted in the course of this project indicates that the aim of the project and most of the objectives were achieved. An efficient structure was designed and constructed and materials with high water collection efficacy identified. Major problems encountered previously during the construction phase were solved.

Important findings of this project were that FWC is not feasible along the West Coast and that a triangular structure is not an effective design to be used for water harvesting. The most suitable design appears to be an open zig-zag system of panels orientated at 60˚ to each other. Other findings were that FWC system does not to have any significant impact on the environment. The quality of water collect by the system is extremely good and suitable for human consumption. Indeed, the quality so good that it could even be bottled to provide an income to local communities.

One of the most important outcomes of this project was the development of novel products such as a water flow meter that can be used to measure low and intermittent flows. Such a device is not currently commercially available and might have application in the market. Another novel product was the development of a rotating FWC system that could improve water collection during periods with low wind speeds, but the structure will have to have a collecting surface sufficiently large to collect appreciable volumes of water.

Five University of Pretoria postgraduate students were directly involved in the project. During the course of the project the research team collaborated with various institutions such as MIT, Denkendorf, FogQuest, and the German Climate Computing Centre (DKRZ). A total of eight papers were presented at national and international conferences. Three articles have been published in accredited journals, and a further two have been submitted and are in the review stage. Other outputs include a data base that can be accessed on www.avitrack.co.za/aws/showmodels.php. Information on the username and password can be obtained upon request from any of the team members. A summary of data spanning the period January 2013 to December 2014 is provided on the CD attached to this report.

This project again confirmed the research team's belief that fog water harvesting is a viable method to provide potable water to isolated mountain communities and, in conjunction with rain water collection, could provide water security in a water stressed environment.

ACKNOWLEDGEMENTS

The Water Research Commission (WRC)

The funding provided by the WATER RESEARCH COMMISSION to make this research possible is greatly acknowledged. A special word of thanks to Mr. Wandile Nomquphu from the Water Research Commission for his leadership and guidance during the execution of the project. Input from Dr Estelle de Coning and Dr George Green who served as Reference Group members is also acknowledged.

The Avontuur experimental site

Mr Jimmy Zondach owner of the Farm Belle-Vue made a great contribution to the success of the project. He made the land, as well as the access to the site, available. At his cost he fenced the entire site. On numerous occasions he made available, free of charge, the use of farm machinery, principally the Bell backacter. The site was visited at least twice a month by members of the project team and on most occasions he insisted that his employees (farm workers) do all the manual labour. This was especially vital during the construction phases of the systems. He also provided overnight accommodation when necessary as well as a venue for the penultimate Reference Group meeting. Mr Bermon Verster is the farm manager at Belle-Vue. Most of the operations involving farm equipment and labour happened under his personal supervision. Despite having wide responsibility ranging from apple production to sheep farming, he always found time to assist. Both these men and their families became firm friends. Mrs Kobie Lombard manages the farm office and she assisted in many ways.

Mr Bob McEwan provided many services to the project. Most of the component design and manufacture was under his supervision, when he did not do it himself. His wide experience was invaluable especially with the Low Flow Meters. He visited the site many times making an invaluable contribution.

Thanks also to Ms Engela Martinson for vital assistance with the EIA.

Many thanks to Dr Mxolisi Shongwe for assisting with the climate change study, and also to the German Climate Computing Centre (DKRZ), through support from the German Federal Ministry of Education and Research (BMBF), for making the computational resources available for the climate / climate change simulations.

The interest shown by Prof Ben van Rensburg (Department Civil Engineering, University of Pretoria) and his support with postgraduate students is greatly appreciated.

The Lamberts Bay Site

Col. Jack Mellet (SAAF, retired) was vital to the Lamberts Bay phase of the project. He negotiated with the owner of Steenbokfontein farm for a suitable site and ensured that all preparation prior to the construction ran smoothly. During the course of the project he visited the site weekly and his expertise in electronics and computers was invaluable. This became especially valuable with the erection and maintenance of the Whirlys. Without his dedication the Lamberts Bay part of the project would have been near impossible.

Mr Hermon Burger, owner of Steenbokfontein, made available the use of farm machinery, workshop and labour, far below cost, during the construction phases. The fact that he prepared the site prior to construction led to considerable saving in time and cost. The use of his tractor hoist made the construction of the systems safe and quick. His wife, Kitta, who runs the restaurant 'The Farm Kitchen', also hosted project team members.

A hearty thanks to Mr Schalk Meintjies for the detailed design and construction of the Whirly and Whirly Mark II, and for Mr Jaco Venter for assistance with the erection of the Whirly at Lamberts Bay.

General

The following person is thanked for supplying samples of material for testing: Dr Bob Schemenauer from FogQuest, the Denkendorf factory in Germany and exchange students from the USA, who supplied MIT material.

Special thanks to Ms Erika Pretorius for site location GIS software research and development, and to Mr Robert Maisha for his coordination of the erection of the triangular FWCS at the Tshanowa School in the Limpopo Province.

It is difficult to express the extent of our gratitude to Ms Nelia Jonker for her invaluable assistance during the first part of this project. Her continued input is sorely missed.

A special thanks to Dr George Green for his assistance in editing the report.

Many thanks to the University of Pretoria for administrative and financial administration. Here Ms Corne van Aardt played a pivotal role.

Team members

Prof J Olivier, Prof J van Heerden, Prof H Rautenbach, Ms E Pretorius, Mr S Meintjes, Dr R van Heerden, Ms N Jonker, Mr B McEwan, Mr J Mellet.

CONTENTS

PREAMBLE

OPTIMISING FOG WATER HARVESTING YIELDS

CHAPTER 3: TESTING THE EFFICIENCY OF DESIGNS AND MATERIALS

CHARACTERISTICS OF THE FOG PHENOMENON

CHAPTER 4: CHARACTERISTICS OF FOG AND RAIN EVENTS

CHAPTER 5: FACTORS AFFECTING WATER COLLECTION RATES

CHAPTER 8: IMPACT OF CLIMATE CHANGE AND LOCAL FOG FREQUENCIES

CONCLUSION

CHAPTER 9: SUMMARY AND CONCLUSIONS

LIST OF FIGURES

LIST OF TABLES

LIST OF ACRONYMS AND ABBREVIATIONS

AMSL	Above Mean Sea Level
AOGCM	Atmosphere Ocean General Circulation Model
AR5	5th Assessment Report
ARC	Agricultural Research Council
AWS	Automatic Weather Station
BMBF	German Federal Ministry of Education and Research
CF	Cold Front
CL	Coastal Low
CMIP5	Coupled Model Inter-comparison Project Phase 5
CORDEX	Coordinated Regional Climate Downscaling Experiment
COSMO	Consortium for Small-scale Modelling Climate Mode
COSMO-CCLM	COSMO – Regional Climate Model
DEM	Digital Elevation data
DJF	December-January-February
DKRZ	German Climate Computing Centre
DMA	District Management Area
DWA	Department of Water Affairs
EC	Eastern Cape
ECMWF	European Centre for Medium Range Weather Forecasting
ED	Endocrine Disruptors
EF	Enrichment Factor
EIA	Environmental Impact Assessment
ERA	ECMWF Re-analysis Data
ESRI	Environmental Systems Research Institute
FTA	Forced Topographic Ascent
FWC	Fog Water Collection
FWCS	Fog Water Collection System
GIS	Geographic Information Systems
ICP-AES	Inductively Coupled Plasma – Atomic Emission Spectroscopy
ICP-MS	Inductively Coupled Plasma – Mass Spectrometry
IPCC	Intergovernmental Panel on Climate
ISCW	Institute for Soil Climate and Water
JJA	June-July-August
KZN	KwaZulu-Natal
LFM	Low Flow Meter
LWC	Liquid Water Content
MAM	March-April-May
MCS	Mike Cotton System
MIT	Massachusetts Institute of Technology
MSLP	Mean Sea Level Pressure
NASA	National Aeronautics and Space Administration
NRF	National Research Foundation
NSSF	Non Sea Salt Fraction
PVC	Polyvinyl Chloride
RCM	Regional Climate Model
RCP	Representative Concentration Pathways

RH	Relative Humidity
SAA	South Atlantic Anticyclone
SAEON	South African Environmental Observation Network
SANPAD	South African – Netherlands Research Programme on Alternatives and Development
SANS	South African National Standards
SAR	Sodium Adsorption Ratio
SAWB	South African Weather Bureau
SAWS	South African Weather Service
SON	September-October-November
SRTM	Shuttle Radar Topographic Mission
SSF	Sea Salt Fraction
SST	Sea Surface Temperature
WC	Western Cape
WHO	World Health Organisation
WRC	Water Research Commission
ℓ	Litre/s

PREAMBLE

CHAPTER 1: INTRODUCTION

1.1 BACKGROUND

Although fog forms the major source of water for plants and animals in arid areas such as the Namib and the Atacama deserts, it was until recently an unexploited source of water for domestic purposes. However, since the 1980s, a number of successful fog harvesting projects have been established in arid countries such as Chile, Venezuela, Guatemala, Peru, Ecuador, Eritrea, Iran, Spain, the Sultanate of Oman, Colombia, Nepal and Morocco (Juvik and Perreira, 1974; Schemenauer et al., 1988; 2001; Schemenauer and Cereceda, 1991; 1992; 1993; 1994; Cereceda and Schemenauer, 1993; Azorin et al., 2010; Baygi, 2008; Esfandiamajad et al.,2010; MacQuarrie et al., 2001; Apigian, 2005; Abyalhamayal and Gandhidasan, 2010; Escobar et al., 2010; Gherezghiher, 2010; Lekouch et al., 2011; Marzol et al., 2011).

Over the past decades extensive research has been conducted in South Africa on the harvesting of fog water. As a matter of fact, the first-ever international research on fog water harvesting was conducted in South Africa, when Marloth (1904 and 1907) measured the amount of water that could be collected from fog (i.e. south easterly wind clouds) on Table Mountain. The first Fog Water Collection Systems (FWCSs) aimed at collecting and using fog and cloud water for human consumption also originated in South Africa. During 1969 and 1970, the Department of Agricultural Technical Services erected two 28 m x 3.66 m FWCSs on the mountain Mariepskop (Mpumalanga Province) to provide water to the staff at a newly established air force radar station on the mountain (Schutte, 1971).

Figure 1.1: *Left: Fog Water Collection System (FWCS) at Mariepskop (1969) (Schutte, 1971). Right: Test fog water collectors at Cape Columbine lighthouse during the research that was conducted in 1995. The 'standard' 1 m^2 fog water collector is shown to the left. The larger test system on the right was donated by a private individual (Maarten van Schoor) and was only deployed at Cape Columbine.*

Fog water harvesting was found to be very successful, averaging yields of 31 000 litres of drinking water per month. Despite these good results, research on fog water harvesting was not pursued until 1995 when a Water Research Commission (WRC) project was initiated to assess the feasibility of fog water harvesting in South Africa (WRC: K5/671: Olivier and van Heerden, 1999; Olivier, 2002). During this project small, 1 m^2 fog water collectors were erected at a total of 10 sites at different locations across South Africa, and yields measured over a period of three years (Figure 1.1).

High elevation sites in the mountains of the Soutpansberg, the Western Cape and those forming the Eastern Escarpment as well as fog prone West Coast, were found to have the highest fog water harvesting potential. For example, maximum yields of >12 $\ell.m^{-2}.day^{-1}$ were obtained in the mountains near Woodbush in the Limpopo Province. Based on these results, two new projects were initiated to implement operational fog water systems aimed at supplying rural communities with water. These projects were funded by the WRC (WRC: K5/902) and by the South African-Netherlands Research Programme on Alternatives in Development (SANPAD) from 1999 to 2001 (Olivier and van Heerden, 2002). The first operational FWCSs were erected at the Tshanowa School in the Soutpansberg Mountains (Figure 1.2) and at Lepelfontein on the West Coast (Figure 1.3) (Olivier and van Heerden, 2002; Olivier and Rautenbach, 2002; Olivier, 2004). These FWCSs consisted of a flat vertical shade cloth screen with a surface area of approximately 70 m^2 supported and anchored by cables, with a gutter attached to the lower end of the screen. During foggy conditions, small fog water droplets are deposited on the screen, drip into the gutter and then flow into a pipe leading to storage tanks. Average daily water yields of 2.85 $\ell.m^{-2}.day^{-1}$ were obtained at the Tshanowa School, while that at Lepelfontein amounted to 1 $\ell.m^{-2}.day^{-1}$, with maximum yields exceeding 3 800 $\ell.day^{-1}$. These FWCSs were specifically designed to be used in poverty-stricken rural areas, to be as cost effective as possible, to use material that is readily available, and to be suitable for areas with no electricity.

Figure 1.2: *The operational Fog Water Collection System (FWCS) erected at the Tshanowa School in 1999 (top) with a view from the first 10 000 litre storage tank, the school and FWCS in the background (bottom).*

Figure 1.3: *The track from the Lepelfontein hamlet along the West Coast towards the top of granite hill (left). The solar panels were erected by the Northern Cape Provincial Government. The Fog Water Collection System (FWCS), facing west on top of granite hill overlooking Lepelfontein (right).*

Similar FWCSs were subsequently erected at schools in the vicinity of Lusikisiki (funded by TEBA) and at Langebaan (funded by the Agricultural Research Council: ARC).

A number of problems were experienced at these sites during severe storms, mainly involving the lack of stability of the flat, vertical nets and the orientation of the FWCSs that had to be perpendicular to the direction of the prevailing fog-bearing winds to ensure optimal water collection. For example, at Lepelfontein it was found that fog-bearing winds vary from NNW to SSW (Olivier 2002, 2004; Rautenbach and Olivier, 2001), and hence the angle of incidence of the water droplets onto a single net may be oblique, compromising yields. Another serious problem was that the design required that the nets are strung vertically, being connected with cable ties to produce a single flat double folded panel of 9 m by 4 m aboveground level. Continuous exposure of these flat nets to turbulent winds caused the nets to tear at the links as well as along the top and sides. Significant modifications to the design were thus necessary.

That is why it was decided to replace the single flat screen FWCS, previously used, with a triangular FWCS in the research conducted for this report. The triangular design was assumed to have greater stability than the original flat screen FWCSs, and to allow water collection from all fog-bearing winds, irrespective of their direction. The connecting panels consisted of two 10 m by 2 m panels linked in the horizontal. The material used was a composite of stainless steel and nylon mesh. The first prototype of the new triangle design, consisting of a 9-panel system with the collecting panels arranged in the form of equilateral triangles (Figure 1.4) was constructed at Cabazana in the Eastern Cape Province during May 2008. Each panel had a surface area of 36 m^2. The entire 9-panel system thus had a collecting surface of around 324 m^2 (Figure 1.5). The triangle system proved to be very robust, withstanding gale force winds and even snow storms (Figure 1.6). An extension to this system that took place in July 2010 made provision for adding another 9-panel system to the existing FWCS (Figure 1.4).

Unfortunately little data were collected at the Cabazana site, and water yields could therefore not be calculated, as the lack of suitable instruments for recording water collection rates proved to be a major problem.

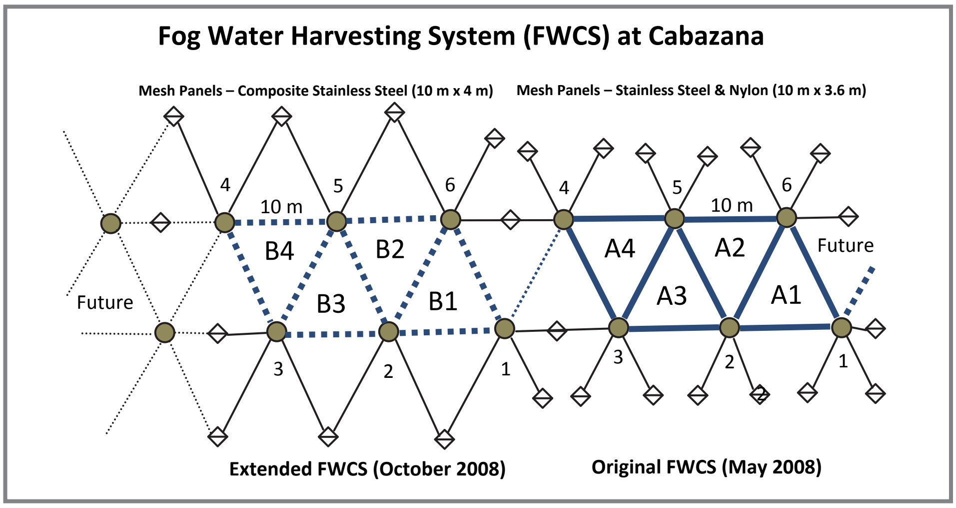

Figure 1.4: *Plan of the original (solid blue lines – May 2008) and the extension of the original (dashed blue lines – October 2008) triangular Fog Water Collection System (FWCS) at Cabazana. Each FWCS has 9 panels, linked by a 10th panel in 2010 (thin dashed blue line). The original panels have a dimension of 10 m by 3.8 m, while the extended panels are 10 m by 4 m).*

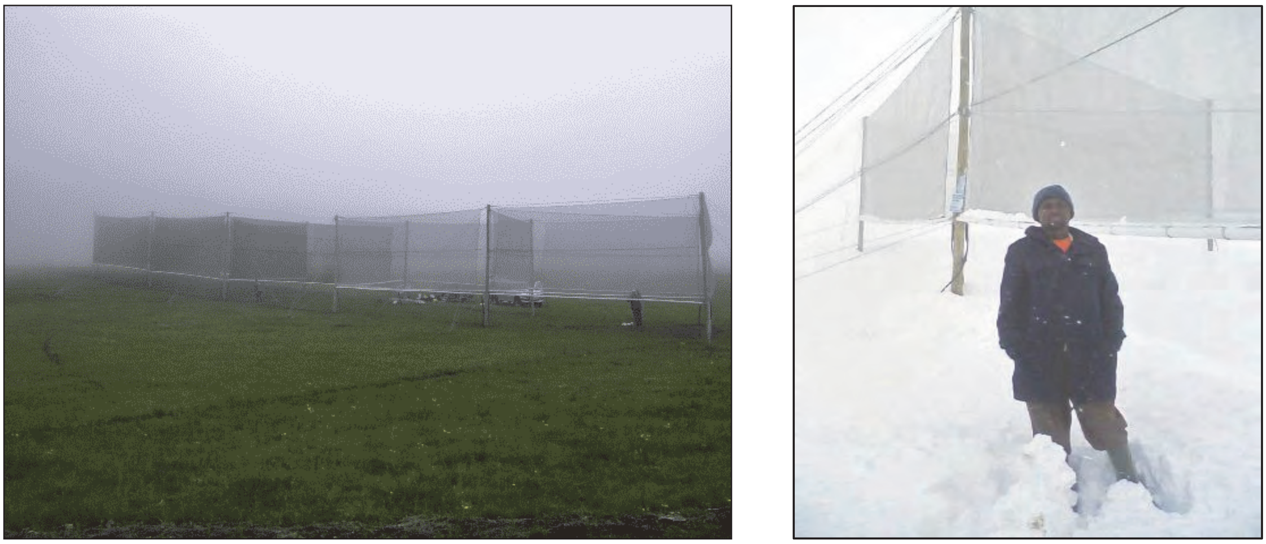

Figure 1.5: *Left: The triangular Fog Water Collection System (FWCS) at Cabazana (Elevation 1650 m Above Mean Sea Level: AMSL) during the final stages of construction in 2008. Note the fog (cloud) advancing from the east. Right: A local resident posing in the snow at Cabazana after the storm on 19-20 September 2008. Snow did not collect on the panels and the newly designed gutters were narrow enough to prevent excessive collection of the snow mas and damage.*

During the operation of the triangular FWCSs at Cabazana several problems were encountered, both with the FWCS structure and with the vertical panels themselves (see Section 1.2 below). It became clear that additional research was required to optimize the functioning of such a FWCS.

At this stage in 2008, no external funding was available for further research. Nevertheless it was decided to continue with the research using personal research funding from Prof Olivier (Unisa). A first step was to find a suitable research site. The primary criteria for such a site were security and ease of access by Prof van Heerden, a principal researcher living in Plettenberg Bay and who had agreed to conduct all constructions and trials. The investigation indicated that the closest fog prone area to Plettenberg Bay is in the Outeniqua-, Zondachsberg and Tsitsikamma mountains. The owner of the farm *Belle-Vue* in the Avontuur district, Mr Jimmy Zondach, has land extending over the Zondachsberg as well as the mountainous region linking this mountain to the Tsitsikamma Mountains. Mr Zondach was interested in fog water collection, and therefore made land and facilities available for further fog water harvesting research. A site, located in the saddle on the northern slopes of the Zondachsberg, at 33.7551°S, 23.1449°E and with altitude 1144 m, was selected as most suitable for the erection of a new experimental FWCS.

Prof Jana Olivier and Prof Johan van Heerden erected and operated a FWCS at this site from late 2008. The FWCS comprised of a single triangular system with each of the side panels measuring 10 m by 4 m. Prof Hannes Rautenbach (University of Pretoria) donated an Automatic Weather Station (AWS) for the recording of water yields. A stainless steel mesh coated with a synthetic material was used for collecting fog droplets. In addition, two storage tanks with a total capacity of 7 500 litre were donated by Mr Jimmy Zondach.

These trial experiments were quite successful, since more than 8 000 litres of water were collected from a single 40 m^2 panel (prior to erection of the two side panels) during October and November 2009. These results were encouraging since this period coincided with one of the most devastating droughts experienced in the Avontuur region. However, a lack of funds prohibited the purchase of proper recording instruments and loggers, and hence prevented the capturing of more data. Nevertheless, the 7 500 litre storage tank remained – and still remains – filled to capacity.

During 2010, a project proposal was submitted to the WRC. The WRC decided to fund and support further fog water harvesting research, with a focus on optimizing fog water harvesting. The resulting project captured in this report commenced during May 2011.

1.2 RATIONALE

1.2.1 Measuring fog water collection rates

The measurement of the amount of water that could be collected by FWCSs is of paramount importance for determining fog water yield. The problem is that conventional water flow meters require a continuous and relatively high flow rate, while fog water collection is sporadic with a variable flow rate, often being very low. In addition, a basic problem with measuring fog water yield is the fact that the first flow of water carries all the dust that collected on the nets during dry periods. Commercially available water flow meters were found not to be able to handle the sporadic flow and this water-borne silt effectively. Commercial water meters, fitted with filters, quickly silted up and also became useless. It was hence regarded as imperative to develop a meter that can measure low intermittent flow and not be affected by the first flush of muddy water.

1.2.2 Structural damage

A collage of photographs in Figures 1.6 and 1.7 illustrates the problems experienced when attempting to implement fog water harvesting on a nation-wide basis.

In some cases, FWCS structures were completely destroyed by wind with speeds in excess of 100 km.hr^{-1}. This applied especially to the flat screen structures erected in the Eastern Cape Province. The main reason for structural failure was either that the anchors slipped or that – because of lack of maintenance – the slack in the structural cables (due to wind stress) was not rectified. This caused the FWCS to vibrate and probably resonate. The vibration caused the poles to loosen and with the nets bulging from the wind, excessive force resulted on the upwind structure cable leading to structure failure. The triangular FWCSs erected at Cabazana in the Eastern Cape Province were structurally stronger than the flat FWCSs and did not collapse. However, flaws in the way that the net panels were attached to the net cables led to the development of horizontal tears (Figure 1.7) in the net material. At both the Cabazana and at the Avontuur sites, stainless steel springs, which were assumed to be stronger, were used to attach the nets, but these proved to be inadequate for avoiding damage by friction.

__Figure 1.6:__ Structural damage to the original flat surface Fog Water Collection Systems (FWCSs) erected during 2005/2006 in the Eastern Cape Province.

Figure 1.7: *Damage to the net panels due to wind turbulence. On the left, net material consisted of double folded 40% shade cloth and on the right a single layer composite stainless steel and poly material was used. The wind caused damage to both materials.*

Another basic reason for constructing a triangular FWCS was the assumption that water would be collected from fog bearing winds, immaterial of the direction of these winds. It was presumed that downwind panels of the system would also collect significant fog water from the fog moving through the first screens. However, it was not known to what extent the upwind screens would modify wind flow patterns and reduce the liquid water content of the fog. It was thus not known whether the triangular system would be the most cost effective in terms of fog water yields.

1.2.3 Materials and on-site construction

Locally manufactured PVC shade cloth (40%) was used as the collecting material. Earlier experiments (Olivier and van Heerden, 1999) indicated that this material is an effective fog water collector. When constructing the nets, three 3 m by 8.5 m lengths of the shade cloth were linked together by means of cable ties and then folded over the top structural cable. The ends of the nets were then attached to rip cord, rope or cables using cable ties. The net panel was then attached to the horizontal net cables – again with cable ties. The final net panel structure therefore had five vertical lines of attachment as well as three in the horizontal. Construction of the screens was carried out on-site, with pauses during adverse weather. When erecting the screen, at least two men were required to drape the net over the top cable. This had to be carried out while standing on ladders and working at between 5 and 6 m above ground. This was especially hazardous during windy conditions since the net would tend to billow and move, shaking the entire structure. Even weak winds created problems with the erection of the screens.

To avoid damage by friction, the completed structure had to allow for some free horizontal movement of the panels. Over time friction could cause the shade cloth to fray and tear. Figure 1.7 (left) illustrates such damage by friction. Much the same thing happened with the stainless poly composite material, but in this case it was the stainless steel springs to which the sides of the net were attached that caused tearing (Figure 1.7 right). It became imperative that alternative way of constructing the net panels be found.

Other, more durable and possibly more efficient materials have subsequently appeared on the market. The efficacy of these should be tested under field conditions. Increasing yields could have a significant impact on the viability of fog water harvesting in South Africa. Currently, an average yield of 3 ℓ.m^{-2}.day^{-1} is assumed to constitute the minimum for a viable fog water collecting system. Large parts of the West Coast experience frequent fogs, but due to other factors have a yield of below this value. If yields could be increased significantly, fog water harvesting could become viable in these areas.

Little change was required with regard to the poles, cables, clamps, etc. used in the construction process of FWCSs and only small modifications were made to the way in which the structure and net cables were attached to each other. However, considerable modification was required in the construction of the anchors. At Cabazana, a backacter was hired and used to dig holes and the anchors and fixtures were of high quality. This is probably the main reason why the FWCS structure withstood the elements, even in conditions of heavy snow. But at remote sites, manual labour is needed to dig the anchor holes and the materials purchased locally are not necessarily of a high quality. These factors play a significant role in the site selection process. It is therefore essential that a fog collection site is accessible with normal vehicles with sufficient ground clearance.

1.2.4 Low yields on West Coast

Despite the high annual frequency of fog (Cape Columbine – 110 days per annum; Port Nolloth – 148 days/annum) (SAWB WB40, 1986), results obtained during the WRC 1995-1999 project showed that fog water yields on the West Coast were relatively low (Olivier and van Heerden, 1999). Cape Columbine fared the best with 2.5 ℓ.m^{-2}.day^{-1}, with yields of only 0.17 ℓ.m^{-2}.day^{-1} being recorded inland of Lamberts Bay and 0.37 ℓ.m^{-2}.day^{-1} at Brand se Baai (Namaqua Sands). This is in sharp contrast to the 12 ℓ.m^{-2}.day^{-1} recorded at Pypkop (Woodbush, Limpopo), the more than 10 ℓ.m^{-2}.day^{-1} at Hanglip (Soutpansberg Mountains near Louis Trichardt (Limpopo)) and the 9.5 ℓ.m^{-2}.day^{-1} at Nuweberg in the Groenland Nature Reserve near Grabouw in the Western Cape. The latter three sites are located at altitudes of more than 1000 m Above Mean Sea Level (AMSL). Altitude thus appeared to play an important role in the magnitude of water yields from the FWCSs. Even small increases in elevation might increase fog water yields. For example, Kalkbaken se Kop (Namaqua Sands) yielded 3.5 times more water than Brand se Baai – a difference in altitude of 118 m (Struthers, 1997). Similarly, an increase in elevation of only 30 m resulted in a three-fold increase in yield at Kleinzee. Increased water harvesting yields are probably due to increased wind speeds and liquid water content of fog with height. Since the largest part of the West coast region lies on a relatively flat, low elevation coastal plain, some method to increase air flow through the collector is necessary to render fog water collection viable.

1.2.5 Data collection

During the previous projects conventional data loggers were used, which required on-site downloading of data. This posed some risks, since data was lost when the data logger ran out of memory or when the battery did not charge. It was also not possible to remotely monitor data logger operation or archive data. This resulted in large gaps in the data sets when failures occurred.

1.3 AIMS AND OBJECTIVES OF THE FOG HARVESTING PROJECT (K5/2059)

The project discussed in this report had three major aims, namely:

1 The understanding of the physical and chemical complexities of fog and its formation -

a) To determine the physical and chemical characteristics of East and West Coast;
b) To determine the factors affecting the occurrence and moisture content of fog (including the relationship between fog occurrence and rainfall, wind speed, sea surface temperature, upwelling extent (West Coast), synoptic conditions (West Coast);
c) To determine the possible influence of climate change on the fog phenomenon and associated environmental and social impacts.

2 The optimisation of the fog water harvesting processes -

a) To delineate optimal sites for fog water collection;
b) To evaluate different materials so as to identify the most effective fog water collector;
c) To assess the impact of the erection of fog water collection systems on the environment;

3 The development of novel products -

a) To design and build a water flow meter for low-flow conditions;
b) To design and develop fog water harvesting systems for unique/specific environmental conditions.

1.4 EXPERIMENTAL SITES

Research conducted during the previous WRC fog projects indicated that fog occurs frequently and that fog water collection could be viable in the mountainous regions of the South-West Cape, Eastern Cape, KwaZulu-Natal, Mpumalanga and Limpopo Provinces, as well as along the West Coast (Olivier and van Heerden, 1999). These areas are depicted in the map in Figure 1.8 which represents fog day frequency values as recorded at 268 weather stations during the period 1960-1990 (SAWB, WB40 1986).

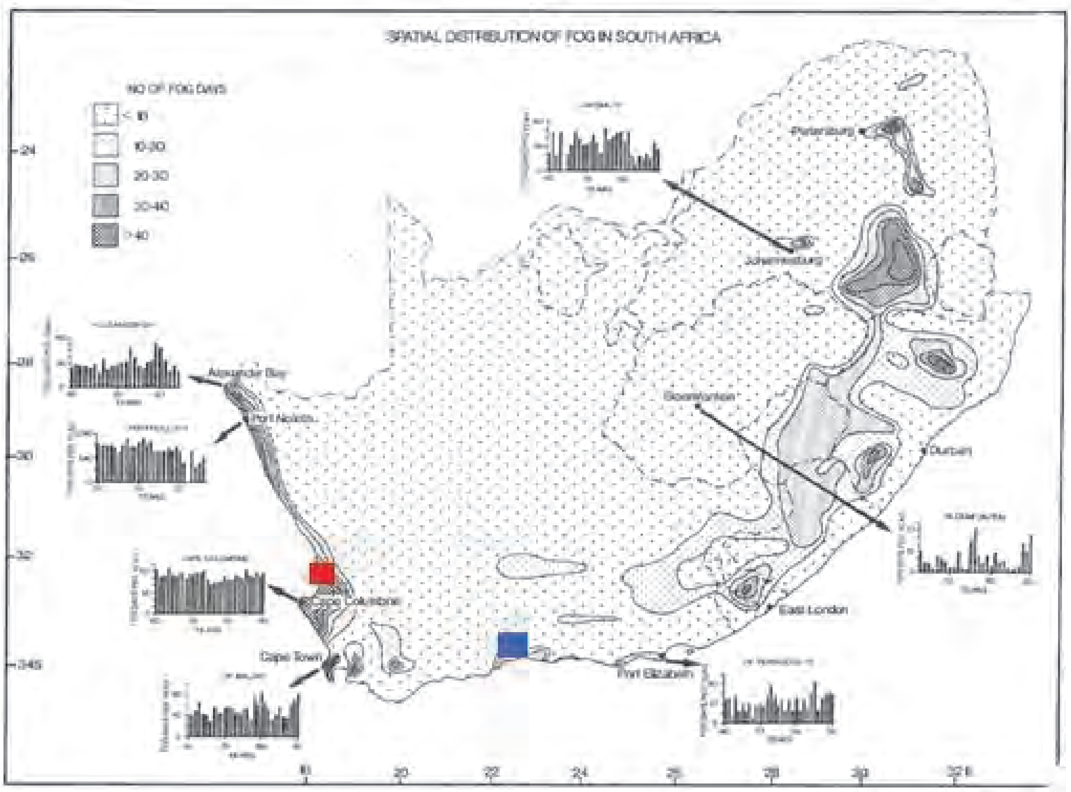

Figure 1.8: *A map depicting the spatial distribution of fog day frequency map across South Africa. Note the higher frequencies in the mountainous eastern escarpment and along the West Coast (Olivier and van Heerden, 1999). The locations of the south-east Coast high elevation (blue) and West Coast (red) experimental sites identified in Sections 1.4.1 and 1.4.2, relative to South Africa, are indicated.*

According to the spatial frequency distribution in Figure 1.8, it was decided that for the purposes of this study two experimental sites were required – one in the eastern mountainous areas of the country and the other on the west coast. In view of past experience, the following factors were crucial in site selection: (1) High fog incidence, (2) Security, (3) Accessibility and (4) Support from local communities.

Unfortunately, sites with the highest incidence of fog are usually located in mountainous areas. These are most often inaccessible and it would be impractical to select such sites as experimental stations – especially where the sites may have to be visited on a daily or weekly basis. For this reason, the fog frequency was not necessarily the most important selection factor, but the selected sites did have to experience sufficient foggy days to provide data for meaningful analysis.

1.4.1 The south-east Coast high elevation experimental site

Since an unofficial experimental site had previously been identified and preliminary research conducted on the farm *Belle-Vue,* a few kilometres south of Avontuur in the Zondachsberg, it seemed prudent to establish the official experimental station on the same farm. However, since the previous experimental site is difficult and dangerous to access without the use of a 4x4 vehicle, another site was sought.

An alternative, more suitable site was found on the large saddle linking the Zondachsberg to the beginning of the eastward extending Tsitsikamma Mountains. This site lies east of the R339 road coming up the Prince Alfred Pass, at 33.7436°S, 23.1808°E, and with an altitude of 1 040 m AMSL. It is located about 2 km (as the Crow flies) to the east of the R339 road at approximately the same elevation (1 076 m AMSL) as the top of the Prince Alfred Pass. This new site was also made available to us by Mr Jimmy Zondach since it was located on his property. An advantage is that the site can be reached with conventional vehicles with sufficient ground clearance. Figure 1.9 shows the location of the new research site, relative to the closest town (Avontuur) and roads.

Figure 1.9: *Location of the East Coast high elevation experimental site in the mountains at Avontuur in the Western Cape Province (indicated by "WRC site") selected as most suitable for erecting an experimental Fog Water Collection System (FWCS).The location of the site relative to South Africa is shown in Figure 1.8 (blue square). (Source: Google Earth)*

Prior to the commencement of this project a 1 m^2 pilot collector was erected at this site to confirm that sufficient fog events occur at the site. Fog water was collected in a 25 litre plastic drum and the volume measured. Satisfactory yields were obtained, indicating that the site would be viable as an experimental site. Thereafter the University of Pretoria made a Mike Cotton Systems (MCS) AWS available for measuring and recording water yields on a continuous basis.

1.4.2 The West Coast experimental site

A number of fundamental factors played a major role in the decision regarding the location of the West Coast experimental site. In view of the distance from Plettenberg Bay (where Prof van Heerden resides) it was essential that technical support be available on an ongoing basis and that the site should be as secure as possible. Fortunately Mr Jack Mellet, a retired businessman living in Lamberts Bay, offered to participate in the project. Mr Mellet has wide experience in data transmission, computer programming and other skills and is well known to the project team.

Figure 1.10: *Location of the West Coast experimental site on the farm Steenbokfontein at Lamberts Bay (indicated by "FWS") selected as most suitable for erecting an experimental Fog Water Collection System (FWCS). The location of the site relative to South Africa is shown in Figure 1.8. (red square). (Source: Google Earth)*

During 2011 Mr Mellet was tasked to find a suitable location for the FWCS. The site had to be near the sea and experience frequent fog events. The site also had to be secure and accessible. He suggested a site on the farm Steenbokfontein, owned by Mr Herman Burger. This farm lies about half way between Lamberts Bay and Elands Bay. Mr Burger indicated that he was willing to participate in the project.

After discussions with Mr Burger, an experimental site was selected to the east of the main Saldanha-Sishen railway line, approximately 2 km east of the shore (Figure 1.20). The site is about 500 m to the west of two granite hills containing caves with Bushman rock paintings. The caves are National Heritage Sites and attract many tourists. The University of Cape Town, Department of Archaeology, also conducts ongoing research in the caves. A FWCS at this location would thus generate a lot of interest and would potentially promote the FWC technology. A good road links the FWCS and the private road along the railway line. Access is excellent. The geographical location of the experimental FWCS is 32°09'51.94"S, 18°19'53.68"E, elevation 74 m (±19 m AMSL).

OPTIMISING FOG WATER HARVESTING YIELDS

CHAPTER 2: FURTHER DEVELOPMENT OF FOG WATER HARVESTING SYSTEM

2.1 DEVELOPMENT OF A LOW FLOW WATER METER

2.1.1 Introduction

In 1999, the WRC funded a project (WRC: K5/902) that was aimed at erecting a fully operational FWCS to supply water to the Tshanowa School in the Soutpansberg Mountains of the Limpopo Province. During this project a large boxed 1 litre tipping bucket was constructed to measure water collection rates from this 70 m^2 FWCS screen. However, the design suffered from serious defects. For example: (1) the 1 litre tipping bucket did not empty completely, resulting in some water being scooped back on the return-tip; (2) some tips were not recorded because of the incorrect placing of the reed switches and (3) during heavy rains, the stream of water falling into the tipping bucket, delayed its up-tip, and large volumes of water flowed directly to the collection tanks without being recorded. In fact, when the water collected from the screen exceeded 50 $mm.hr^{-1}$, the entire box, housing the tipping bucket became filled with water, preventing it from tipping (Olivier and van Heerden, 2002). Before entering the measuring device, the water was filtered by a sand filter, which was also associated with problems. For example, dust collected on the nets and gutters and formed a fine clay mud/compound, which when dry, formed a water tight seal across the sand filter inlet. The only way to rectify this was to remove this layer on a weekly basis, which was not practical due to the remoteness of the site.

The newly designed FWCSs, first operated at Cabazana (Eastern Cape) and Avontuur (Western Cape), comprise panels of approximately 40 m^2. It should be borne in mind that despite the fact that relatively large amounts of water can be collected from these large systems, the flow rates are extremely low when compared to the flow in municipal water supply systems and rivers, as it was estimated that an maximum of only around 500 litres of water can be collected per hour from a 40 m^2 FWCS.

Various flow meters were tested that could measure the intermittent and low flows from FWCSs, including municipal water flow meters which were inserted into the pipe leading to the storage tanks. However, since the flows are intermittent, the water in the flow meter evaporated leaving a residue of mud and dust, blocking the flow meter. The inability for conventional water flow meters (using a water wheel principle) to record very high, very low and intermittent flows became a major problem at the operational-scale systems erected at the Tshanowa School and Lepelfontein (Olivier and van Heerden, 2002).

By 2008 it became obvious that a more suitable water meter that can handle low intermittent water flow and also pass the first flush of silt from FWCSs with the onset of each new fog event, had to be developed.

2.1.2 Requirements and development of the flow meter

The aim of the first deliverable was to develop a low flow meter that could be used for the unusual flow patterns arising from fog water harvesting systems. It required the following characteristics:

- Measurements had to be taken directly below the gutters for comparison between water collection rates from different FWCSs. Since the gutters were only about 1 m above the ground, the hydrostatic pressure in the pipes below the FWCS is too low to activate a conventional flow meter. The new flow meter thus had to be able to be functional at very low hydrostatic pressures;
- For a fog screen of 30 m^2 or more the device had to be able to accommodate water flows from less than 1 $ℓ.hr^{-1}$ to as much as 500 $ℓ.hr^{-1}$ (in a heavy drizzle);
- Because dust is collected on the FWCSs during dry periods, the device had to be able to cope with an initial inflow of muddy water;
- The device had to operate and record accurately despite the deposition of a thin layer of silt in the meter when a minor fog event occurs after a dry spell;
- The device had to require only little maintenance and operate for extended periods of time without service;
- It had to be able to work efficiently at wide range of temperatures and humidities;
- The device had to be robust and require minimum re-calibration in the field;
- The device had to be tamper-proof to limit interference from animals like monkeys and baboons;
- The device had to be able to record data and to transmit signals to a logging device. Since there is usually no electricity available on-site, 6V or 12V batteries charged by means of solar panels or power provided by the logging device, are the only power sources that can be used for the recording, storage and transmission of data.

During 2011, a number of low flow meters were constructed and tested in the laboratory and under field conditions. These included a system based on a water wheel design, a round tipper and one based on a tipping bucket. However, all suffered from various shortcomings. A Low Flow Meter (LFM) which works well and meets all the criteria outlined above, was eventually designed and constructed. This device, referred to as the *Big Tipper*, is shown in Figure 2.1.

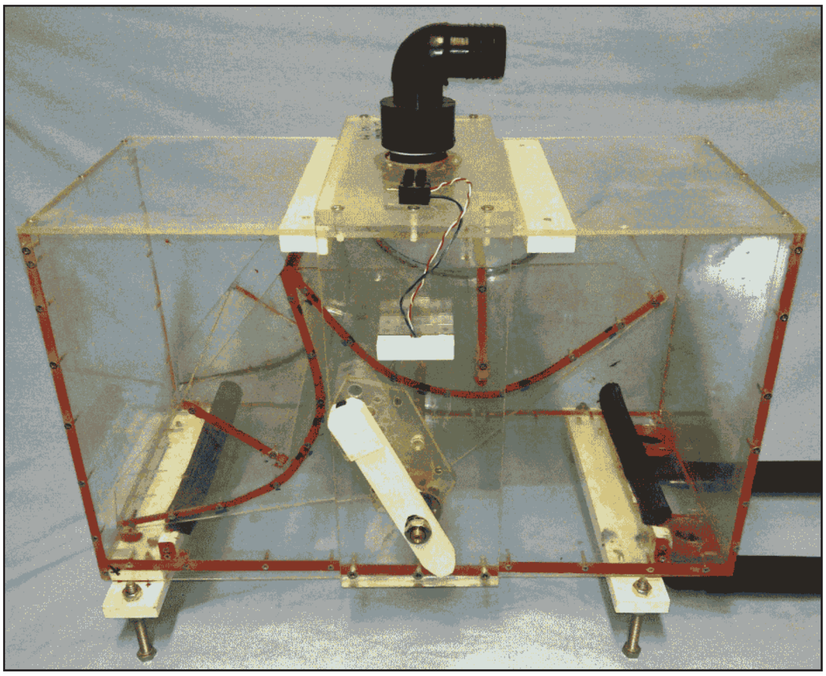

Figure 2.1: *The newly developed "Big Tipper" was the first Low Flow Meter (LFM) that was constructed for the project.*

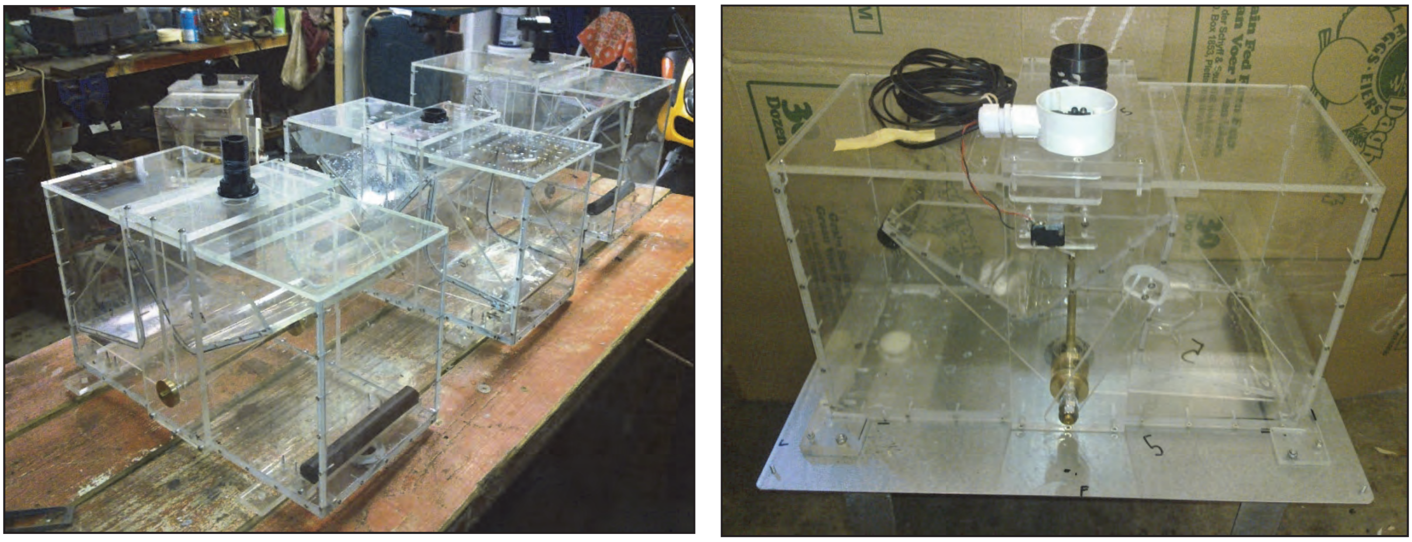

Figure 2.2: *Three Low Flow Meters (LFM's) assembled by McEwan Enterprises (left) with the completed system on the right resting on the base plate. Note the flattened tipper sections, the shock absorbers and the 50 to 32 reducer with acts as a funnel for the water from the gutters.*

With the *Big Tipper* in place, modifications followed. The units arms were straightened, the double outlets replaced by a single outlet and the reed switch was replaced by a more reliable micro-switch. The LFM was housed in a black PVC 96 litre container with lid, which in turn was bolted to a galvanized steel base fitted into the soil with the top horizontal.

However, it became clear that the PVC Box was not the ideal container because the LFM had to be removed (a difficult operation) for maintenance. Further modifications included the mounting of the LFM on a base plate with the outlet located in the centre of the LFM through the base plate. A sheet metal (galvanized) box protects the LFM and allows vertical flow of the fog water from the gutter through a water tight seal (Figure 2.2). The first five modified LFMs were deployed at Avontuur and Lamberts Bay (Figure 2.3).

Figure 2.3: *Top: Mr Jack Mellet fitting the Low Flow Meter (LFM) into the PVC box at the Fog Water Collection System (FWCS) at Steenbokfontein, Lamberts Bay (left). Note the horizontal inflow from the gutter to the LFM (right). The pink foam pieces are used to eliminate vibration of the LFM.* ***Bottom:*** *Mr Markus Geldenhuys fitting the Low Flow Meter (LFM) electronics at the Avontuur Fog Water Collection System (FWCS) (left). On the right is the completed LFM assembly, stand, base plate and cover box all connected to the net gutters and the outflow to the storage tank.*

These LFMs operated smoothly, and apart from minor hitches with slight friction that build up on the brass axles, no problems were encountered with their mechanical functioning during the last three years of the project.

2.2 OPTIMISING THE DESIGN

2.2.1 Stationary structures

2.2.1.1 The triangular system: Avontuur

As mentioned in Chapter 1, numerous problems were encountered with the design and construction of suitable and efficient FWCSs. A first step in modifying the original triangular FWCS was to change the scale and the nets. This modified system consists of three panels (Net1, Net2 and Net3 in Figure 2.4), each with a dimension of 10 m x 3 m arranged in a triangle with side lengths of 11 m. The FWCS is supported by three 6 m poles, and anchored to 6 independent anchors. Wind data from the pilot system indicated that major fog-bearing winds are from the south at Avontuur and hence Net1 was orientated at right angles to these winds (Figure 2.4). At the Avontuur experimental site, provision was also made for five 1 m^2 nets to be used to test the efficiency of different materials. The position of the test nets (T1 to T5) with four loggers are also indicated in Figure 2.4.

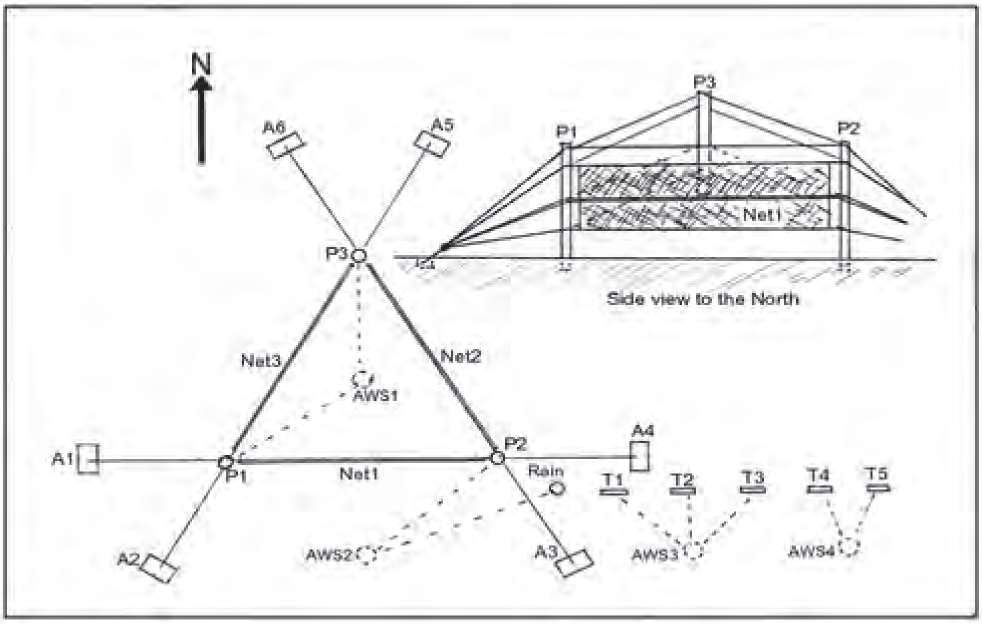

Figure 2.4: *Plan and side view of the triangular Fog Water Collection System (FWCS) Avontuur. A1-A6 depict the anchors. P1 to P3 represent the three 6 m supporting poles. Net1-Net3 reflect the three net panels made of double folded 40% shade cloth. The positions of the four Automatic Weather Stations (AWSs), AWS1-AWS4, as well as the proposed five 1 m x 1 m test nets, T1-T5, are also shown. Pole to pole distance is 11 m.*

Materials

The research team decided to use double-folded 40% shade cloth manufactured by Alnet as standard for fog water collection. This material was also used extensively during the research funded by the WRC during the 1990s (WRC: K671/1/99 and K902/1/02). The material is light, durable and strong with good fog capturing qualities.

Component parts

To prevent rust, certain components of the FWCSs were galvanized. These included the anchor rods, cable support brackets and pole top brackets (Figure 2.5).

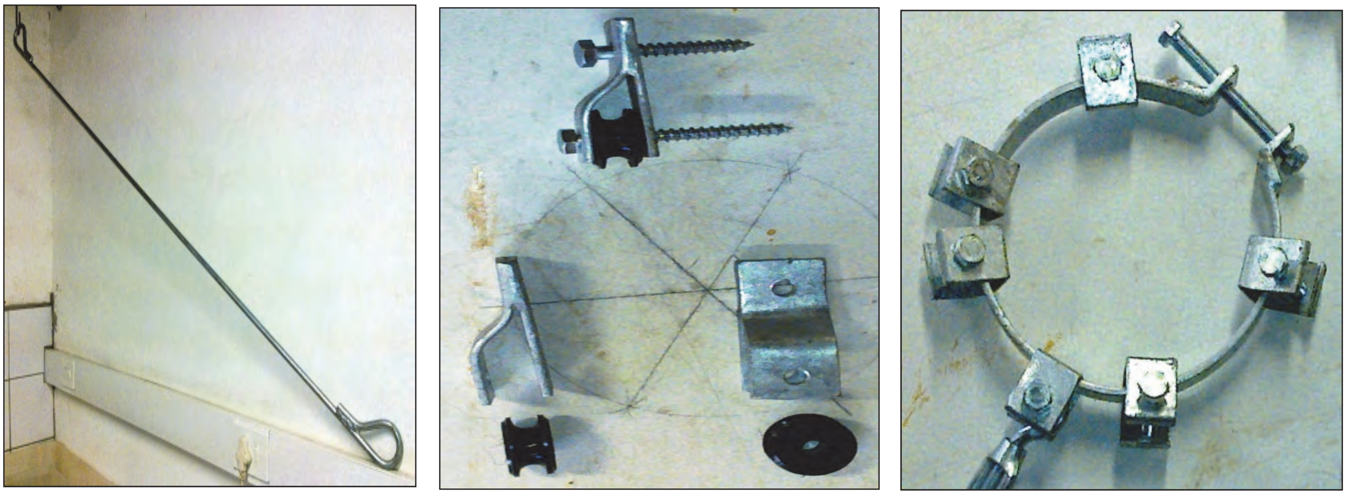

Figure 2.5:
Left: The 12 mm diameter galvanized anchor rod (1.5 m) with loops at both ends for rebar and cable attachment. Centre: The pole brackets. A side view of the assembled bracket appears on top. Note that the rod cable runs over the nylon pulley. Right: The pole top bracket. This bracket clamps around the pole top and provides sturdy and adjustable cable attachment fittings.

The anchor rods had to be placed in the 1 m x 0.6 m and 1 m deep anchor holes with at least one 1 m by 16 mm rebar rod through the bottom loop. Where large rocks were encountered at the anchor positions, several 12 mm threaded rods chemical anchor fixed deep into the sandstone. This is a viable and strong alternative. The pole brackets are essential attachments to the vertical poles. The net support cables run through them. Their main purpose is to provide a sturdy adjustable fixture to the poles for the net support cables. Using these brackets, the wind stresses on the nets were transferred to the anchors ensuring system stability. Experience gained over the past 15 years indicated that if the net support cables are attached directly to the poles, the wind-generated horizontal forces soon destroys the FWCS. The pole top brackets must be fitted over the pole top to provide rigid and strong fittings for the attachment of the structure cables. The structure cables keep the 3-panel FWCS vertical and ensure that most of the force acting on the poles is in the vertical plane. The bracket is protected with a piece of aluminium flashing. This allows the pole top to be free from water penetration and rot.

Net panel construction

In order to minimise difficulties encountered during on-site construction of the FWCSs, pre-construction of the net panels was carried out in a large shed. Working in the shed resulted in quality panel assembly. Temporary fittings were attached to the steel beams of the storage and tool shed. This allowed the top and bottom 5 mm cables of each panel half to be tensioned under considerable force and locked in position with Crossby clamps. This sturdy assembly allowed the 10 m by 3 m 40% shade cloth to be folded over the top and bottom cables/pipes. This double net was attached to the cables and pipes with cable ties spaced ≤ 50 mm apart. The vertical sides of the nets were attached to vertical cables with cable ties. These vertical cables were in turn attached to the horizontal cables with Crossby clamps. Figure 2.6 (left) shows the temporary cable fixtures while Figure 2.6 (centre) shows the fitting of the net. The photo on the right illustrates the net top folded over the 15 mm Polycop pipe. This entire procedure assured a net system well tied to the cables and most importantly, eliminating the dangerous on-site construction process, and also allowed the nets to be erected under windy conditions.

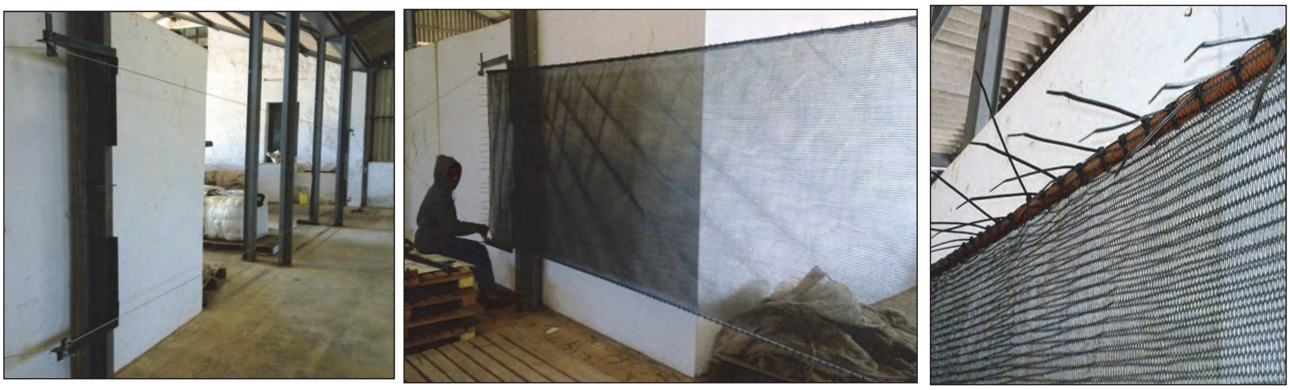

Figure 2.6: *The net panel assembly that took place off-site in a shed on the farm.*
Left: The temporary fittings to hang and tension the cables. Centre: Attaching the shade cloth to the cables with cable ties. Right: Top of the panel folded over the polycop pipe and fastened with cable ties (prior to cutting).

On-site activities

Mr Jimmy Zondach provided four labourers and use of a Bell backacter machine. The holes for four of the anchors were dug quickly using this machine and then squared off and cleared by hand. At least three 16 mm rebar rods of 1 m length were placed in the concrete as reinforcement. One of these re-bar rods passes through the bottom eye of the anchor rod. In addition, two rectangular pieces of 6 mm steel matt were placed in the upper third of the concrete. This reinforcing proved to be more than adequate for the forces that the nets will transfer to the anchor rod. At the 2 other positions chemical anchoring was used. A galvanized 10 mm chain and 12 mm shackle was fitted through the eye-nuts to facilitate the cable attachment (Figures 2.7 and 2.8).

Figure 2.7: *Top left: The south-facing pole positions marked. Top right: The backacter machine digging the anchor hole. Bottom left: Hand mixing the dry concrete. Bottom right: Water seepage into the anchor holes allows the concrete to be mixed in the hole.*

Figure 2.8: *Left: Eye-nuts screwed onto the 12 mm threaded rods chemically fixed in the sandstone rock. Note the deep cavity in the rock. Right: Concrete poured into the cavity and over the eye-nuts for added strength. Note the chain section in the bottom half of the picture fitted for future extension of the system.*

The next step was to fit the pole top brackets as well as structure cables. All the 5 mm wire rope (cables) fitted to the pole top brackets were attached using two Crossby clamps per cable. In Figure 2.9 (top left) the fitting of the pole top bracket as well as the aluminium flashing covering the pole top are depicted.

Figure 2.9: *Top left: The pole top bracket and protective aluminium sheet. Top right: Raising the pole using the ladder as support. Bottom left: Using the tractor to raise the pole and keep things steady. Bottom right: Fitting the structure top cables and tightening the pole top turnbuckles (straining screws).*

Figure 2.9 (top right) illustrates how the pole was carefully slipped into the hole. Apart from the structure cables fitted to the pole top bracket, at least three sections of 10 mm ski rope were attached near the top of the pole and tied as temporary anchors. Some of the ski ropes, temporarily anchored, can be seen in Figure 2.9 (top right and bottom left). This entire process was repeated until all the poles were vertical. With this achieved, the pole to anchor cables were clamped. This process was repeated for each of the three poles. With all three poles stable, the ladder was placed carefully against the outside side of the pole, tied to the pole and, supported by the staff, the pole-to-pole cables were then fitted and the turnbuckles tightened. This remained the only potentially hazardous part of the construction and can be totally eliminated if a hoist is available. The next step was to fit all the pole brackets to the poles. Thereafter, the net support cables were simply slipped over the bracket pulleys and tensioned using the hand held hoist and commercial Vineline Twisters. The two nets panels were linked using cable ties, attached principally to keep the net panels in line (Figure 2.10).

Figure 2.10: *Left: The bottom panels are fitted. Right: Spacing of the linking cable ties in comparison with the net fixtures.*

Gutters to collect the fog water were made by adapting the well tried-and-tested method and design used by the Chilean fog harvesting group at El Tofo, Chili (Schemenauer and Joe, 1989). The gutters were manufactured using twelve 3 m lengths of 80 mm white PVC gutter downpipe. Six (end-gutter) sections were fitted in the ends using PVC material. Each of the three (lower-end) sections was fitted with a 25 mm grommet (tank connector). These grommets allow connections to the 25 mm down pipes which feed into the three low flow water meters. The gutters were attached to the net bottom cable using 2.1 mm stainless steel wire, again adapting the Chilean design, bent in such a way to keep the top of the gutter above the lower net cable and also allowing for movement of the gutter in the wind. The fitting of the gutters is illustrated by in Figure 2.11 (centre). Figure 2.11 (left) shows Mr Bobby McEwan fitting gutters while Figure 2.11 (right) shows the completed gutter system. The final step was connecting the LFMs.

Figure 2.11: *Left: Mr Bobby McEwan fitting gutters. Centre: Gutter bending with the net in the moderate wind. Right: All three panels with gutters and downpipes fitted.*

2.2.1.2 The triangular FWCS at Lamberts Bay (Steenbokfontein)

<u>*Site preparation and construction*</u>

Detailed plans (depicted in Figure 2.12) for the positioning of the poles and anchors were provided to Mr Burger, the owner of Steenbokfontein, who was contracted to complete the anchors. The major difference between the Avontuur and Lamberts Bay sites was that at Lamberts Bay the research team operated on 11 m-deep sand.

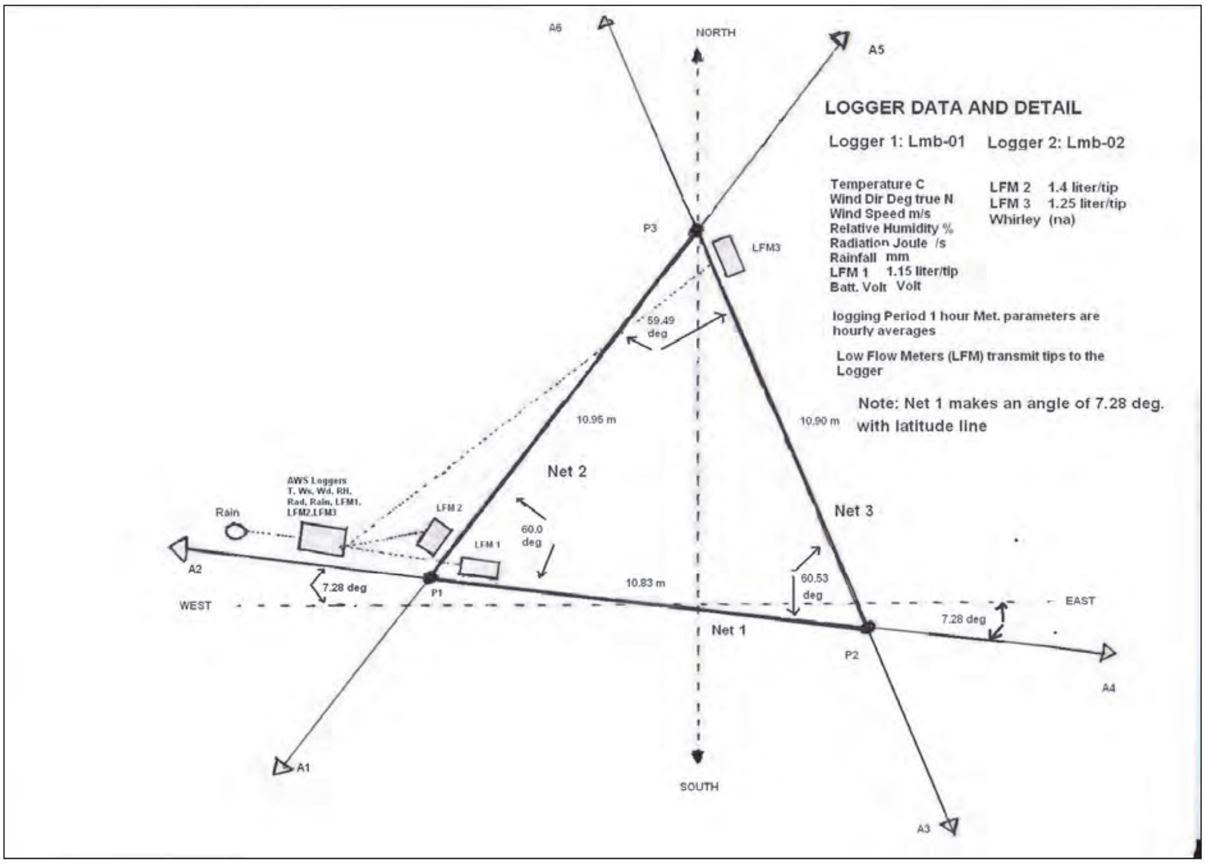

Figure 2.12: *Detailed plans for the triangular Fog Water Collection System (FWCS) erected at Lamberts Bay on the farm Steenbokfontein.*

The anchors were all made of 12 mm chain, well concreted and reinforced in the sand at a depth of 1 m. The work was completed during early March 2012. By then all the net panels, brackets and other fittings were assembled in Plettenberg Bay, and Prof J van Heerden travelled to Lamberts Bay on 26 March 2012 starting construction on 27th March 2012. All procedures closely followed the Avontuur site example with the additional advantage that Mr Burger made a tractor hoist and driver available. This speeded the process enormously and the system was complete within 3 days. The steps followed during the erection of the FWCS are briefly illustrated in Figure 2.13.

Figure 2.13: *Left: Slipping the pole into the hole using a sling and the tractor hoist. Right: Fitting the pole structure cables from the stable pallet.*

In Figure 2.14 (left) the completed Lamberts Bay triangular FWCS is illustrated, and in Figure 1.14 (right), the LFM and complete MC Systems AWS and logger are displayed. The MC System loggers allowed for remote access of data through a GPRS signal, thus permitting real-time monitoring and regular (1 hourly) archiving of data.

Figure 2.14: *Left: The basic triangular FWS at Lamberts Bay. The closest net panel faces towards north-east. Right: LFMs and AWS fully operational.*

2.2.1.3 Expansion of the FWCS at Avontuur

The expansion of the existing three-panel FWCS at Avontuur to a 9-panel system, as originally indicated in the project proposal, required the addition of another three triangular systems. However, preliminary results obtained from the 2011 data revealed that Net1 (Figure 2.4), facing towards the south, collected twice as much water as Net2 and 18 times as much as Net3. This could have been due to the direction of moisture-laden winds, but may also have been due to a screening effect of the nets. This suggests that the triangular FWCS, although very stable, might not be the optimal design for fog water collection. It was then decided to abandon the 9-panel system and rather to investigate the efficacy of an open zig-zag arrangements of nets facing into the predominant fog-bearing wind.

This raised the question as to: *What should the angle between 2 net panels facing into the fog bearing wind be so as to optimise the collection of water?* It was decided to construct three sets of 2-net panels at 60^o, 90^o and 120^o, to each other, respectively. However, all other components in structure had to be retained so as to test only the efficacy of the open zig-zag system. Water yields from these FWCSs could then be compared with those from the existing triangular FWCS to determine structure efficiency. By linking all the cables with a top structure cable, triangular stability was retained. In Figure 2.15 the expanded open zig-zag systems in relation to the existing 3-panel triangular system is displayed.

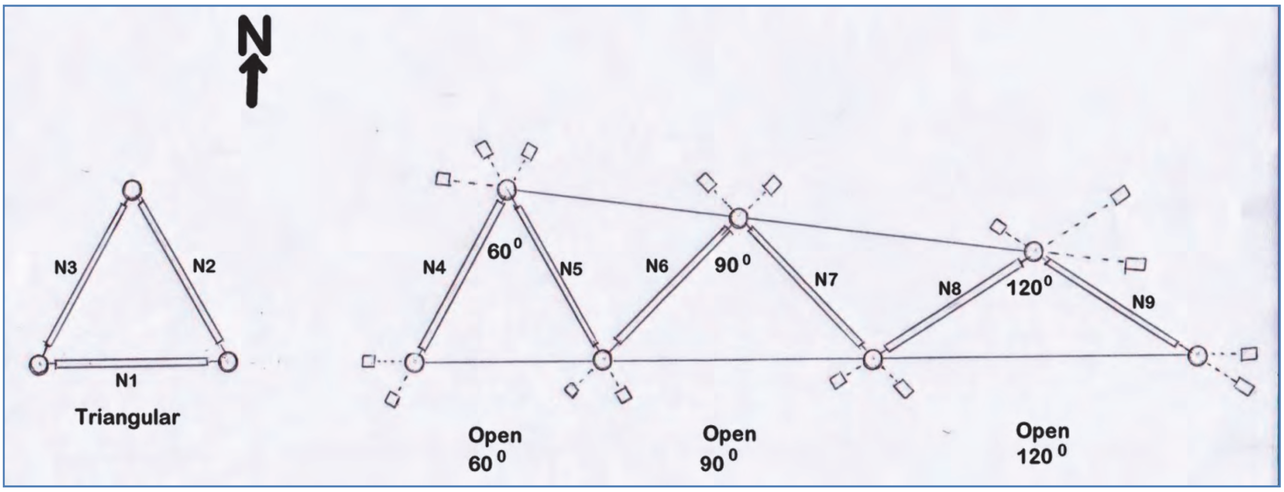

Figure 2.15: *An illustration of the expansion of the Fog Water Collection System (FWCS) at the Avontuur experimental site. Note that anchor-to-pole distances are not according to scale.*

The 60^o, 90^o and 120^o systems are open to the southern quadrant, which is the direction of the dominant fog bearing wind. All panels are linked to the top of the pole structure cable on the open side of the systems. This functions to form a closed triangle that provides structural stability of the system. This zig-zag FWCS provided the opportunity to determine the angle between the net panels for optimal yields. Net N1 in Figure 2.15 of the triangular FWCS can be considered as a 180^o system with respect to fog bearing winds from the south. Only occasionally does fog arrive from the northeast or the north – in such cases the open systems would become 75^o and 105^o systems, respectively.

Construction and Instrumentation

The construction of the 60° and 90° FWCSs commenced early in 2013 (Figure 2.16). Procedures followed those used for the construction and erection of the triangular FWCSs and will not be discussed in detail. The six new individual net panels that were fitted with LFMs and two additional MC Systems AWS loggers were installed to capture data. The first test data were captured during February 2013 and comparisons of water yields from these structures are dealt with in Chapter 3.

Figure 2.16: *The Avontuur extensions as illustrated in Figure 2.15 near completion – note the lack of gutters and instrumentation which were added later.*

Structure failure

During June 2014 a severe north-westerly wind, gusting well in the excess of 100 km.hr^{-1}, caused the centre pole of the 120° FWCS to collapse. Except to the pole, no other damage occurred and the problem was quickly rectified – as illustrated in Figure 2.17.

In order to prevent this from happening again, two additional anchors now support this centre pole. However, it was concluded that a 120° FWCS may be stretching the limits (almost equivalent to a flat FWCS) and should rather be avoided in future. During the same storm the linking cable ties between nets N2 and N3 of the original triangular system (left in Figure 2.15) snapped. This was easily fixed, but it does indicate that short wave radiation may be responsible for the hardening of the cable ties. It would therefore be advisable to use Ultra-Violet (UV) resistant materials/cable ties.

No other damage occurred to the FWCSs during the entire course of the project – not even a single tear in the nets.

Figure 2.17: *Left: Wind stress fracture to the centre pole of the 120° system. Right: Two channel brackets bolted to the pole solved the problem and left the structure stronger.*

2.2.2 Rotating systems

As indicated in Chapter 1, the basic principle of the triangular and zig-zag systems is to trap liquid water droplets on the panel material as fog is blown through the stationary panels. However, advection sea fog that prevails along the West Coast is often associated with very weak winds and hence the efficiency of this process falls drastically as the mechanism to drive the fog through the panels virtually disappears. An alternative would be to design a system that could move the panels through the fog. Such a system was devised and a prototype erected during February 2013. For convenience, this system will be referred to as the '*Whirly*'.

2.2.2.1 The Whirly

The prototype fog water collector consisted of a base frame with collection tank, a vertical shaft and a rotor with three panels (Figure 2.18). The panels were constructed from a double layer of 40% shade cloth, similar to that comprising the nets of the triangular FWCSs. The total surface area of the three Whirly panels is 1.38 m^2.

During foggy conditions the rotor rotates around the vertical shaft at a constant speed allowing the panels to sweep through the fog. Water trapped by the panel material flows downwards to a small gutter at the base of each panel. This water is channelled to a rain gauge to measure water yields. However, the water could be collected and stored in a storage tank. The rain gauge is connected to a data logger so that simultaneous water collection data can be collected from the Whirly and the panels of the triangular system. The rotor assembly driven by a small motor is connected to the base of the vertical shaft. The motor is driven by a 12 Volt battery that is stored in the base frame of the collector. The battery is charged by means of the large solar panel, as shown in Figure 2.18.

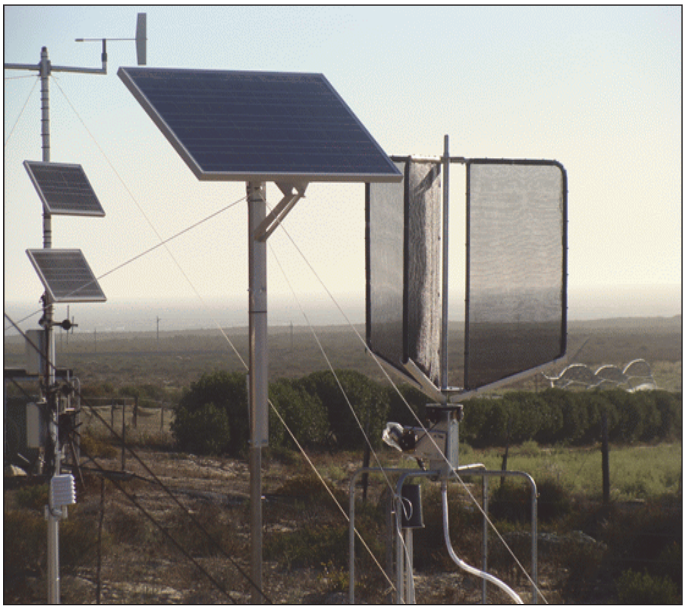

Figure 2.18: *Photo of the 'Whirly', with its 3 fog water collection panels and rotation mechanism, at the Lamberts Bay experimental site. The solar panel used to charge the battery for the Whirly is shown in the foreground while the sea can be seen in the distance.*

During the second half of 2013 Mr. Jack Mellet and Mr. Mike Cotton (owner of MC Systems), devised a mechanism which activates the Whirly when the Relative Humidity (RH) reaches ~98% and the wind speed is < 4 $m.s^{-1}$. The Whirly switches off (stops rotating) when the RH drops below 95%.

However, a few problems were encountered relating to the structure of the Whirly. One involved the accumulation of wind-blown dust on the net panels. On becoming wet during foggy conditions, dust forms a muddy deposit which blocks the small hole in the automatic rain gauge. As a solution, Mr. Mellet designed and installed an ingenious mud trap device capable of handling the water flow from the Whirly. The device traps mud in a 110 mm PVC pipe.

2.2.2.2 Whirly Mk II

Analysis of the results (to be discussed in Chapter 3) showed that, per m^2 of collecting surface, the Whirly was more efficient than the triangular FWCS. However, the amount of water collected was small due to the small surface area of the panels. It was decided to construct and install a second unit, called Whirly Mk II (Figure 2.19). The main goal with Whirly Mk II was to obtain higher water yields. Whirly Mk II was constructed and installed during August 2014 in the same region, but approximately 1 km away from the prototype.

The construction of Whirly Mk II was similar to that of the Whirly, with the following exceptions:

- The area of each rotating panel was increased to 1.99 m^2 which resulted in a total area of 7.96 m^2 for four panels;

- A special imported net with a higher efficiency was used on the rotating panels;
- The centre rotor and rotating panel frames were constructed from aluminium;
- Stainless steel bolts and nuts were used where possible.

Figure 2.19: *Whirly MK ll with Mr. Mellet. In the centre is the Automatic Weather Station (AWS) and on the left a modified rotary Fog Water Collection System (FWCS).*

Unfortunately, shortly after installation the Whirly Mk II was damaged by gale force winds. Illustrations of this damage incurred are shown in Figure 2.20.

Figure 2.20: *Wind damage to the Whirly Mk II (left) and to the aluminium drive ring (right).*

As a result, the damaged frame had to be disassembled for repair work to be carried out at the local workshop. Damage was isolated to the aluminium drive ring and centre pin of the rotor assembly. After repair work was carried out, it was also decided to construct a secondary reinforcing frame across the rotating panels (Figure 2.21) to prevent further wind damage.

Repairs took longer than expected and, at the time of submission of this report, no data had been gathered from this system.

Figure 2.21: *The Whirly Mk II's secondary reinforcing frame.*

2.3 STRUCTURES FOR SPECIAL REQUIREMENTS

2.3.1 The variable direction fog catcher

Good quality water is a prerequisite for the viability of fog water harvesting. One of the questions that had to be answered was whether the quality of water varied during different synoptic conditions. To answer this question, different water samples had to be collected for each wind direction.

Figure 2.22: *Left: The variable direction fog catcher with the fog water collection container. Right: The container with six plastic bottles fitted. Note the nozzle attachment on the down pipe.*

For this purpose a variable direction FWCS was constructed to capture wind-direction specific water samples. The system consisted of a small screen (0.5 m^2) with a weather vane attached. The weather vane keeps the screen facing the wind. A gutter is attached to the screen as well as a tray to collect the fog water. All the rotating parts were made from aluminium. The small screen assembly rotates freely on an axle, constructed from 50 mm pipe fitted with Vasconite bushes. This axle is fixed to the supporting bracket by a large clamp constructed from 50 mm angle iron. Two of these are also fitted to the downpipe ensuring free rotation of the system with the wind. The water outlet from the tray flows down the aluminium pipe into containers labelled clearly to indicate wind direction. This device allows the fog water to be stored from six different wind directions (Figure 2.22). This system has performed faultlessly. With enough water collected, the collector was replaced with an Automatic Rain Gauge. Wind data is also collected at the site and this allows capturing the fog water/ direction yield.

2.3.2 Fog collator to measure droplet size

The liquid content of fog is a function of fog density and fog droplet size. The goal of this part of the project was to measure the size of fog droplets by linearly extrapolating the effect of fog droplet size on the intensity of a focused light beam. A prototype fog collator was developed that measures the extent to which the intensity of a light source is affected by fog. Other methods, such as using digital images and lasers, were not applicable due to power constraints at remote sites. The prototype had to operate on minimal power, and was placed in an environment that was physically remote. By definition the fog collator must withstand moisture and humidity.

The prototype functions as shown in Figure 2.23.

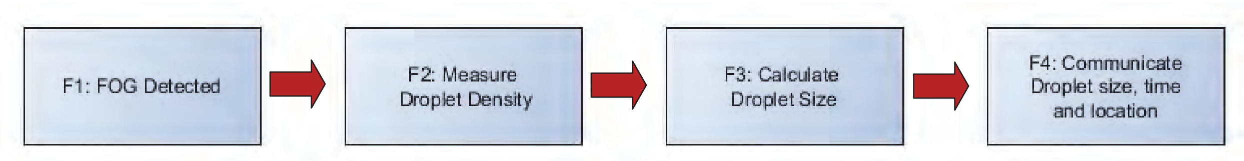

Figure 2.23: *The steps in fog collator prototype operation.*

F1: Fog Detected: The prototype has to detect that a fog event is taking place. Thus the fog collecting system has to send a pulse that can be measured to identify a fog event. This can be problematic if false pulses are generated, or if the interval between pulses is too small. A pulse from the water flow measuring system can be used, or the droplet measurement prototype can be externally prompted to take a measurement.

F2: Measure Droplet Density: Historically fog droplet measurement was obtained by the impact method (Garland, 1971) or by the effect on light attenuation (Kumai, 1973). The impact method is not a viable method due to the requirement for human interaction, thus the light attenuation methodology was selected. Fuzzi et al. (1980) used a linear factor to measure fog droplet samples.

F3: Calculate Droplet Size: An effect of droplet size on light attenuation was shown by Dorathy et al. (1982). Thus the prototype attempts to match the droplet size to measured light attenuation using a predetermined linear equation established via the method of least squares.

F4: Communicate Droplet size, time and location: The following information is required to be communicated by the droplet measurement prototype:

- Size: The estimated size of the droplet
- Time: The date and time of the measurement
- Location: The location from which the measurement was taken.

A successful communication system was developed based on the Adriano chipset (Thompson, 2008). This communication system is capable of hosting a basic web site, from which all data collected by the fog measurement droplet prototype could be retrieved. The prototype uses 3G Cell communication to make the data available throughout the Internet (Zaghloul, 2014).

Light attenuation was measured by measuring the light density via a light tube with a light sensitive LED. The light tube has a 5 cm opening through which the mist must flow.

Measurement of light attenuation by the prototype was found to be not consistent. This device was not completed, but because of its potential, testing and improved designing continues.

CHAPTER 3: TESTING THE EFFICIENCY OF DESIGNS AND MATERIALS

3.1 TRIANGULAR SYSTEMS

3.1.1 Avontuur

As discussed and illustrated in Chapter 2 (Section 2.2.1.1 and Figures 2.4 to 2.11) a triangular FWCS was erected at the Avontuur experimental site during December 2011. Data collected at this site over the period January 2012 to December 2014 are presented in Figure 3.1 and summarised in Figure 3.2. The raw data are available in Appendix A.

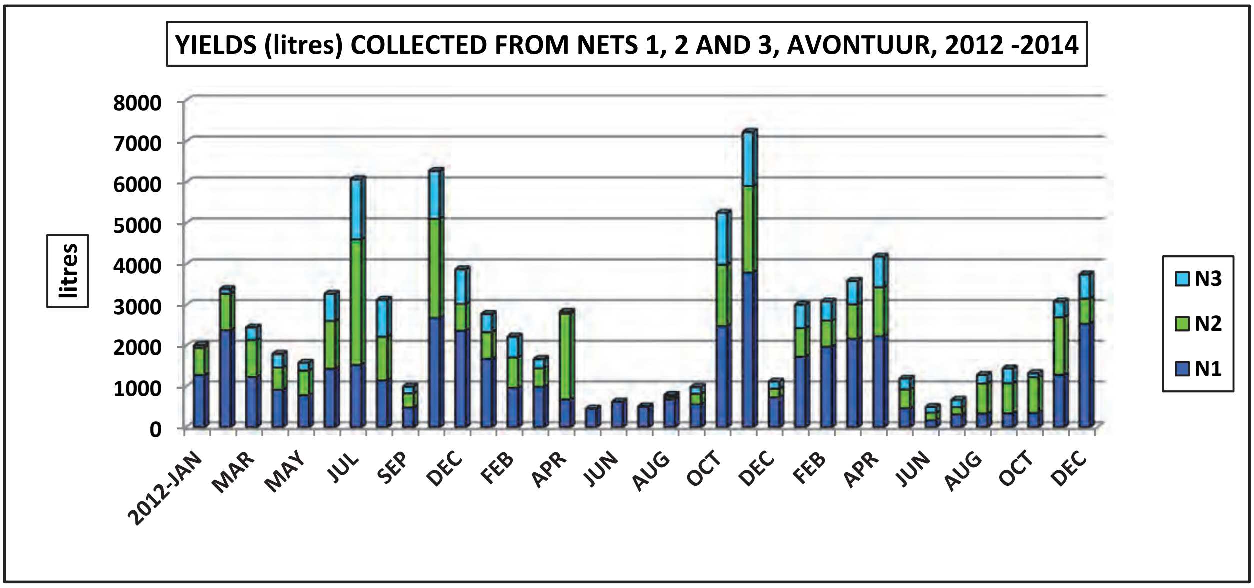

Figure 3.1: *Comparison of mean monthly water yields (ℓ.m^{-2}) over the period January 2012 to December 2014 from nets N1, N2 and N3 (see Figure 2.15, left) that form the triangular FWCS at the Avontuur experimental site.*

Over the entire 3-year period (35 months, excluding November 2012), a total of 53 534.5 litres of water was collected by the triangular FWCS. This amounts to >1 500 litres per month or about 17 ℓ.m^{-2}.month^{-1} (i.e. 0.56 ℓ.m^{-2}.day^{-1}). During the study period the largest yields are obtained during the summer months with the highest value of 7 225.3 litres recorded during November 2013.

The yields obtained during this period indicated that the front south-facing, net (N1 in Figure 2.15, left) outperforms nets N2 and, especially net N3 during most months (except for July 2012, April 2013 and October and November 2014). Net N3 underperforms in comparison to nets N1 and N2 throughout the period. Comparison of yields from the three nets shows an almost perfect ratio between nets N1:N2:N3 of 3:2:1 (27 $\ell.m^{-2}.month^{-1}$: 18 $\ell.m^{-2}.month^{-1}$: 9 $\ell.m^{-2}.month^{-1}$, respectively).

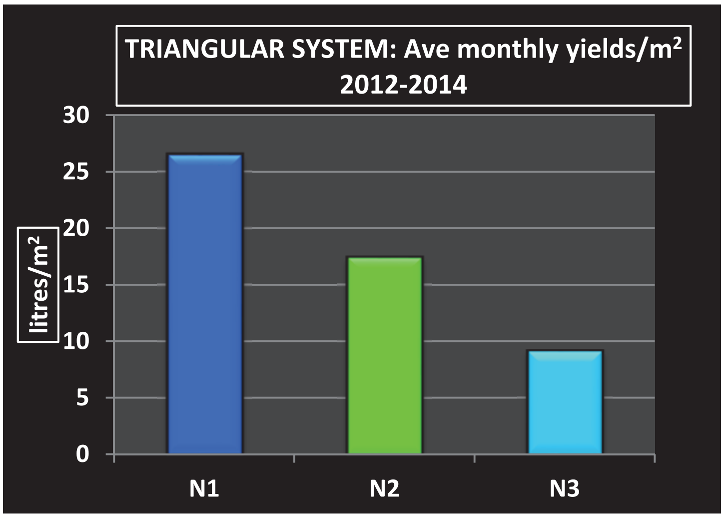

Figure 3.2: *Comparison of water yields ($\ell.m^{-2}$) from nets N1, N2 and N3 in Figure 3.1 over the period January 2012 to December 2014.*

A possible cause of the differences in collection rates is variations in prevailing wind directions and speeds. Wind roses for February and July 2012 are shown in Figure 3.3 (Honours project by Markus Geldenhuys in 2013), reflecting conditions during periods when nets N1 and N2 produce higher monthly water yields, respectively.

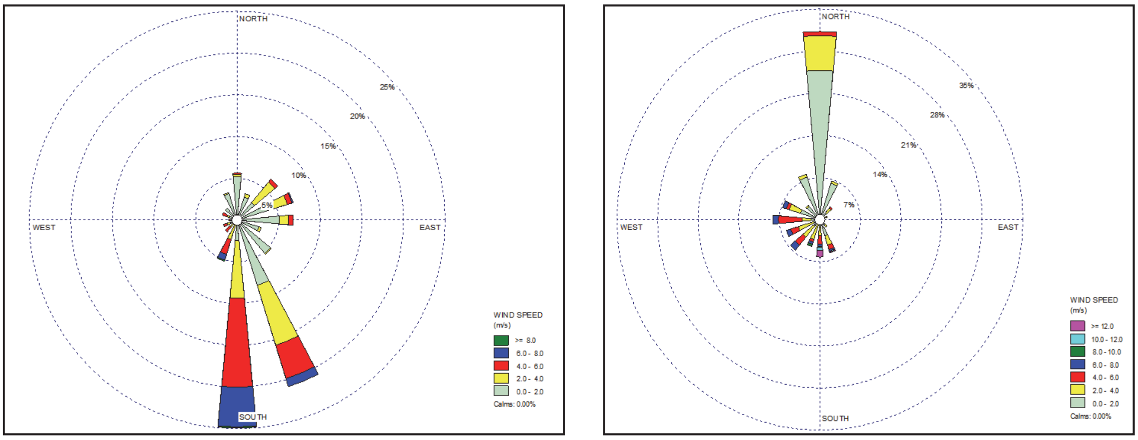

Figure 3.3: *Wind roses for foggy conditions during February 2012 (left) and July 2012 (right), as measured at the Avontuur triangle Fog Water Collection System (FWCS).*

Winds from the south are found to be dominant when net N1 collected most water during February 2012 (Figure 3.3, left). However, the greater proportion of winds from the north and north-west during July 2012 may account for the higher collection rates measured from nets N2 and N3 during this month. Moreover, the February 2012 winds – and especially the winds with a southerly component – are markedly stronger than those originating from other directions. Approximately 5% of the southerly winds exceed speeds of 6 $m.s^{-1}$, while 11% of the winds have speeds of between 1 $m.s^{-1}$ and 6 $m.s^{-1}$. In contrast, less than 1% of the northerly, easterly and westerly winds reach 6 $m.s^{-1}$. Wind speed has been found to play a significant role in fog water yields, driving air with high liquid water content through the nets and therefore allowing for water deposition on these nets.

Rainfall also has a significant influence of the volumes of water collected from FWCSs. Pearson's correlation coefficients calculated between the total water collection measured from the triangular FWCS and rainfall collected from a separate rain gauge gave values of $r = 0.87$ for 2012 and 0.9 for 2013. These are significant at $p = 0.01$ (99% confidence level). These results give an indication that there is a strong linear relationship between the total water yields from the Avontuur FWCS and rainfall.

The high water yields associated with winds from the south (especially during February 2012) can be explained by the prevailing circulation during rain events. Rainfall at Avontuur is usually as a result of counter-clockwise circulation around the South Indian Ocean Anticyclone and a low pressure system over the South African interior – both are associated with southerly component winds. As the high pressure system ridges in to the south of the continent, wind directions change from south to east, and even north-east.

Fog events at Avontuur are invariably associated with winds from the south and south-east, and occur when moist air is advected inland from the ocean and forced to ascend against the slopes of the continental escarpment. The contribution of rainfall vs fog to water collection rates is discussed in Chapter 6.

3.1.2 Lamberts Bay

The triangular FWCS at Lamberts Bay was only constructed during January 2013, and observational records therefore span the period January 2013 to December 2014. Unfortunately, a number of problems were experienced with data capturing, and all data loggers were fully functional for only a period of 15 months. The yields collected from Net1, Net2 and Net3 (Figure 2.12) are shown in Table 3.1.

Analysis of the data in Table 3.1 revealed that a total of 3 553 litres of water was collected from all three nets of the triangular FWCS during this period. This amounts to a meagre average of 237 litres of water per month, i.e. 2.68 $\ell.m^{-2}.month^{-1}$ or 0.08 $\ell.m^{-2}.day^{-1}$. Water yields are especially low during the austral summer months, but increase during the wetter winter season. Maximum monthly water yields were obtained during May 2015, when a total of 508 litres of water was recorded.

Table 3.1: Water yields (litres) obtained from the triangular Fog Water Collection System (FWCS), nets Net1, Net2 and Net3) at Lamberts Bay (2013, 2014)

	2013JAN	FEB	MAR	APR	MAY	JUN	AUG	OCT	NOV	DEC	2014 JAN	MAR	MAY	AUG	NOV	TOT
Net1	31	65	93	188	162	378	246	68	10	23	46	191	97	48	146	1792
Net2	29	63	34	207	67	25	6	135	20	36	28	76	279	98	78	1181
Net3	13	34	36	32	40	69	6	88	4	5	9	33	133	28	53	580
Total litres	**73**	**161**	**163**	**427**	**269**	**472**	**258**	**290**	**34**	**65**	**83**	**299**	**508**	**174**	**277**	**3553**

The relative effectiveness of the three nets of the triangulat FWCS at Lamberts Bay are illustrated in Figures 3.4 and 3.5. Net N1, which faces towards the south, collects most the water. However, yields from net N2 (facing north-west) are better than those of net Net1 for April, October, November and December 2013 and May 2014. Net N1 is 3.1 times as effective as net N3, whereas, net N2 is twice as effective.

Water collection is due to both rainfall and fog. A Pearson's correlation coefficient value of $r=0.5$ shows that there is a statistically significant linear relationship between total water yields from the triangular FWCS and rainfall (significant at $p < 0.05$, 95% confidence level). However, rainfall only explains 25% of the variation in water collection rates and hence fog appears to play a relatively more important role. Winter rainfall over the West Coast is usually associated with an approaching cold front, and therefore north-westerly winds. It was therefore expected that net N2 would record higher water yields during winter. This is, however, not the case, but the water collected on net N2 could also be the result of fog. Fog, on the other hand, may occur when (1) the South Atlantic Anticyclone is located to the south-west of the African continent; (2) an approaching cold front occurs; (3) a coastal-low is sweeping from north to south along the coastline and (4) when sea-land breezes occur.

Characteristically, (1) prefrontal conditions are associated with western to north-western winds; (2) onshore winds arising from the South Atlantic Anticyclone have south-west to western components, depending upon the position of the high pressure cell; (3) fog-bearing winds related to a coastal-low may vary from south-west through to west and north-west with an approaching coastal-low, and may even impinge from the north and north-east once the coastal-low has passed and (4) sea breezes are invariably from the west to west-south-west. Fog-bearing winds thus vary in direction, but often have a southerly component. In addition, summer rainfall over these regions occurs when a deep continental low pressure system moves southwards near the Atlantic coast. Individual, or a combination of these events, could therefore contribute to the water yields from nets Net1, Net2 and Net3.

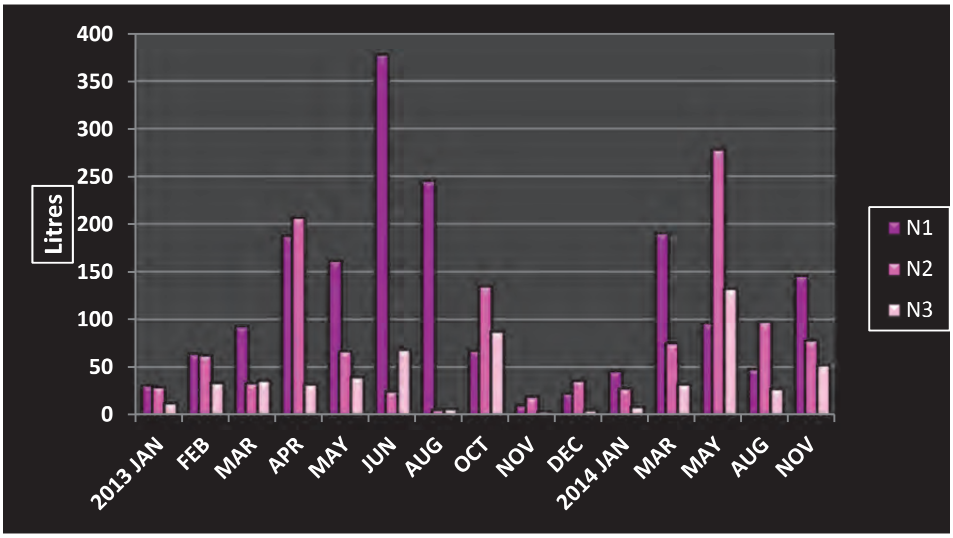

***Figure 3.4**: Monthly water yields obtained from nets Net1, Net2 and Net3 at Lamberts Bay during 2013 and 2014*

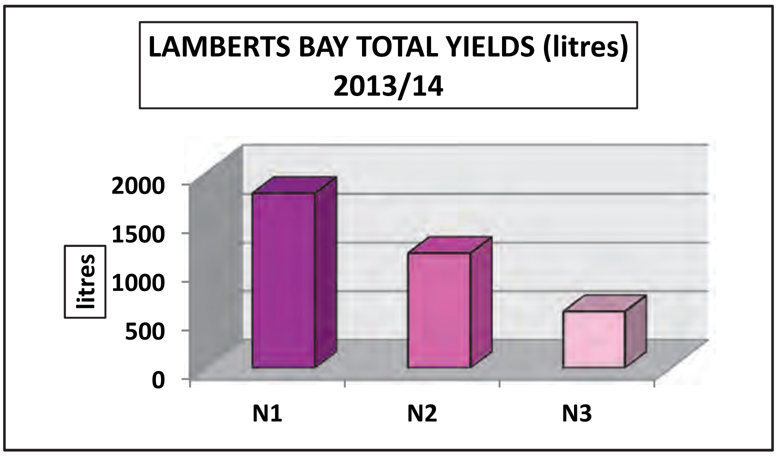

***Figure 3.5:** Comparison of the effectiveness in terms of water yields of the the three nets (Net1, Net2 and Net3) of the trangular Fog Water Collection System (FWCS) at Lamberts Bay.*

3.2 ALTERNATIVE DESIGNS

3.2.1 Open systems

Barring the prevailing circulation, lower yields on the downwind side of the triangular FWCS could also possibly have been due to a ‘shielding’ effect of N1 on nets N2 and N3. To test for this possibility, alternative FWCS designs were tested at the Avontuur experimental site. For this purpose a further six nets were erected immediately adjacent to the original triangular system. Figure 2.15 in Chapter 2 illustrates the layout of the original and expanded FWCSs. All nets had a surface area of 30 m^2. Nets N4 and N5 were erected at an orientation of 60^o

to each other with the open end facing south or into the prevalent fog bearing winds. Nets N6 and N7 formed an angle of 90^{o} to each other and nets N8 and N9 were erected at an angle of 120^{o} to each other.

The full dataset of water yields recorded at the Avontuur experimental site are presented in Table 3.2, while Figure 3.6 gives a summary of yields from all four FWCSs at Avontuur (triangle, 60^{o}, 90^{o} and 120^{o}). The 60^{o}, 90^{o} and 120^{o} systems were erected during January 2013, August 2013 and October 2013, respectively. Since net N9 was only completed during October 2013, the comparison of the systems is based on the total yields during the October 2013 to December 2014 period during which all nets were functional.

The 60^{o} open FWCS was clearly the most effective with respect to water collection. Per square meter of collecting surface, the 60^{o} open FWCS collected 2.7 times more water than the conventional closed triangular FWCS. The 120^{o} open FWCS was almost twice as efficient and the 90^{o} open FWCS 1.6 times better. Net N1, representing a single system facing into the main moisture-bearing winds, was also much more efficient than the closed triangular FWCS in terms of water yield per area – note that the net area of the closed triangular FWCS is approximately 3 times the net area of Net N1. These results show conclusively that there is a significant shielding effect within the triangular FWCS, indicating that is not regarded as an effective design if one considers water yield per area. The FWCS is, however, stronger in structure. Not only is the 60^{o} open FWCS more effective in terms of water harvesting, it also has the advantage of structural stability in comparison to the 90^{o} and 120^{o} open FWCSs. However, the reason why the 60^{o} and 120^{o} systems outperform the 90^{o} system is not clear. These results suggest that future FWCS should be comprised of a zig-zag pattern of nets orientated at 60^{o} to each other.

Table 3.2: Summary of water yields (litres) from nets N1 to N9 (see Figure 2.15) at the Avontuur experimental during the period January 2013 to December 2014.

YEAR	MONTH	TRIANGULAR FWCS			60^{o}		90^{o}		120^{o}	
NETS		N1	N2	N3	N4	N5	N6	N7	N8	N9
2013	JAN	1668.6	665	443.8	1194.7	1201.9	904	-	-	-
	FEB	961	749.8	509.6	1292	1521.5	924	-	-	-
	MAR	982.8	461.3	226.8	1801.2	1133.9	669.9	-	-	-
	APR	672.3	2107.6	53.2	825.4	924.8	354.8	-	-	-
	MAY	452.3	0	0	509.2	680	204.6	-	-	-
	JUN	625.1	0	0	705.5	831.3	460.4	-	-	-
	JUL	504.9	0	0	814.7	787.1	356.4	-	-	-
	AUG	679.1	68.5	42.4	588.2	1056	638.6	679.4	-	-
	SEP	558.9	259.2	165.2	395.2	759.9	293.7	552	-	-
	OCT	**2477.3**	**1509.4**	**1262.8**	**1766.2**	**3063.4**	**1729.2**	**2144.3**	**1937.5**	**1720.4**
	NOV	**3792.2**	**2115.7**	**1317.4**	**1938**	**4464.2**	**2550.9**	**3404.5**	**3718.5**	**4163.3**
	DEC	**727.7**	**216.8**	**172.2**	**459**	**731**	**656.7**	**656.2**	**940.9**	**887.4**
2014	**JAN**	**1726.7**	**699.3**	**578.2**	**972.8**	**1883.6**	**1394.3**	**1530.5**	**2280.1**	**1973.7**
	FEB	**1969.7**	**642.3**	**471.8**	**1117**	**2018**	**972**	**1735.1**	**2573**	**2230.4**
	MAR	**2162.7**	**850**	**575.4**	**1205.4**	**2385.1**	**1664.9**	**1848.9**	**2828.8**	**2420.8**
	APR	**2234**	**1199.7**	**747.6**	**1143**	**2696.2**	**1579.1**	**1235.2**	**2993.1**	**2522.8**
	MAY	**457.7**	**464.6**	**267.4**	**322.2**	**992.8**	**176.6**	**34.7**	**370.5**	**219.3**
	JUN	**167.4**	**182.6**	**145.6**	**185.4**	**345.1**	**107.3**	**139**	**156.6**	**164.9**
	JUL	**310.5**	**176**	**180.6**	**193**	**421.6**	**224.4**	**328.1**	**573.5**	**0**
	AUG	**328.1**	**741.7**	**212.8**	**301**	**889.1**	**358.1**	**660.1**	**792.1**	**666.4**
	SEP	**336.2**	**741.7**	**359.8**	**630.8**	**1604.8**	**1069.2**	**1308.5**	**2056.9**	**1642.2**
	OCT	**347**	**875.3**	**100.8**	**19754**	**13321.2**	**7364**	**1105.9**	**1884.8**	**1375.3**
	NOV	**1283.9**	**1408.3**	**387.8**	**1170.4**	**2777.8**	**1590.6**	**1931.9**	**3540.2**	**2422.5**
	DEC	**2532.6**	**617.8**	**602**	**1714.6**	**2771**	**2187.9**	**2146.2**	**4493.5**	**2799.9**
TOTAL LITRES 0CT2013-DEC2014		**20853.7**	**12441.2**	**7382.2**	**32872.8**	**40364.9**	**23625.2**	**20209**	**31140**	**25209**
TOTAL ℓ.onth^{-1} OCT2013-DEC2014		**1390.2**	**829.4**	**492.1**	**2191.5**	**2691.0**	**1575.0**	**1347.3**	**2076.0**	**1800.7**
ℓ.m^{-2}.month^{-1} OCT2013-DEC2014		**46.3**	**27.6**	**16.4**	**73.1**	**89.7**	**52.5**	**44.9**	**69.2**	**60.0**
ℓ.m^{-2}.month^{-1} PER SYSTEM OCT2013-DEC2014		**30.1**			**81.4**		**48.7**		**64.6**	

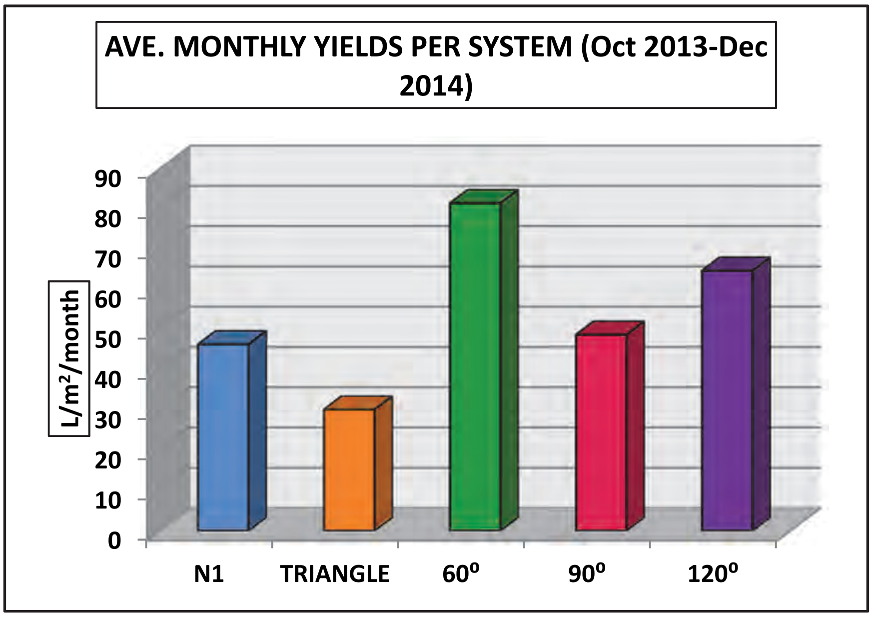

***Figure 3.6**: Comparison of water harvesting efficacy of the different Fog Water Collection Systems (FWCSs) (nets N1 to N9 in Figure 2.15) at the Avontuur experimental site (October 2013 to December 2014).*

The water yields of the 60^o open FWCS amount to a mean of 2.7 ℓ.m^{-2}.day^{-1}. This is still low for a high elevation site, but similar to water yields obtained at Tshanowa School. However, it should be kept in mind that the selection of the *experimental* site was not based on fog water harvesting potential, but rather on security and accessibility. A number of factors, such as rainfall, fog collecting materials, wind speeds and local topography might explain the lower yields.

3.2.2 Rotational systems – the Whirly

Yields obtained from the Whirly (see Chapter 2, Section 2.2.2.1) were compared with those recorded for the stationary nets forming the triangular FWCS. Comparison could only be conducted for concurrent periods when all data loggers were fully functional. Moreover, since each of the stationary nets had a surface area of 30 m^2, whereas the Whirly's was only 1.38, yields could only be compared if calculated per square meter of collecting surface. The entire dataset can be found in Appendix B. Monthly water yields of the nets forming the triangular FWCS and the Whirly are shown in Figure 3.7.

Figure 3.7 illustrates that the Whirly collects more water (per square meter) that the stationary nets over a period of eight months of the 13 month period that spans from February 2013 to November 2014 when more than 14 litres were collected per m^2. The highest water yield of 14.6 ℓ.m^{-2} were collected from the Whirly during May 2014. For the corresponding period, the highest water yield from net Net1 was 12.6 ℓ.m^{-2} during June

2013; 9.3 ℓ.m^{-2} from net Net2 during May 2013 and 2.3 ℓ.m^{-2} from net Net3 during June 2013. The relative greater yields from the rotational system are also reflected in Figure 3.8, which gives a comparison of the overall yields during this period.

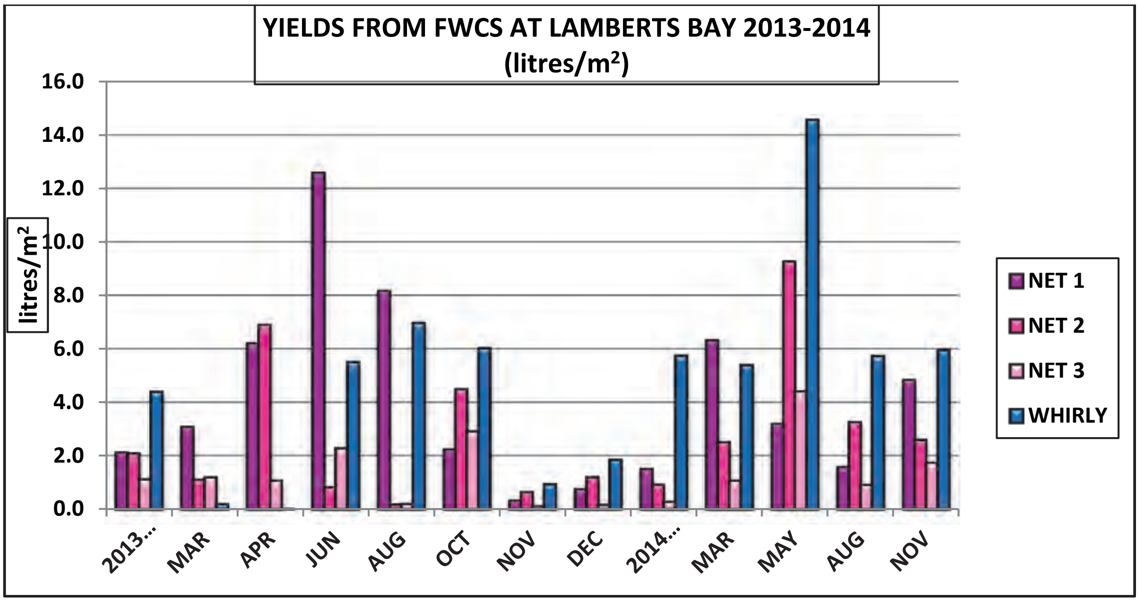

Figure 3.7: *Water yields (ℓ.m^{-2}) from the three panels (Net1, Net2 and Net3 in Figure 2.12) of the triangular Fog Water Collection System (FWCS) as well as from the Whirly at the Lamberts Bay experimental site (2013-2014).*

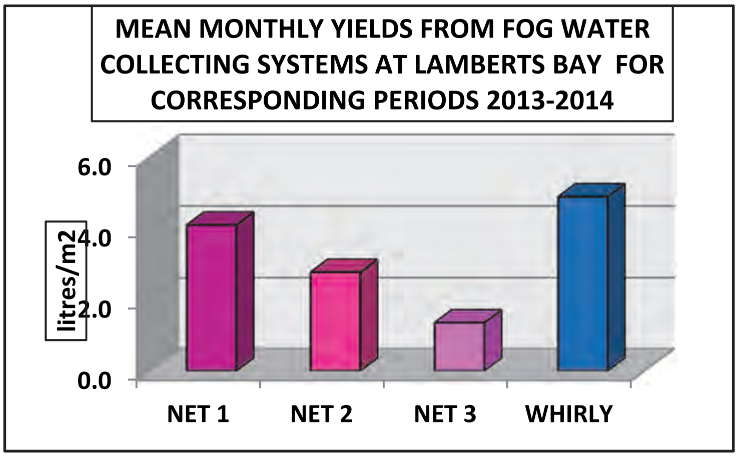

Figure 3.8: *Comparison of mean monthly water yields (ℓ.m^{-2}) from the stationary Fog Water Collection Systems (FWCSs) and Whirly at Lamberts Bay experimental site (2013, 2014).*

It should however, be kept in mind that the surface area of the Whirly is small (only 1.38 m^2) and hence the total volume of water collected is minimal (around 6.7 litres per month or 0.2 ℓ.m^{-2}.day^{-1}).

3.3 COMPARISON OF WATER COLLECTION EFFICIENCY OF DIFFERENT MATERIALS

Five test nets (T1 to T5) were erected at the Avontuur experimental site during 2012 (see Figure 2.4). These nets were used to determine the water collection efficiency from different materials. The surface area of each of the nets was 1 m^2 with the exception of the two samples obtained from MIT (Massachusetts Institute of Technology) which was 0.73 m^2. The efficacies of 12 different materials were tested. These comprised: Materials developed by *MIT*; *Denkendorf* from Germany; *Rachel* used in numerous South American countries; South African 40% Alnet *shade cloth* (double and single layers); 80% shade cloth; a knitted Steel-*polypropylene* produced by KnitMesh Ltd in Port Elizabeth (but not widely available to the general public); a net commonly used by the fishing fleet and referred to as *Anchovy* net and an impenetrable cloth made by Alnet (popularly known as *ground sheet*). During March 2013, a 1 m^2 sample of the Denkendorf material was obtained from the factory in Germany. Preliminary results obtained during the course of 2013 showed that this material was the most efficient water collector. For this reason, a large roll of material was purchased during 2014. This material had a different appearance to the original sample and thus it was decided to test this 'new' Denkendorf. Unfortunately, this was only done towards the end of 2014 and thus only very limited data were available. The materials on T1, T2, T4 and T5 in Figure 2.4 were replaced during the course of the experiments; however, that of T3 was kept the same. Since the double layer of 40% shade cloth is used for the large systems, this material (T3) was used as reference for comparison purposes. Figure 3.9 provides a summary of the efficacies of the materials (in the form of ratios of yields of material *x* to that of T3 over a corresponding period), while Table 3.3 lists the number of litres per m^2 collected from each net during the period January 2012 to December 2014.

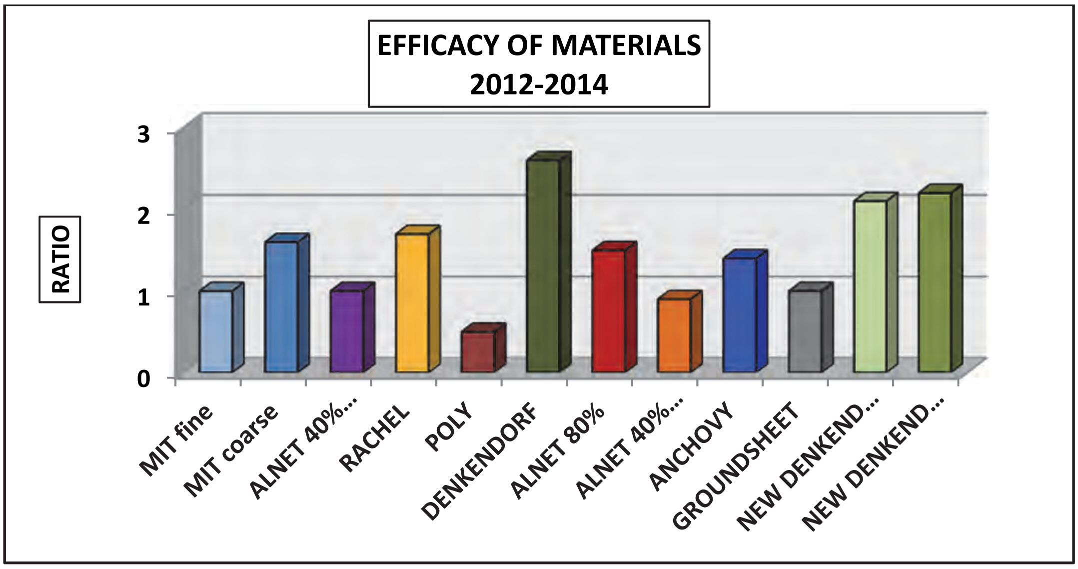

Figure 3.9: *Comparison of the efficacy of different materials as fog water collectors in the form of ratios of yields of material x to that of test screen T3 over the corresponding period January 2012 to December 2014.*

Figure 3.9 and Table 3.3 indicate that there appeared to be little difference in the efficiency of the three lots of Denkendorf. Moreover, the German material was found to be the most effective fog and rain water collector – collecting twice as much water as the double layer of 40% Alnet shade cloth (the reference material). A double layer of the Rachel net collected 1.7 times more than the reference material, while the coarse MIT net and the dense (80%) Alnet shade cloth lagged slightly behind (1.6 and 1.5 times, respectively). There was little difference in the water collection efficiency of the Anchovy net and the single layer of the Alnet material. The poor results obtained for the double layer of 40% shade cloth (Alnet) was surprising since experiments conducted during 1995-1998, indicated that shade cloth was slightly more efficient than Rachel (Olivier and van Heerden, 1999). Indeed, there was little difference in the amount of water collected from the double layer of shade cloth and a single layer of the same material. Even the ground sheet gave comparable results. The only tested material that is less efficient than the double layer of 40% shade cloth was the polypropylene material. It is surmised that the poor performance of the polypropylene material was due to its water absorption properties. Instead of allowing water to run downwards to the gutter, the material became wet and heavy. This is clearly not suitable for fog water collection.

A material which can small droplets, allow them to coalesce and grow in size – and then repel them when they reach a certain size – would be optimal for fog water harvesting. A considerable amount of research is being conducted internationally to create such a material. It is indeed a pity that this part of the original project had to be abandoned, but there is a good indication that National Research Foundation (NRF) funding has been obtained by the University of Pretoria for further material research in 2015 and 2016.

Table 3.3: Water collection efficiency of different materials (ℓ.m^2).

	MIT fine	MIT coarse	Alnet (40% double)	Rachel (double)	Poly	
2012	**T1**	**T2**	**T3**	**T4**	**T5**	**N (wet hrs)**
JAN	32.3	34.3	34.8	34.3	3.2	164
FEB	49.4	49.7	44.6	50.6	8.1	181
TOTAL (Jan & Feb)	**81.7**	**84.0**	**79.4**	**84.9**	**11.3**	**345**
	Denken	MIT coarse	Alnet 40%	Rachel	Poly	**N**
MARCH	55.1	39.3	24.3	46.2	7.1	137
APRIL	33.9	25.2	19.6	21.0	3.7	160
MAY	34.8	32.2	0.1	19.4	4.2	139
JUNE	64.1	53.0	27.3	35.3	7.8	200
JULY	59.4	43.7	20.8	42.4	11.6	159
SEPT	20.8	15.5	10.7	14.0	2.0	143
OCT	165.0	98.5	54.0	97.9	17.2	328
DEC	72.5	53.9	34.4	45.1	8.8	214
JAN-2013	56.3	48.5	36.1	48.9	46.5	743
FEB	58.8	47.9	28.3	47.4	46.0	672
TOTAL	**620.6**	**457.8**	**255.6**	**417.5**	**154.8**	**2895.0**
	Denken	**Alnet 80%**	Alnet 40%	Rachel	**Alnet 40% single**	
MAR	24.0	14.9	11.3	20.4	13.9	744
APR	0.2	0.1	02	17.5	4.2	720
MAY	19.0	3.5	5.6	15.8	3.5	744
JUN	0	0	0	19.4	4.7	720
JUL				12.0	5.8	744
AUG	4.3	2.6	2.5	19.8	7.4	744
SEPT	7.8	4.5	4.5	11.3	6.9	720
OCT	70.4	48.6	27.5	58.6	22.0	744
TOTAL (Mar to Oct for months not in red)	**114.6**	**71.5**	**48.9**	**106.2**	**46.1**	**2952**
	Denken	**Anchovy**	Alnet 40%	Rachel	**Ground sheet**	N
NOV	102.0	67.1	42.6	85.6	56.9	722
DEC	17.0	8.7	8.0	14.6	4.7	744
JAN-2014	58.8	32.9	26.5	48.3	20.8	744
FEB	65.4	40.8	29.6	52.8	23.9	672
TOTAL	**243.1**	**149.5**	**106.5**	**201.3**	**106.3**	**2882**
	Denken	Anchovy	Alnet 40%	Rachel	-	
MAR	70.9	46.8	35.3	59.2		744
APR	78.2	55.9	35.0	69.3		720
MAY	12.7	9.5	7.5	13.8		744
JUNE	6.0	9.4	3.5	6.4		720
JUL	10.7	5.6	5.3	8.7		744
AUG	29.7	18.6	10.1	20.3		744
SEPT	47.0	28.4	21.1	29.1		720
OCT	55.9	33.7	19.2	32.0		744
TOTAL	**680.1**	**431.6**	**300.2**	**541.3**		**5880**
	Denken	Anchovy	Alnet 40%	**New Denkend double**		
NOV	**75.0**	**46.7**	**29.3**	**51.5**		**720**
	Denken	**New Denkend single**	Alnet 40%	New Denkend double		
DEC	**74.7**	**71.2**	**35.2**	**83.8**		**744**

CHARACTERISTICS OF THE FOG PHENOMENON

CHAPTER 4: CHARACTERISTICS OF FOG AND RAIN EVENTS

4.1 CLASSIFICATION OF EVENTS

In order to distinguish between the characteristics of rain and fog, monthly data sets were divided into dry hours, foggy hours and rain hours based on the presence or absence of yield data from the FWCS and rain gauge data. A *fog event* was defined as hours during which the water was collected on the low flow meter (LFM) but where the rain gauge did not record any rain. On the other hand, hours during which both the rain gauge as well as the LFM recorded tips, was defined as a *rain event*. A *wet event* was a period during which either rain or fog was collected. It was assumed that a *dry event* comprised of hours with neither rain (measured on the rain gauge) nor fog (tips on the low flow meter but not on the rain gauge) water recorded.

Table 4.1: Definition of classified events

<table>
<tr><th>Tips recorded by LFM (from the FWCS)</th><th>Tips recorded by the rain gauge</th><th colspan="3">TYPE OF EVENT</th></tr>
<tr><td>X</td><td>X</td><td>DRY</td><td></td><td></td></tr>
<tr><td>✓</td><td>X</td><td>FOG</td><td></td><td rowspan="3">WET</td></tr>
<tr><td>✓</td><td>✓</td><td>RAIN AND FOG (R&F)</td><td rowspan="2">RAIN</td></tr>
<tr><td>X</td><td>✓</td><td>RAIN ONLY</td></tr>
</table>

Anomalous results were found on a number of occasions when the rain gauge registered rainfall, but where there was no corresponding yield from the FWCS. On closer examination, it was found that during these periods the rain gauge registered only a single tip, equivalent to 0.2 mm rain. A possible explanation for these ‘rain only’ events is that they occurred during windless conditions, resulting in a near-vertical drop path. It is also possible that the minute rain droplets deposited on the net were too small and too few to coalesce to form drops sufficiently large to overcome the adhesive properties of the net, thereby preventing drops from running downward and dripping into the gutter. Another possible cause is dew. Observations have indicated that copious amounts of dew form on surfaces such as roofs and vehicles soon after sunset. The inclusion of these records do not affect the determination of yields, but play an important role in identifying temporal characteristics of fog and rain on the west coast have thus been included in the temporal analyses. All data were captured and analyses were conducted using the Microsoft 2010 Excel spread sheets.

4.2 COMPARISON OF FOG CHARACTERISTICS

The two experimental sites are located on opposite sides of the country at approximately the same latitude (Avontuur: 33.7^{o}S; Lamberts Bay: 32.1^{o}S). These two sites have different elevations (>1000 m at Avontuur; 74 m at Lamberts Bay) and are subject to totally different synoptic conditions. Comparison of the characteristics of fog versus rain events and their relative contributions to water collection potential could cast some light on the water characteristics of fog and rain events along the West Coast and south-east coast of South Africa. For purposes of comparison, corresponding periods were used for analysis of the Avontuur and Lamberts Bay data. Since there were considerable breaks in the data collected from Lamberts Bay for 2014, only 2013 data were considered in the analysis.

4.2.1 Frequency of fog and rain events

Table 4.2 provides a summary of the daily and hourly statistics of fog and rain water collected during selected periods during 2013. Analyses of the data record for Avontuur and Lamberts Bay reveal that fog was recorded on 111 days during the 335 day data record at Lamberts Bay (approximately 1 out of every 3 days, i.e. 33%) and 134 days during the 213 day record at Avontuur (63% of the days).

Table 4.2: Daily and hourly rainfall and fog data from the Lamberts Bay and Avontuur experimental sites.

DAYS	LAMBERTS BAY	AVONTUUR	HOURS	LAMBERTS BAY	AVONTUUR
Length of record	335	213	Length of record	8 040	5 112
Fog frequency	111	134	Fog frequency	463	722
Rain frequency	108	86	Rain frequency	266	400
Wet	148	143	Wet	729	1 107

During the same periods, Lamberts Bay experienced 108 days with rain, while at Avontuur there were 86 days with rain. (It should be kept in mind that rain and fog can be recorded on the same day, and hence the number of wet days is not necessarily the sum of the number of fog days plus the number of rain days. The total number of wet days at Lamberts Bay amounted to 148 and at Avontuur, 143. The corresponding rainfall was 159 mm at Lamberts Bay and 415 mm at Avontuur.

Although there are no long-term rainfall records available for Lamberts Bay, the annual mean rainfall of 244 mm recorded at Cape Columbine, with an average rain day frequency of 67 (with a rain day defined as precipitation of > 0.1 mm) (SAWB WB40, 1986) could serve as an estimation of West Coast average rainfall. Although the fog day frequency for 2013 at Lamberts Bay is in accordance with that previously recorded along the West Coast (Cape Columbine – 111 days. yr^{-1} and Port Nolloth, 148 $day.yr^{-1}$) it seems that Lamberts Bay experienced lower-than-normal rainfall during 2013, but with small amounts falling more often than usual. The mean rainfall at Avontuur is 580 mm per year.

Comparison between Lamberts Bay and Avontuur indicated that Avontuur experienced fog more frequently (63% (134/213) against 33% (111/335) at Lamberts Bay); received more rain (415 mm against 159 mm at Lamberts Bay), but had only slightly more frequent rain events (40% against 32% at Lamberts Bay) than Lamberts Bay. The frequency of wet days (rain and/or fog) was virtually the same at the two experimental sites (148 days at Avontuur against 143 days at Lamberts Bay) but the proportion of wet days differed considerably between the two sites. On the one hand, 44% (148/335) of the days at Lamberts Bay recorded some form of precipitation, while at Avontuur this amounted to 67% (143/213) of the data record. The proportion of wet hours to the total number of hours comprising the data set shows a similar picture, with 21% of the recorded hours at Avontuur recording water, while at Lamberts Bay this only amounts to 9%. Surprisingly, the contribution of rain and fog to the total number of wet hours was the same for the two sites (Figure 4.1).

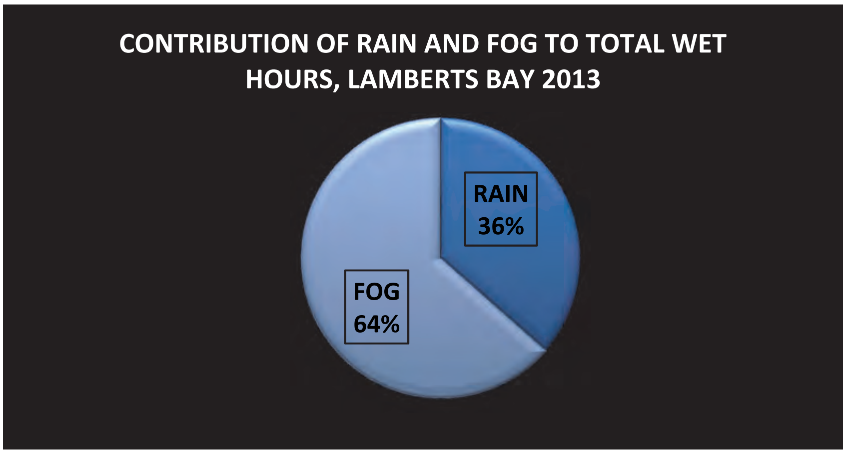

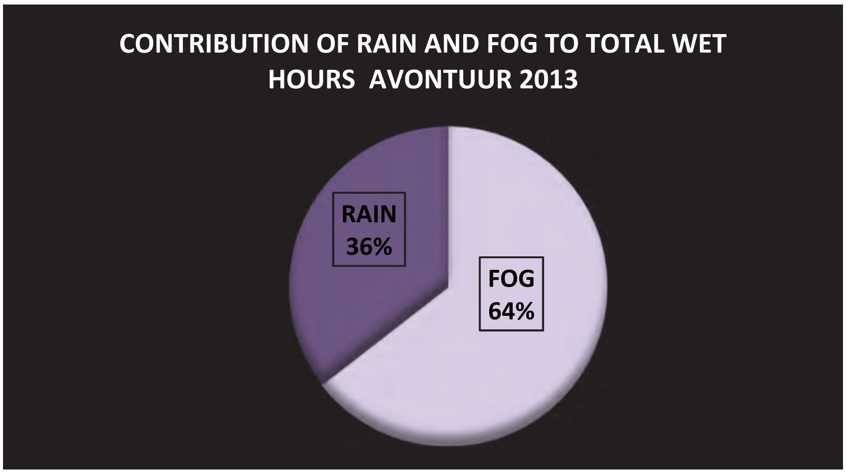

Figure 4.1: *Proportion of fog and rain recorded at the Lamberts Bay (top) and Avontuur (bottom) experimental sites, calculated as percentage (%) to total number of wet hours during 2013.*

4.2.2 Monthly patterns

The rainfall pattern (as reflected by rain day frequencies) for Lamberts Bay during 2013 (Figure 4.2, top) is typical of that for a South African austral winter rainfall region, with maxima occurring during June, July and August. The seasonal incidence pattern of fog, however, does not coincide with the rainfall, but rather reflects a year-round phenomenon. Peak incidence is during the late winter and spring months. It is noticeable that there were proportionately more foggy days during the drier summer months (October to February) and thus fog water harvesting could contribute significantly to augmenting water supplies during these low rainfall periods.

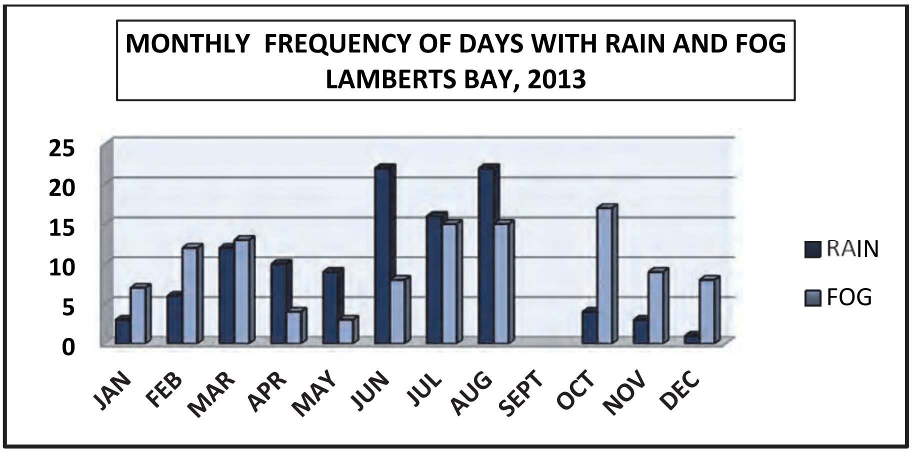

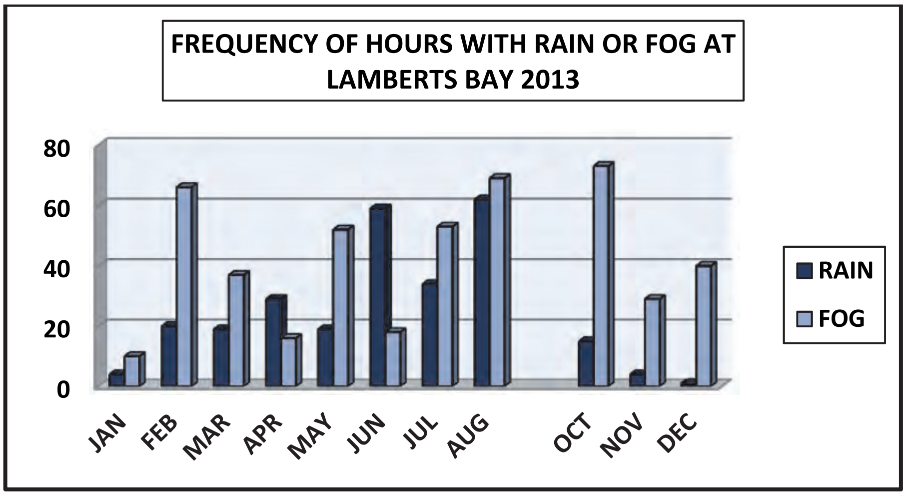

Figure 4.2: *Monthly variability in days with rain and fog (top), and monthly frequencies with hours with rain or fog (bottom) as recorded at Lamberts Bay during 2013.*

The number of *hours* during which rain was recorded at Lambert Bay (Figure 2.6, bottom) also shows a winter maximum. The monthly frequency of rain days and rain hours thus seem to vary in tandem with each other. A Spearman's Rank correlation coefficient (r_s) of 0.96 between these two variables confirms this ($\alpha < 0.05$). By contrast, neither the daily nor hourly fog frequency exhibit any 'seasonal' trends, although there is a statistically significant (α, 0.05) relationship between the number of fog days and the number of fog hours per month ($r_s = 0.72$). The largest anomaly between these two parameters occurs during May 2013 when only 3 days with fog were recorded, but the hourly frequency was 52. This suggests that each fog event was protracted. Indeed, the longest fog event was recorded during May 2013. This event lasted from 06:00 on 30 May 2013 until 24:00 on 31 May 2013, preceded by fog from 09:00 on 29 May 2013 until 01:00 on 30 May 2013. A fog event was defined as a period in which fog is recorded over a number of consecutive hours, with a fogless interval (break) of no more than one hour within this period. Comparison of Figure 4.2 and Table 4.1 suggests that fog occurs much more often than rainfall and is of longer duration than rainfall. This is in accordance with previously findings for general fog versus rainfall trends throughout foggy regions in South Africa (Olivier and van Heerden, 1999).

As indicated earlier, some gaps in the data record at Avontuur prohibited the differentiation between fog and rainfall. Nevertheless, the monthly incidence of rain and fog, as well as the volumes for water collected, are presented in Figure 4.3.

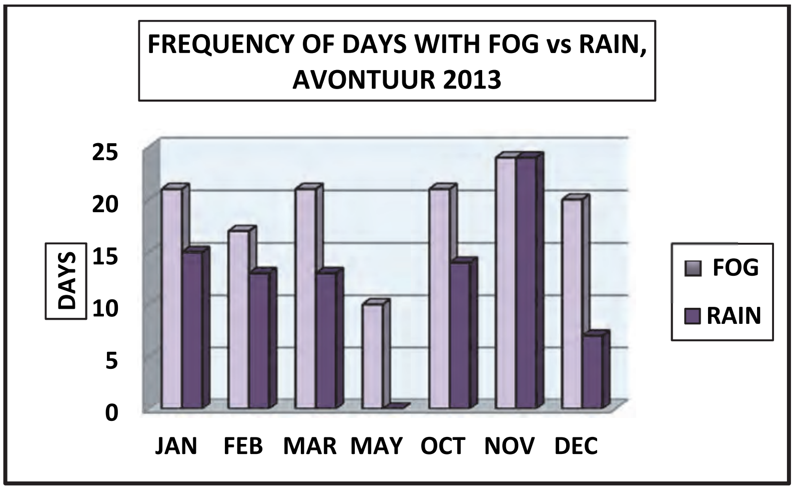

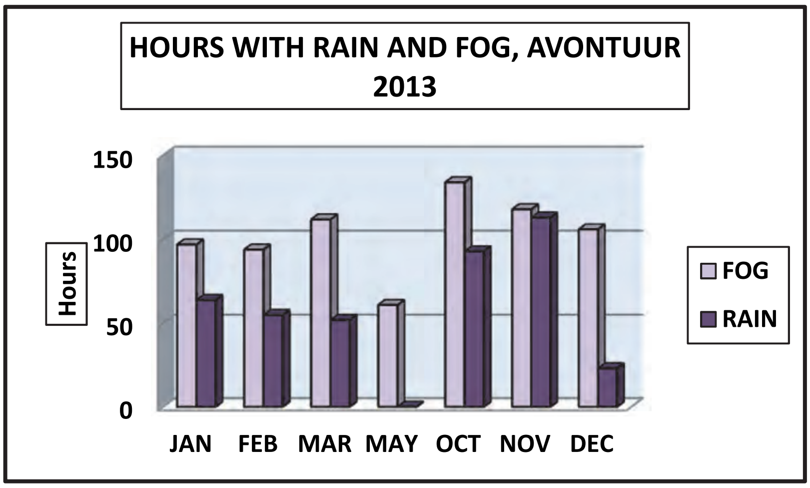

Figure 4.3: *Monthly variability in days with rain and fog (top), and monthly frequencies with hours with rain or fog (bottom) as recorded at Avontuur during 2013.*

At the Avontuur experimental site there was no discernible seasonal pattern in fog incidence, although there is a sight maximum during October and November. The lack of clear seasonality in fog incidence agrees with that at Lamberts Bay, and emphasizes the importance of fog precipitation and its potential harvesting during the low rainfall months.

4.2.3 Diurnal patterns of rain and fog

The diurnal incidence of wet events at Lamberts Bay is depicted in Figure 4.4. Although rain occurs most often during the period between 05:00 and 11:00 at Lamberts Bay, there is no clear pattern during the rest of the day. Conversely, fog events show a clear diurnal cycle, increasing during the early evening and peaking between 06:00 and 08:00 local time in the morning. These trends are not unexpected since rainfall is associated with synoptic-scale events, primarily north-westerly winds originating from mid-latitude cyclones that approach the country from the south west.

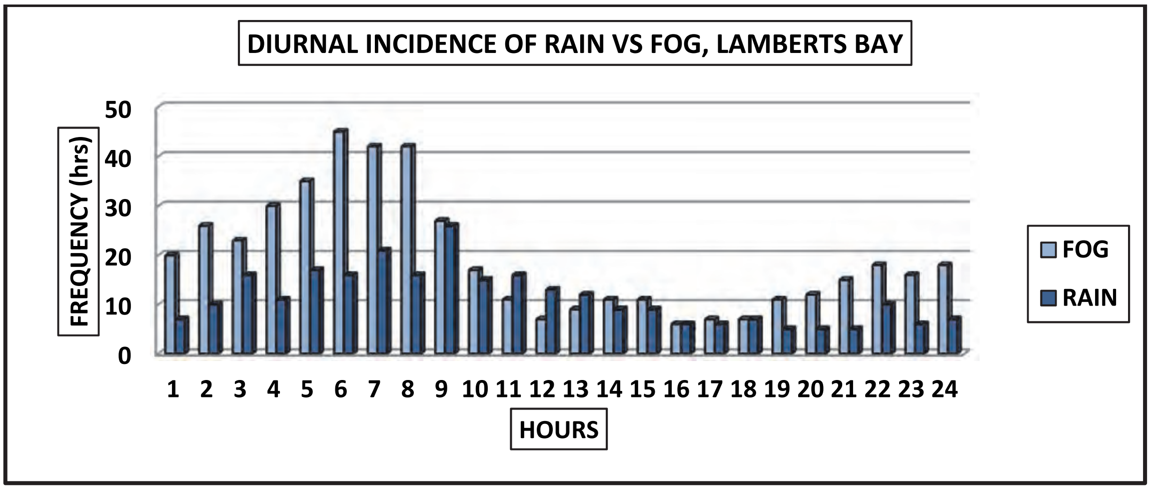

Figure 4.4: *Diurnal incidence of hours during which rain and fog was recorded at the Lamberts Bay experimental site during 2013.*

While this is also an important system producing advection sea fog, other conditions such as the South Atlantic High (situated to the south-west of the continent), coastal lows and local sea-land breezes may be responsible for fog formation (Estie, 1984; Olivier and van Heerden, 1999; Olivier, 2004). Moreover, the midday heating of the land surface dissipates fog as the day progresses. The isolated events where fog occurs during the midday probably reflect cloudy conditions that ameliorate long-wave terrestrial emissions.

At Avontuur (Figure 4.5), the probability for rain is the same throughout the hours of the day. However, while fog is predominantly an early morning event, a secondary peak occurs during early evening (19:00 and 20:00). The latter may be due to a local heat low pressure system that develops over the Little Karroo over the area during the afternoon. This could literally ‘suck in’ moist maritime air from south of the mountains, which then forms a fog as the ascending air cools to saturation by adiabatic expansion.

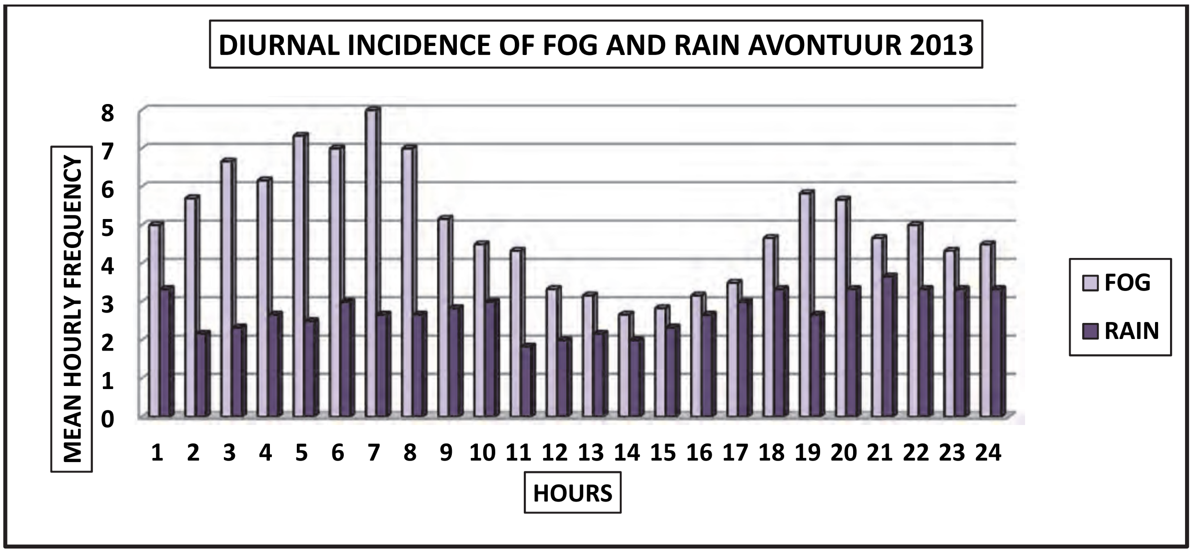

Figure 4.5: *Diurnal incidence of hours during which rain and fog was recorded at the Avontuur experimental site during January, February, March, May, October, November, December 2013.*

Early evening radiative cooling of the ascending air enhances the fog formation, peaking at 20:00 after which the thermal low over Little Karoo collapses. The more common 'normal' early morning peaks in fog are probably caused by synoptic scale forcing which causes an ascending motion against the mountains, resulting in saturation, condensation and fog formation in the ascending air. During the early morning, at about sunrise, the radiative cooling of the ascending air peaks and minimum temperatures occur. This enhances (thickens) the fog. At about the time of the minimum temperatures the stability of the ascending air reaches a maximum and this may contribute significantly to thickening of the fog because of mixing by turbulence with drier environmental air.

4.2.4 Contribution of fog and rain to water collection

As indicated earlier, it is extremely difficult to determine the relative contributions of rainfall and fog to the total volume of water collected. A rough estimate may, however, be obtained by assuming that all water collected during hours when rainfall was recorded on the rain gauge, was due to rain alone; while water collected when the rain gauge did not record rain, was due to fog. This obviously under-estimates the contribution of fog to the total water yields.

An indication of the relative contribution of rain and fog to the volumes of water collected at Lamberts Bay and Avontuur in Tables 4.3 and Figure 4.3, respectively.

Table 4.3: Water collection (litres) due to fog and rain at the Lamberts Bay experimental site during 2013

LAMBERTS BAY 2013	JAN	FEB	MAR	APR	MAY	JUN	JUL	AUG	OCT	NOV	DEC	TOTAL
FOG	9.5	28.2	110.5	84.5	187.5	18	14.4	23.2	167.4	25.6	63.3	**732.1**
RAIN	63.5	94.1	27	331	67.3	451	105.3	235	108	6.8	0	**1488.1**
TOTAL WATER (FOG + RAIN)	73	122.3	137.5	415	254.8	469	119.7	258	275.4	32.4	63.3	**2220.2**
PERCENTAGE FOG TO TOTAL WATER	13.0	23.1	80.4	20.4	73.6	3.8	12.0	9.0	60.8	79.0	100.0	**33.0**

The contribution for fog water to the total water collected was only 33% (732/2220) at Lamberts Bay. This is considerably less than 88% that was found at Lepelfontein (Olivier, 2004). The elevation of the site is clearly definitive in water yield potential and re-affirms findings by Schemenauer and Cereceda (1991, 1992, 1994), Struthers (1997) and Olivier and van Heerden (1999). An important observation is that fog yields contribute more to total water yields during low rainfall months. A Spearman's rank correlation coefficient (r_s) of -0,81 bears this out. This is significant at $\alpha<0.05$. Fog water harvesting may thus make a considerable contribution to water availability during the dry summer months along the west coast.

Table 4.4 indicates that fog contributes only 20% of the water collected at Avontuur, the bulk being supplied by rainfall interception. As expected, this is considerably less than at Lamberts Bay, and is slightly less than the 28% contribution recorded at Pypkop in Limpopo (Olivier and van Heerden, 1999). But, similar to Lamberts Bay, the contribution of fog to water collected was greatest during the dry season.

Table 4.4: Water collection (litres) due to fog and rain at the Avontuur experimental site during 2013

2013	JAN	FEB	MAR	MAY	OCT	NOV	TOTAL	% OF TOTAL
FOG	505.5	343.1	572.1	1057	785.5	863.3	4126.5	**20%**
RAIN	2253.7	2190.6	1081.5	0	4456.1	6325.8	16307.7	**80%**
TOTAL WATER (FOG + RAIN)	2759.2	2533.7	1653.6	1057	5241.6	7189.1	20434.2	
PERCENTAGE FOG TO TOTAL WATER	18.3	13.5	34.6	100.0	15.0	12.0	20.2	

CHAPTER 5: FACTORS AFFECTING WATER COLLECTION RATES

5.1 INTRODUCTION

The total volumes of water that were collected at the Lamberts Bay and Avontuur experimental sites were considerably lower than expected from previous research results. At Lamberts Bay, for example, the mean yield of 0.07 $\ell.m^{-2}.day^{-1}$ is an order of magnitude lower than those previously obtained at Lepelfontein (1 $\ell.m^{-2}.day^{-1}$), with the two sites being about 140 km apart (Rautenbach and Olivier 2001; Olivier and Rautenbach, 2002). Avontuur, too, records much lower yields than mountainous areas researched in previous WRC projects (WRC: K5/671/ and WRC: K5/902/1). For example, at the Tshanowa School in the Soutpansberg, mean daily yields of 2.85 $\ell.m^{-2}.day^{-1}$ were obtained, while maximum yields obtained from one square metre test screens reached maxima of 12.2 $\ell.m^{-2}.day^{-1}$ at Pypkop near Woodbush (Limpopo Province) and 10.5 $\ell.m^{-2}.day^{-1}$ at Hanglip (near Louis Trichardt in the Limpopo Province). In the Groenlandberge near Grabouw in the Western Cape, an average of 8.7 $\ell.m^{-2}.day^{-1}$ of water was collected over a period of seven months. A number of factors could be responsible for the meagre yields recorded at Lamberts Bay and Avontuur, including the differences in the design and size of the structures, the frequency and duration of wet events, distance from the sea, the liquid water content of the fog, and wind direction and speed (Nagel, 1956; 1959). These in turn depend to a large extent on altitude and on the presence of certain regional climatic factors such as the pressure distribution in the area and the sea-surface temperature. The direction and speed of the wind are also affected by the type of terrain and on the micro-topography of the area (Fuenzalida, 1988). Clearly, one or more of these factors must account for the low water yields at the experimental sites.

5.2 SYSTEM DESIGN FEATURES

It was shown in Chapter 3 that the nets of the triangular system have a blocking effect on each other, lowering yields significantly. Even the highest yielding systems at the current experimental sites have yields (2.7 $\ell.m^{-2}.day^{-1}$ from the 60^{o} open zig-zag system at Avontuur and 0.16 $\ell.m^{-2}.day^{-1}$ from the Whirly at Lamberts Bay) which are still below those expected from previous research. Although the structural designs of the systems do contribute to the low yields at the experimental sites, direct comparison between different types of fog water collection systems is not possible since structural characteristics are clearly not the sole reason for the meagre yields.

5.3 GEOGRAPHICAL FACTORS

5.3.1 Distance from the sea

The distance from the sea – the source of moisture – does not appear to the major factor affecting yields at Lamberts Bay and Avontuur. The Lamberts Bay site is 2 km from the sea, while Lepelfontein is 15 km from the Atlantic Ocean seaboard. Moreover, the Avontuur site is 40 km from the Indian Ocean. On the other hand, Tshanowa is 400 km away, and Hanglip even further, at 270 km from the sea.

5.3.2 Altitude

The West Coast region is relatively flat with minor hills protruding from the coastal plain. Rainfall obviously makes a contribution to the volume of water collected by the nets of the triangular system at Lamberts Bay. However, altitude does not influence rainfall in this region since rainfall is associated with large-scale synoptic events. Cloud bases are usually some distance above ground level and thus little to no cloud interception occurs in the coastal zone to the west of the escarpment. Fog is formed by the advection of moist air over the cold Benguela Upwelling region. Topographical forcing and adiabatic cooling of air at elevated sites may thus account for the higher fog water collection rates at Lepelfontein.

In mountainous regions, altitude of a site influences the liquid water content of fog as well as wind speeds (Schemenauer and Cereceda 1991, 1992, 1994), Struthers (1997) and Olivier and van Heerden (1999) and is of crucial importance to the volume of water that can be collected.

The impact of mountain altitude on fog water harvesting potential is influenced by various factors. Firstly, fog in the mountainous regions of the country originate from different sources such as frontal systems, orographic lift and the interception of stratocumulus clouds that originate over the Indian Ocean. Each of these may give a unique altitude-FWC potential profile since the temperature, moisture contents, wind speed and height of the cloud base and cloud tops may differ. Information on these variables is not readily available. No research has been conducted on the occurrence frequency of the different types of fog in South Africa. Secondly, fog, drizzle and rain often occur simultaneously in mountainous areas. Although no research has been published on the relationship between altitude on fog occurrence, some work has been done on the effect of altitude on rainfall. It is generally assumed that rainfall increases with height (Tyson et al. 1976) in mountainous terrain. Research conducted in the Drakensberg by Schulze (1979) confirmed this, but only up to a certain height, where after rainfall decreased. Nel et al. (2010) found the same trend when comparing rainfall at the Sentinal Peak (3165 m AMSL) in the Drakensberg of the KwaZulu-Natal Province with that at the Royal Natal National Park station (1392 m AMSL) at the foothills. The former was found to be lower. Conflicting results have also been found regarding the relationship between altitude and the frequency of rainfall events (Nel and Sumner 2005; Nel et al. 2010). Since fog water harvesting includes both rainfall and fog collection from a vertical collector, it is not yet certain how altitude will affect fog water harvesting potential.

An attempt is made in this chapter to determine the relationship between altitude and water yields in mountainous areas using data obtained from research on fog and rainfall that was conducted by the South African Department of Water Affairs during the period 1968 to 1970. A series of rain gauges and fog catchers (rain gauges fitted with a gauze cylinder with a height twice the diameter of, and a vertical cross-sectional are equal to, the catching area of the rain gauge to which it was attached) were placed at numerous sites in the then Northern Transvaal (currently the Limpopo and Mpumalanga Provinces). Details of these experiments were described in a Departmental Technical Report (Schutte, 1971). Since the report is not readily accessible and was written in Afrikaans, the results are reproduced in the first 5 columns of Table 5.1. A severe shortcoming of these results is the short length of the data record which spans only a few months.

Table 5.1: Rain and fog water yield in mm and ℓ.m^{-2}.day^{-1} (fog water harvested from a 1 m^{2} vertical screen) as recorded at 16 selected mountain sites in the Limpopo and Mpumalanga Provinces (after Schutte (1971) and Olivier and van Heerden (1999)*).

	Altitude (m)	Total rain (mm)	Total rain and fog (mm)	Water yield (mm.month^{-1})	Water yield (ℓ.m^{-2}.day^{-1})
Broederstroom	1555	1082.7	3032.8	337	9.2
Entabeni	1401	1079.4	2126	236.2	6.4
Goedehoop	811	412.6	621.6	88.8	2.4
Voorspoed	1065	630.6	912.8	114.1	3.1
Matiwe	1376	872.3	1627.8	203.5	5.5
Spelonken	1082	452.3	575.2	71.9	2.0
New Agatha	1097	868.5	1138.4	126.5	3.4
Roodewal	1065	500.5	685.4	85.7	2.3
Tate Vondo	960	508.3	1008.5	252.1	6.9
Vondo	1152	528.7	1142.8	285.7	7.8
De Hoek	1219	735.1	1000.5	166.8	4.5
Zomerkomst	792	507.7	534.2	133.6	3.6
Mamathela	914	705.5	828.2	92	2.5
Pypkop*	1903	N/A	N/A	447	12.2
Hanglip*	1719	N/A	N/A	353	10.5
Mariepskop	1944	N/A	N/A	430.5	11.7

The fog and water yields obtained in this research were recorded in mm. Fortunately the experiment at Mariepskop included concurrent measurements of water yields obtained from the vertical fog collecting screens (Figure 1.1) and from a fog catcher. These findings could be used to convert total fog catcher readings in mm to yields in ℓ.m^{-2}.day^{-1}. These are shown in the last column of Table 5.1. Fog water yields for Mariepskop, Hanglip and Pypkop that were obtained from research conducted by Olivier and Van Heerden (1999) were included in Table 5.1.

Fog water collection values were plotted against altitude (Figure AMSL) for the sites shown in Table 5.1. In all cases the data records exceeded 3 months. A Pearson's Correlation Coefficient of +0.88 was obtained, explaining 78% of the variability in water yields in areas with altitudes spanning 800 m to 2000 m amsl. Although these results refer to data obtained in the mountains of the Limpopo and Mpumalanga Provinces, it is assumed that they also apply to mountains in other parts of the country.

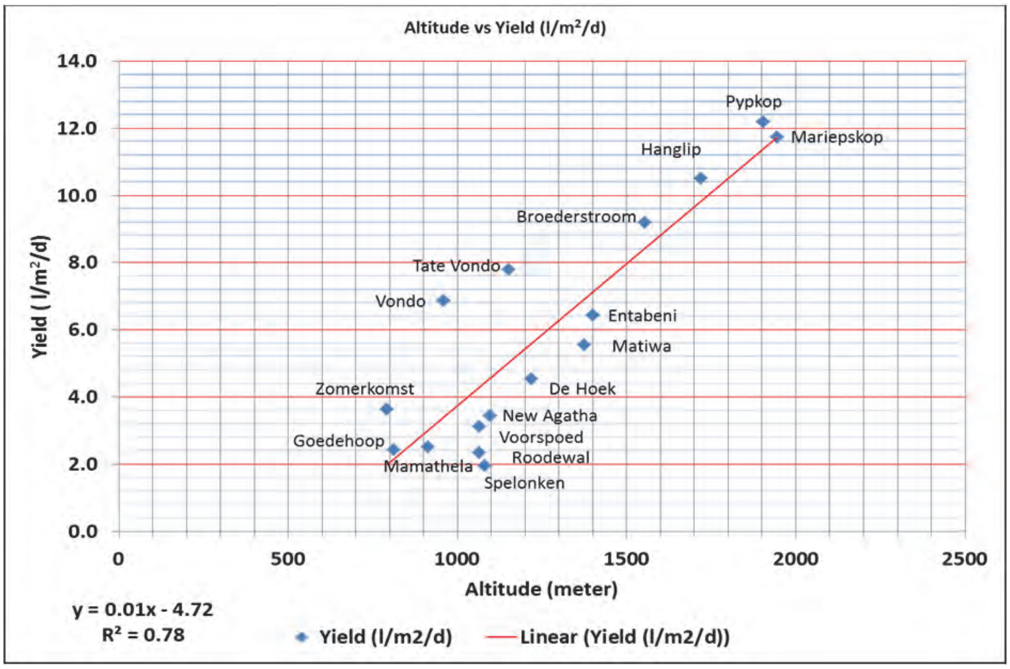

Figure 5.1: *The relationship between fog water collection potential and altitude in the Limpopo and Mpumalanga Provinces showing a positive regression line fit. Altitude explains 78% (R^2 = 0.78) of the variability in water yield in areas with altitudes spanning 800 m to 2000 m Above Mean Sea Level (AMSL).*

5.3.3 Topography

It is clear that altitude is the major geographical factor that controls the amount of water that can be harvested from fog (Schemenauer et al., 1987). However, the occurrence of fog can vary significantly from one point to another at places with the same altitude due to micro and meso-topographic features of a site. These features comprise aspect, i.e. orientation of topographic features, relief of the surrounding areas, and slope.

Aspect is important since it is imperative that a potential fog water harvesting site is exposed to moisture-bearing winds. Under suitable conditions extensive clouds or fog layers tend to form against mountain slopes overnight, and can last well into the day if the terrain generally slopes downhill towards the coastal region. Such slopes ensure that if maritime air ascending to a potential fog water harvesting site, it will cool by adiabatic expansion as well as due to heat loss to the surface at night, which could result in more dense fog. Sites located on the lee side of a ridge or hill, especially where the wind is flowing down-slope, will experience adiabatic heating and evaporation of the fog droplets. Such sites must be avoided (Suau, 2010).

It is also important that there are no major obstructions to wind flow upwind of the site. These may cause sub-mesoscale circulation eddies in the wind field, thereby increasing patchiness in fog incidence.

Another important topographic factor affecting yields is the general slope of the terrain. A sharp slope immediately seawards of a potential fog water harvesting site is considered very beneficial to fog water collection. The sharp ascent up such slopes will result in rapid adiabatic cooling (approximately 1°C per 100 m for unsaturated air), which will result in condensation of water vapour in the moist ascending air and the formation of broad front of orographic cloud.

Taking altitude alone into account, a yield of almost 4 $\ell.m^{-2}.day^{-1}$ can be expected at Avontuur. Aspect is probably the most important factor responsible for the low yields at Avontuur since the experimental site is located on the saddle linking the Zondachsberg and the start of the Tsitsikamma Mountain ranges. It is also some 2 km from the top of St Alfred Pass. This illustrates the importance of site location and the impact of topography on yields. For this reason, it is important to try to estimate the extent of impact of these factors on yield.

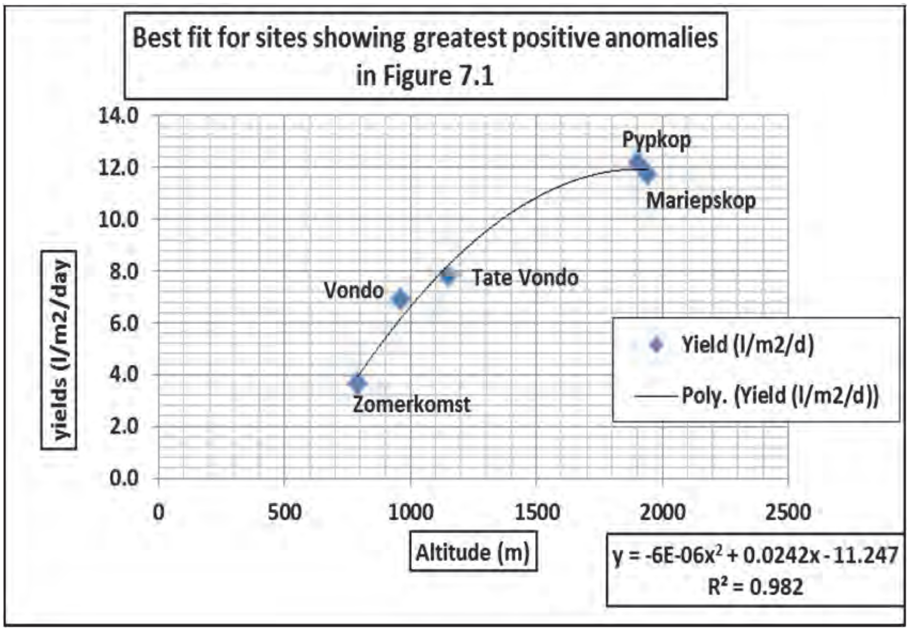

Figure 5.2: *Fog water yield (ℓ.m^{-2}.day^{-1}) as a function of altitude (m Above Mean Sea Level: AMSL), with the line providing the best fit between these most suitably located sites.*

An estimate of the negative effects of unfavourably topographic features can be obtained by assuming that the sites with yields showing the largest positive deviations from the linear trend line shown in Figure 5.1, as the most suitably located topography. Using this criterion, Pypkop, Mariepskop, Tate Vondo, Vondo and Zomerkomst were located at the most suitable locations for water harvesting. A polynomial function provided the best fit between yield and altitude for these five sites with altitude explaining 98% of the variation in yields (Figure 5.2). The extent of impact of topography on yield can thus be estimated by comparing the actual yields at sites to potential yields as derived from Figure 5.2.

The role of topographic obstacles, aspect and slope for sites such as Entabeni, Matiwa, De Hoek, New Agatha, Voorspoed, Roodewal and Spelonken can only be determined by detailed analysis of terrain features and possibly, site visits. Nevertheless, this concept could be used to identify the most suitable sites for fog water harvesting on a national basis and to quantify potential yields.

5.4 ATMOSPHERIC AND CLIMATIC FACTORS

5.4.1 Liquid water content of fog

The moisture content of fog is a function of the type of fog and the altitude AMSL. Numerous experiments have shown that radiation fogs have the least amount of moisture, followed by advection sea fog. High elevation mountain fogs comprising orographic fog and cloud contain the highest levels of moisture (Nagel, 1959). The moisture content also changes within a cloud. It increases with height, but only up to a level equivalent to about two-thirds of the cloud thickness above the base, where after it decreases (Suau, 2010). The altitude of a fog water harvesting site is thus of crucial importance.

Lamberts Bay experiences advection sea fog and consequently yields are considerably lower than at Avontuur where fog is mostly topographic in nature and may also be due to cloud interception.

The contribution of fog yields to the total water yields may give an indication of the liquid water content of the fog at similar sites (west coast sites and mountainous sites). At Lamberts Bay, the contribution for fog water to the total water collected was only 33%. This is considerably less than 88% that was found at Lepelfontein (Olivier, 2004). This difference in liquid water content could be influenced by altitude with the higher-lying Lepelfontein being exposed to fog with a higher liquid water content. Similarly, fog at Avontuur contributes only 20% to the total amount of water collected. This is also less than its 24.5% contribution at Tshanowa. This discrepancy is also probably due to differences in altitude as well as adiabatic heating and evaporation of moisture from descending air on the leeward slopes of the Zondachsberg.

5.4.2 Wind speed

Another factor that might assist in explaining the low yields at Lamberts Bay and Avontuur may be the wind speed. The amount of fog water captured by static nets is dependent upon the volume of fog-bearing air passing through the net per unit time and hence, the wind speed. It has been shown (Chapter 3) that the triangular system affects the wind speed since this structure probably lowers the droplet collection efficiency by lowering the wind speed at the screen surfaces at the downwind sides of the FWCS. Atmospheric conditions might also be associated with stronger or weaker winds. The effect of wind speed during dry, foggy and rain events at Lamberts Bay are shown in Table 5.2.

Table 5.2: Mean hourly wind speed ± standard deviation (m.s^{-1}) during fog and rain events at Lamberts Bay (with statistically significance in differences in means reflected by t-test)

WIND SPEED	JAN	FEB	MAR	APR	MAY	JUN	JUL	AUG	OCT	NOV	DEC
DRY	3.60± 1.63	**3.40± 1.64**	**2.90± 1.45**	2.60± 1.43	2.26± 1.19	*2.73± 1.63*	2.41± 1.26	3.03± 1.63	**3.17± 1.65**	**3.38± 1.71**	**3.25± 1.54**
FOG	*3.28± 1.52*	*1.98± 1.24*	2.77± 1.50	*1.66± 0.89*	*1.70± 0.73*	3.19± 1.47	2.44± 1.27	*2.71± 1.64*	*2.26± 1.29*	*2.56± 1.44*	*2.63± 1.01*
RAIN	-	2.21± 1.29	*1.81± 0.79*	**4.39± 1.42**	**3.22± 0.45**	**4.21± 1.46**	**3.40± 1.23**	**3.84± 1.73**	2.63± 0.95	-	-
SIGNIFICANCE USING T-TEST											
P dry.fog	0.27	**8.93E-13**	0.20	**0.0001**	**0.0002**	0.11	0.43	0.07	**1.34E-7**	**0.003**	**0.0003**
P dry.rain	-	**0.001**	**0.0007**	**9.8E-5**	**0.5E-6**	**2.02E-6**	**0.0002**	**0.002**	**0.05**	-	-
P fog.rain		0.26	**0.002**	**0.01**	**1.04E-9**	**0.01**	**0.001**	**0.0005**	0.13	-	-
for frequencies of < 5 events; highest wind speeds and significance values of P<0.05 are highlighted; slowest wind speeds are shown in italics											

During most austral summer months (October to March), winds are stronger during dry conditions than during wet periods. This trend is reversed during winter, when rain events are characterised by strong winds. However, fog-bearing winds are significantly weaker than those prevailing during dry conditions during February, April, May, October, November and December and during rain events from March to August (winter). The overall mean wind speeds recorded during dry, rainy and foggy conditions are shown in Figure 5.3 for the 11 month study period in 2013.

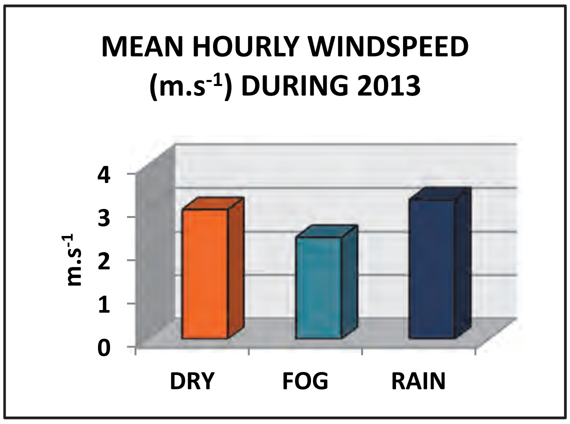

Figure 5.3: *Summary of mean hourly wind speeds (m.s^{-1}) during dry, rainy and foggy events during 2013.*

Wind speeds associated with dry, foggy and rainy conditions at Avontuur are depicted in Figure 5.4.

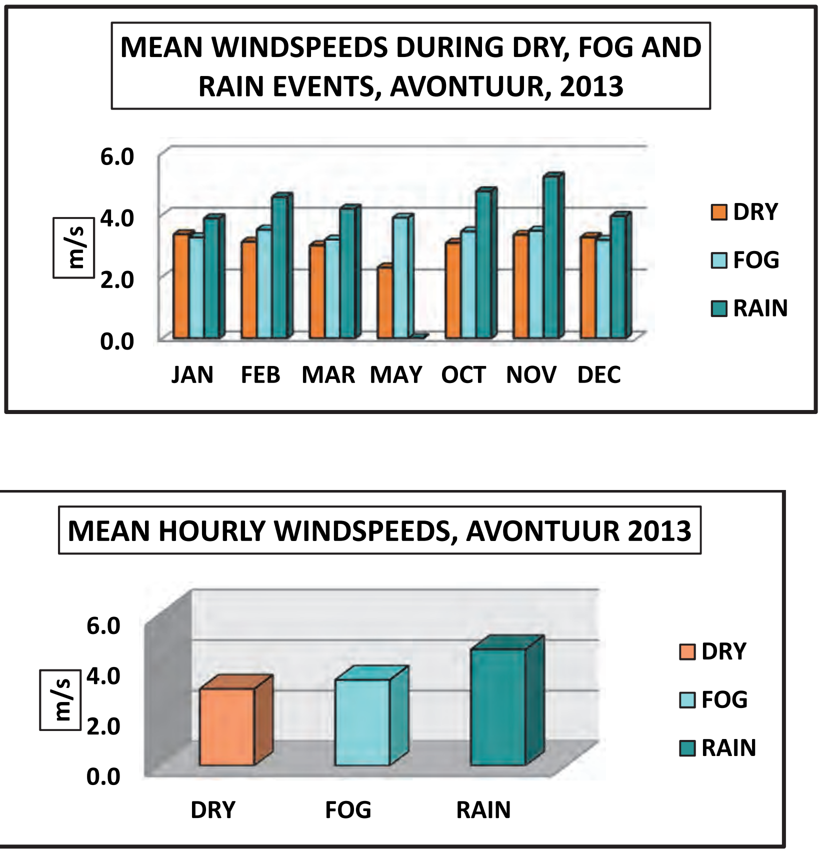

Figure 5.4: *Mean monthly and annual wind speeds during dry, fog and rain events at Avontuur, 2013*

Comparison of wind speeds during dry, fog and rain events during these seven months in 2013, indicates that winds are significantly (p=0.05) stronger during rain events, but there is little or no difference in mean monthly or annual wind speeds during dry and fog events at Avontuur.

5.5 SYNTHESIS – IDENTIFICATION OF AREAS WITH FOG WATER COLLECTION POTENTIAL

5.5.1 Elevation as indicator

The elevation of the site plays in water yield potential is well known, since it influences both the liquid water content of fog as well as wind speeds (Schemenauer and Cereceda (1991, 1992, 1994), Struthers (1997) and Olivier and van Heerden (1999)). Altitude was thus used as a proxy variable to depict areas with high fog harvesting potential. That said, it should be noted that it is not the altitude *per se* that is the important factor, but rather the elevation since a relatively steep upward slope is required for the formation of orographic fog. High altitude regions on the plateau are thus not necessarily prone to fog episodes. Taking this into account, GIS tools were used to obtain a more detailed fog water yield potential map of South Africa.

GIS software packages generally provide several surface analysis tools that are valuable for this project. In this analysis, the functions and tools embedded in licensed ArcGIS 9.3.1 software, a product from the Environmental Systems Research Institute (ESRI) were applied in the analysis of raster- as well as vector data sources. All data sets used in this project were obtained from the Centre for Geoinformation Studies at the University of Pretoria.

As a basis for the initial elevation and slope analysis, raster based 90-meter Digital Elevation data (90 m DEM) as obtained from the NASA Shuttle Radar Topographic Mission (SRTM) was used. The raster data model is useful for representing continuous geographic data such as elevation values. However, it typically comprises of large data sets that require more computer storage space than corresponding vector data such as contour lines or elevation points. To decrease the amount of data storage space needed and to optimize data processing speed, specific focus areas were delineated by using vector layers such as provinces and quaternary catchment polygons. Because elevation and influx of maritime are important parameters in determining the potential for fog water collection, the polygons representing fog receiving coastal winds (Limpopo, Mpumalanga, KwaZulu-Natal, Eastern Cape and Western Cape Provinces) where selected and a computer shape-file was created with the selected provinces as a separate layer. This layer was then used as a mask to extract the DEM data for the coastal areas. As the selected provinces still included areas that are low lying or too far inland, the layer with DWA river catchment polygons was used to manually select only the catchments which include higher lying areas and are located on the coastal side of the escarpment and/or other coastal mountain ranges.

The DEM values within the different selected provinces were classified into elevation zones with an equal interval of 800 m. For most of the targeted regions, the elevation zones of 800 m AMSL and higher may be suitable for fog water harvesting.

An example of a GIS generated map is given as Figure 5.5.

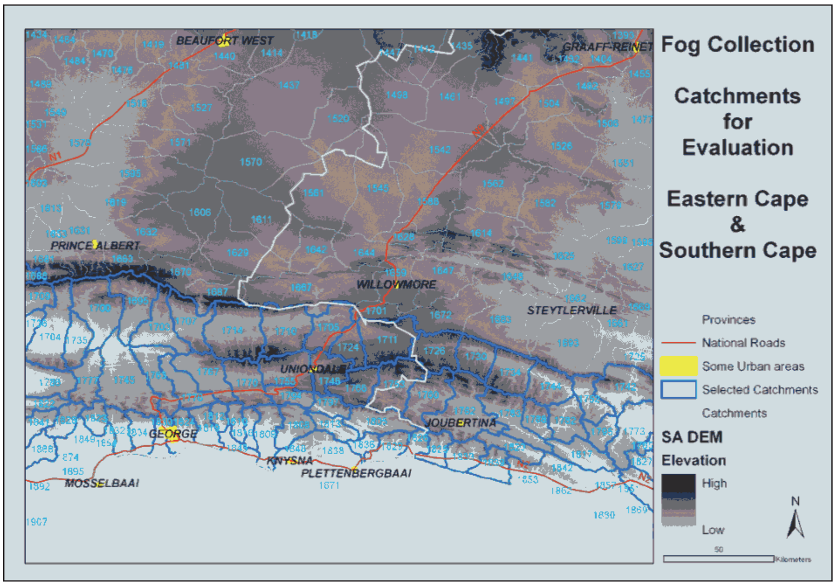

Figure 5.5: *Catchment areas (blue lines) identified to have high fog water harvesting potential along the south coast of South Africa.*

Conditions along the west coast are considerably different to those in other fog prone regions. Elevation zones are much lower than along the eastern and southern coastal regions and influx of moist air is from the west, north west and south west. The differences in elevation along the coastal region are relatively small. Therefore a much finer raster resolution, a 20 m DEM derived from 20 m contours, was applied. It is clear that the fog prone areas here are located in a narrow sliver running parallel to the western coastline. The communities in need of water are also usually situated at the coast.

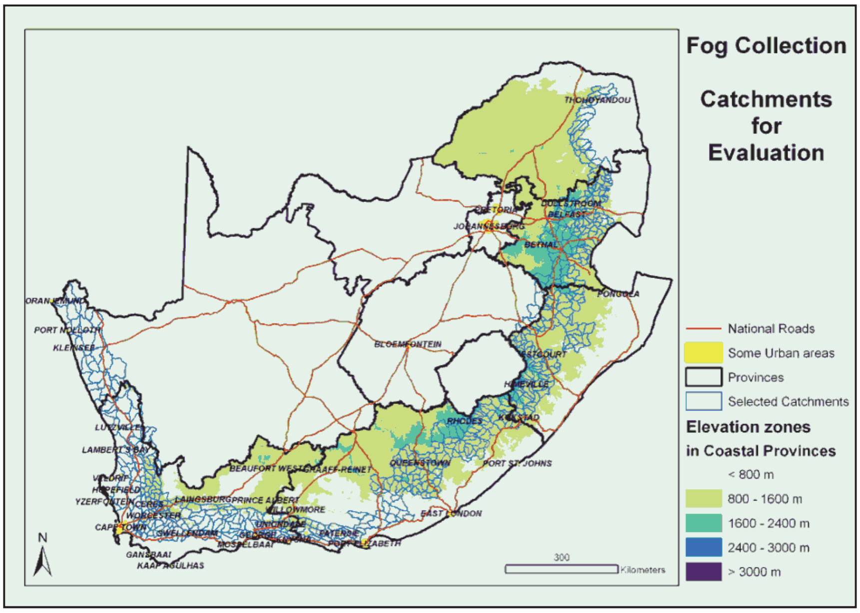

Figure 5.6: *Catchment areas (blue lines) across South Africa identified to have high fog water harvesting potential.*

GIS maps were created for all regions in South Africa and presented in Deliverable 2 (compiled by Erika Pretorius and presented as Appendix C). A composite map of all catchment areas with high fog potential is given in Figure 5.6 and represents the first step in compiling a Fog Atlas for South Africa.

5.5.2 Topographic ascent as indicator

As will be discussed in detail in Chapter 8, Forced Topographic Ascent (FTA) of moist marine air against the slopes of the eastern and south-eastern escarpments of South Africa frequently results in adiabatic cooling and mountain fog formation. Although slopes are less profound along the West Coast, FTA also plays a role in forcing moist marine air upwards which might also result in fog formation. FTA could therefore be used as an alternative indicator for identifying domains with the potential for fog formation. In this section (as in Chapter 8), FTAs were calculated over the 20-year period 1986 to 2005 using Equation (2), from where daily frequencies of FTA in 1km x 1km domains over the entire South Africa were calculated, regardless of the wind direction. Daily frequency percentages larger than 70 % (red) and larger than 80% (blue), for four seasons of the year, are depicted in Figure 5.7.

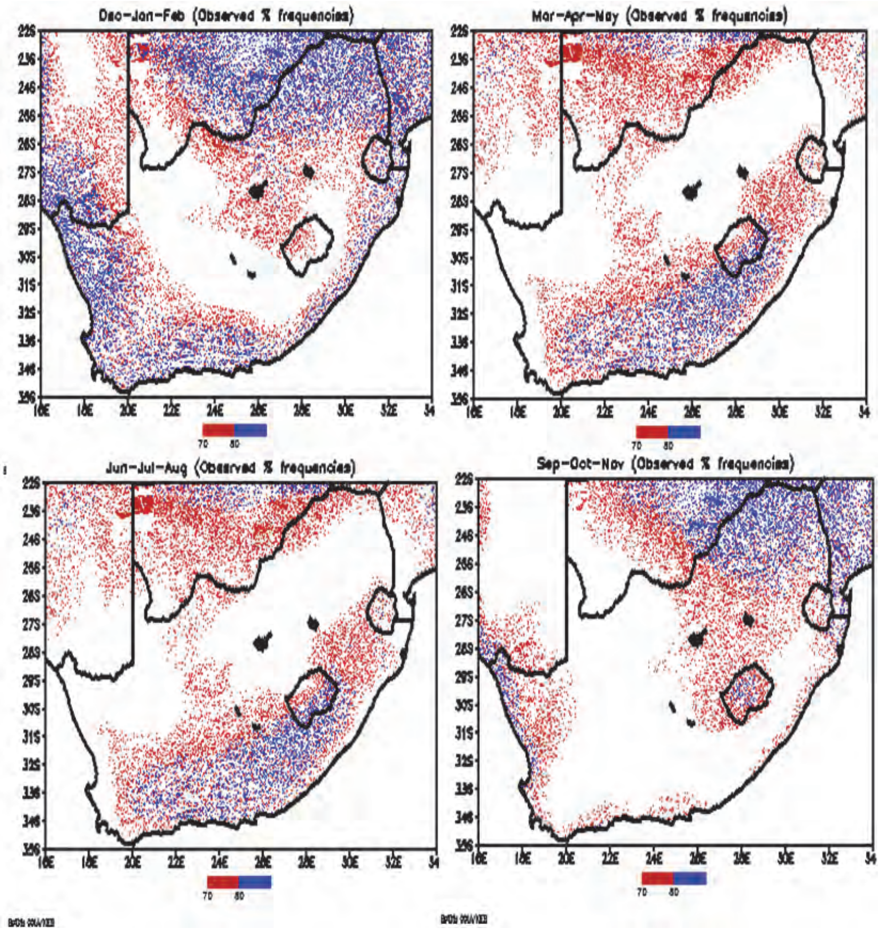

Figure 5.7: *Seasonal (Dec-Jan-Feb, Mar-Apr-May, Jun-Jul-Aug and Sep-Oct-Nov) frequency percentages (%) of positive daily Forced Topographic Ascent (FTA) as calculated for South Africa in 1 kmx1 km domains over the 20-year period 1986 to 2005. Red and blue domains represent positive FTA frequency percentages of > 70% and > 80%, respectively.*

Domains with the potential for fog formation will obviously depend on the availability of moisture in the atmosphere, which make coastal domains with a positive FTA (FTA > 0), and where the topographical slope faces towards the ocean, more favourable for fog formation than inland domains.

In Figure 5.7 selected domains along the entire coastline appear to have a good potential for fog formation (daily frequency of FTA > 0 is > 70 %) during the season Dec-Jan-Feb, while domains in the south and south-east coastlines have a greater potential for fog formation during the seasons Mar-Apr-May and Jun-Jul-Aug. The lowest potential for fog formation in the FTA > 0 frequency range of > 70% occurs during the season Sep-Oct-Nov.

Both altitude and FTA could serve as good indicators for the potential for fog formation. However, further research, preferably with atmospheric modelling involved, is required to combine these indicators in order to develop integrated optimum fog formation potential maps for South Africa.

CHAPTER 6: CHEMICAL CHARACTERISTICS OF WATER COLLECTED

6.1 INTRODUCTION

Water samples were collected from the FWCSs at the Avontuur and Lambert Bay experimental sites, and chemical analyses were conducted for two main reasons. Firstly, to test the potability of water should it be used for human or animal consumption. This step included analyses of the physical and chemical characteristics of the water, including pH, pHs, SAR and Electrical Conductivity (EC) ($mS.m^{-1}$), macro-elements and trace elements using ICP-MS and ICP-AES. All samples were tested at the ARC's Institute of Soil, Climate and Water (ISCW) accredited laboratories in Pretoria.

In addition to these analyses, research was conducted at the University of Pretoria's Medical Sciences laboratories at the Steve Biko Hospital (Pretoria) to test for the presence of Endocrine Disruptors (EDs) in the water. EDs are organic toxicants with the potential to alter hormone action within the body (Sharp and Irvine, 2004), thus interfering the function of the endocrine system, which is responsible for growth, sexual development and many other essential physiological functions both in males and females (Lovekamp-Swan and Davis, 2003). Well-known EDs include phthalate esters that are used in the manufacture of certain plastic materials (Tsutsumi et al., 2004). Phthalates are not bound chemically in the plastics material; therefore they can migrate into water, juices and food products (Nerin et al., 1993; Latini et al., 2004) with the potential of serious health effects in humans and animals (Parks et al., 2000; Ema and Miyawaki, 2001; Wilson et al., 2004. Since the FWCS nets are composed of polyethylene, it was deemed prudent to test water for the possible presence of these toxins in the water. The recombinant Yeast Estrogen Screen (YES) and the T47D-KBluc reporter gene assay were used for this purpose.

The second motivation for conducting chemical analyses was to determine whether factors such as the prevailing wind directions (and consequently the synoptic systems) affect the composition of collected water. This could have consequences in determining the feasibility of harvesting fog water in the event of climate change or other factors affecting the incidence of different mesoscale fog-producing systems. For this purpose, a special rotating fog system to collect water originating from the 6 main compass directions. This was mounted at the Lamberts Bay experimental site during February 2014 (see Section 2.3 and Figure 2.22).

The possible origin of various constituents of the water – albeit maritime or continental – was also included in the study. The method proposed by Ahmed et al. (1990) was used to determine the Enrichment Factor (EF), and hence the fraction of ions originating from the sea (Sea Salt Fraction) (SSF) and from other sources (Non-Sea Salt Fraction) (NSSF).

Further details of the methods used are given in the relevant sections.

Table 6.1 provides a summary of the dates on which water samples were collected at the two experimental sites for analyses.

Table 6.1: Experimental research site, source from where water was collected and dates of sample collection

SITE	SOURCE	COLLECTION DATE
LAMBERTS BAY	Tank	1/3/2013
LAMBERTS BAY	Gutter	21/11/2013
LAMBERTS BAY	N bottle	13/5/2014
LAMBERTS BAY	N bottle	24/6/2014
LAMBERTS BAY	N bottle	31/7/2014
LAMBERTS BAY	N bottle	23/8/2014
LAMBERTS BAY	S bottle	24/6/2014
LAMBERTS BAY	S bottle	23/8/2014
LAMBERTS BAY	WSW bottle	24/6/2014
LAMBERTS BAY	WSW bottle	23/8/2014
LAMBERTS BAY	WNW bottle	13/5/2014
LAMBERTS BAY	WNW bottle	24/6/2014
LAMBERTS BAY	WNW bottle	31/7/2014
LAMBERTS BAY	WNW bottle	23/8/2014
LAMBERTS BAY	ENE bottle	24/6/2014
LAMBERTS BAY	ENE bottle	31/7/2014
AVONTUUR	Tank	Dec 2009
AVONTUUR	Tank	13/1/2010
AVONTUUR	Tank	21/5/2012

6.2 RESULTS: WATER QUALITY AT AVONTUUR AND LAMBERTS BAY

Tables 6.2 and 6.3 reflect the average physical and chemical properties of the water collected at the Avontuur and Lamberts Bay experimental sites, as well as the trace element composition of the samples, respectively. Full data sets of the original data are provided in Appendices 6.1 and 6.2.

The concentration of cations is in the following order: Ca^{2+} > Na^{+} > Mg^{2+} and > K^{+} for Lamberts Bay and Na^{+} > $Mg^{2+>}$ Ca^{2+} > K^{+} for Avontuur, while the anions are predominantly chloride (Cl^{-}) at both sites (Table 6.2). The only trace elements that exceed 10 ppb are Cr, Zn, Sr, Br and NH_4 at Lamberts Bay and Mn, Zn, Sr and Br at Avontuur (Table 6.3).

Table 6.2: Physical and chemical properties of water from FWCS

	pH (5-9.7)	pHs	SAR	EC (mS/m)	F (<1.5)	NO_2 (<0.9)
Ave LB	6.89	9.09	0.63	15.50	0.24	0.00
Ave Avontuur	6.60	9.95	2.18	20.33	0.03	0.07
	NO_3(<11)	**Cl(<300)**	**SO_4(<500)**	**PO_4**	**CO_3**	**HCO_3**
Ave LB	0.66	32.30	2.96	2.24	0.00	34.16
Ave Avontuur	9.04	45.24	10.11	0.12	0.00	12.20
	Na (<200)	**K (<50)**	**Ca (<150)**	**Mg (<70)**	**B**	**TDS (<1200)**
Ave LB	8.31	2.20	8.69	4.04	0.05	77.93
Ave Avontuur	25.05	1.10	2.89	3.23	0.06	102.57
Values in brackets: SANS 241:2011 standards for Drinking Water						

Table 6.3: Concentration of trace elements at Lamberts Bay and Avontuur

SUMMARY TRACE ELEMENTS (ppb)					
Element	**Lamberts Bay**	**Avontuur**	**Element**	**Lamberts Bay**	**Avontuur**
Li	1.25	0.6	**Ba**	0.76	5.91
Be	0.01	0.0	**W**	0.16	0.00
Ti	1.60	0.0	**Pt**	0.00	0.00
V (<200)	6.20	4.3	**Hg (6)**	0.00	0.00
Cr (<100)	24.27	0.5	**Tl**	0.00	0.00
Mn	0.00	44.9	**Pb (<20)**	0.77	0.00
Co	0.00	0.3	**Bi**	0.00	0.00
Ni	0.00	0.0	**U (<15)**	0.03	0.00
Cu	4.05	0.1	**Br**	40.09	40.82
Zn	10.48	627.5	**B**	8.51	0.00
As	1.24	0.0	**La**	0.08	0.00
Se	1.91	1.6	**I**	6.81	6.94
Rb	1.21	0.9	**Fe (mg/l)**	0.06	0.05
Sr	46.01	44.6	**NH4 (mg/l)**	14.37	-
Mo	0.23	0.0	**Si (mg/l)**	0.42	-
Cd (<5)	0.00	0.0	**Al (mg/l)**	0.08	0.07
Sn	0.00	0.0	**S (mg/l)**	-	7.20
Sb (<20)	0.06	0.1	**E coli**	neg	neg
Te	0.00	0.2	**Coliform**	0	0
Cs	0.00	0.0	**Tot bact**	640	>3000
Values in brackets: SANS 241:2011 standards for Drinking Water					

The presence of Zn and Cr probably originate from the system itself since some parts of the FWCS was galvanised whereas South African soils appear to be high in Sr. Avontuur is close to the Swartberg – renowned for its black colour due to the presence of manganese-rich rocks. The Sr and Mn ions are thus probably due to dust while Br (and I) are likely to be of maritime origin. The role of the ocean and continent in the mineral composition of the water samples are discussed in greater details in Section 6.3.

The pH of both samples is near-neutral and fall within the South African National Standards for drinking water (SANS 241:2011) recommended values of 5-9.7 set for domestic water use. Indeed, all of the guidelines for domestic water quality are met in samples collected from both sites. This makes the water eminently suitable for human and animal consumption. The very low TDS values of 77.9 and 102.6 at Lamberts Bay and Avontuur, respectively, attest to the purity of the water. The high quality of the water is further confirmed by the lack of harmful bacteria such as *E.coli* and other coliforms in the water. The presence of heterotrophic bacteria is not uncommon in water that is exposed to the atmosphere and is not a cause for concern.

Assays conducted by van Zijl and Aneck-Hahn in 2012 to determine the presence of EDs in the water at Avontuur (Appendix C), showed no estrogenic activity in the sample using the YES assay. Slight cytotoxicity was observed in ten times and higher concentrations of the sample. It is important to note that cytotoxicity could mask estrogenic activity if it is present in the sample. No estrogenic or anti-estrogenic activity was observed in the T47D-KBluc assay" (Van Zijl and Aneck-Hahn, 2012). However, continuous testing of samples should be undertaken to ensure that there is no change in status of the water.

In contrast to the high degree of potability of the water, the relatively high pHs values would translate to a Langelier Stability Index (Box 6.1) value of between +2 and +3 at the two sites, indicating a high probability of scaling.

Box 6.1 The Langelier Stability Index (LSI)

The Langelier Stability Index is a calculated number used to predict the calcium carbonate stability of water. It indicates whether the water will precipitate, dissolve, or be in equilibrium with CaCO3. In 1936, Wilfred Langelier developed a method for predicting the pH at which water is saturated with CaCO3 (called pHs).

The LSI = pH (measured) – pHs.

For LSI > 0, water is super saturated and tends to precipitate a scale layer of $CaCO_3$. For LSI = 1 (I.e. -0.5 - +0.5) water is saturated with $CaCO_3$. No scale is precipitated or dissolved. For LSI < 0 water is under saturated and tends to dissolve solid $CaCO_3$, i.e. corrosive. LSI of < +1 and > -1 has relatively low corrosion impact on metallic compounds.[Wikipedia accessed 25/12/2014]

In addition, the relatively high Sodium Adsorption Ratio (SAR) (Box 6.2) at Avontuur also mitigates against its use for irrigating plants whereas this does not appear to present a problem with the water collected at Lamberts Bay.

Box 6.2 The Sodium Adsorption Ratio (SAR)

SAR is a measure of the suitability of water for use in agricultural irrigation, as determined by the solids dissolved in water. SAR = $Na^+ / \sqrt{½(Ca^{2+} + Mg^{2+})}$ where Na, Ca and Mg are in milli-equivalents/litre. In general, the higher the SAR, the less suitable the water is for irrigation. Continuous irrigation with water with SAR values of >2 could induce sodic soil conditions whereby the Ca and Mg are replaced by Na. This will cause a decrease in the ability of the soil to form stable aggregates and a loss of soil structure and tilth.

6.3 SOURCES OF CHEMICAL CONSTITUENTS OF WATER

In order to determine the possible origin of the various macro-constituents of the samples, the Enrichment Factor (EF) as proposed by Ahmed et al. (1990) and given in Eckardt and Schemenauer (1998) was calculated. The basic assumption here is that if deposition on the FWCS was due to fog originating over the ocean, the chemical composition of the deposited aerosols should reflect the composition of sea water. Using Na^+ as the sea salt tracer element, the ratio of the element (X) (where X = Ca^{2+}, Mg^{2+}, etc.) to Na^+ in the water sample to that occurring in the ocean should thus give an indication of enhancement due to non-maritime aerosols. The following equation is used to determine the EF:

$$\mathrm{EF_{Na}(X)} = \frac{\left(\frac{\mathrm{X}}{\mathrm{Na}}\right)_{\mathrm{fog}}}{\left(\frac{\mathrm{X}}{\mathrm{Na}}\right)_{\mathrm{sea}}} \qquad (1)$$

An EF approximating 1 indicates a purely marine origin, while ratios exceeding unity reflect enrichment from other sources. The EF can thus be used to determine the Sea Salt Fraction (SSF) and Non-Sea Salt Fractions (NSSF) of the deposited aerosols where the SSF = 100*(1/EF) and the NSSF = 100-SSF (Lekouche et al., 2011). The EF, SSF and NSSF for Lamberts Bay and Avontuur are presented in Table 6.4.

Table 6.4: sea Salt Fraction (SSF) and Non-Sea Salt Fraction (NSSF) of deposited aerosols collected on fog nets at the Lamberts Bay (LB) and Avontuur (Av) experimental sites.

Element (X)	Sea salt ratio*	Aerosol ratio at Lamberts Bay	EF (LB)	SSF(%) (LB)	NSSF(%) (LB)	Aerosol ratio at Avontuur	EF (Av)	SSF(%) (Av)	NSSF(%) (Av)
Ca^{2+}	0.044	1.05	23.75	4.21	95.79	0.17	3.89	25.67	74.33
Mg^{2+}	0.227	0.49	2.14	46.75	53.25	0.13	0.57	176.07	-76.07
K^+	0.022	0.26	12.03	8.31	91.69	0.04	2.00	50.11	49.89
Cl-	1.166	3.89	3.33	30.00	70.00	1.81	1.55	64.58	35.42
*Sea salt ratios as given by Kennish (1989) In: Lekouche *et al*. (2011)									

The concentration of all four elements shown in Table 6.4 for Lamberts Bay, are higher in the water sample than would be expected from a solely maritime origin. This applies especially to the Ca and K ions, where the NSSF exceeds 90%. A relatively greater proportion of the Cl and Mg ions originate from the ocean but with some enrichment from other sources. Aerosols deposited during fog events that are associated with an approaching cold front or the proximity of the South Atlantic Anticyclone (SAA), will clearly be of marine origin, while those associated with Coastal Lows (CLs) might contain some aerosols of continental origin. A large proportion of the NSSF fractions of Ca and K ions were probably due to contamination from dust deposited on the nets. This explanation is plausible since the FWCS is located on a sandy plain with plentiful remnants of sea shells interspersed among the sand grains. It is clear that if a FWCS is to be used to supply water to the community, some technique will be required to allow the first flush of dust-laden water to be drained away.

It is interesting to note that the SSFs of all four aerosol constituents (Ca, Mg, K and Cl) at Avontuur exceed those at Lamberts Bay. At first glance, this appears to be contrary to expectation in view of the distance from the sea of Avontuur in comparison to that of the Lamberts Bay site. However, it must be kept in mind that the fog occurring at Avontuur originates from maritime air from the Southern Indian Ocean which is forced to ascend the escarpment by onshore breezes. Clearly, all of the Mg and a large proportion of the K and Cl ions originate from the sea. As at Lamberts Bay, the Ca aerosol component in water collected at Avontuur, probably arises from dust.

6.4 THE ROLE OF SYNOPTIC CONDITIONS ON THE COMPOSITION OF WATER AT LAMBERTS BAY

Since it was not logistically possible to collect water samples on a wet-event or daily basis, the instrument depicted in Figure 2.22 was used to collect samples associated with different wind directions over a period of time. It was assumed that wind direction is a function of synoptic conditions.

The synoptic conditions that could be responsible for continental fog at Lamberts Bay were identified and discussed in terms of the associated wind directions in Section 3.2.1.

The predominance of northerly and west-north-westerly liquid water-bearing winds is reflected by the frequency during which water was collected from the relevant collecting bottles. As a matter of fact there was water present in the north and west-north-west containers on all four collecting dates (Table 6.1), while water was found in the south and west-south-west containers on two of the four occasions. Only a small amount of water was present in the east-north-east container on one of these collection dates.

The average concentrations of macro- and trace elements are given in Tables 6.5 and 6.7, respectively while the sea salt fraction of four aerosols are presented in Table 6.6. No water was collected from winds originating in the ESE.

Table 6.5 Physical and chemical properties of water samples associated with different wind directions.

	pH	pHs	SAR	EC	F	NO2	NO3	Cl	SO4	PO4	CO3	HCO3	alk	Na	K	Ca	Mg	B	TDS
				(mS/m)															
Ave S	7.2	8.5	9.7	296.5	0.3	12.6	24.8	223.4	47	1	0	43.0	35.3	537.0	28.8	45.5	72.4	0.1	1015.0
Ave N	6.5	8.5	10.6	280.5	0.4	18.7	41.6	808.8	133	1	0	30.0	24.6	464.0	21.5	46.2	57.5	0.1	1607.2
Ave WSW	6.9	8.5	10.1	288.5	0.3	15.6	33.2	516.1	90	1	0	36.5	29.9	500.5	25.1	45.8	64.9	0.1	1311.1
ENE	7.5	8.8	4.2	68.0	0.2	0.8	17.2	218.8	25	0	0	31.7	26.0	97.9	4.8	18.7	13.9	0.1	413.1
Ave WNW	6.8	8.3	13.3	371.0	1.0	9.7	23.4	820.7	139	1	0	49.1	40.3	664.1	30.4	52.3	82.0	0.1	1847.2

It is noticeable that the northern and west-north-western winds have the highest loading of dissolved solids, followed by water associated with west-south-westerly winds (Table 6.5). The dissolved solid concentration is mostly due to the high concentrations of Na and Cl ions (and Mg to a lesser extent) in this water which seems to indicate its marine origin, probably associated with rainfall and prefrontal fog. This is borne out by calculation of the SSFs (Table 6.6). All the Mg ions in these moisture-bearing winds as well as the largest proportion of Cl are of marine origin. The Ca-fraction of the minerals in water collected during west-north-westerly winds also originates from the sea. For water advected from all directions except west-south-west, around half of the K-containing aerosols are also of oceanic origin. Interestingly, all of the Cl ions in the southerly wind originate from the sea, while between 30% and 50% of the Cl in water associated with north, west-south-west and east-north-east wind has a non-maritime origin. The water collected during east-north-east wind conditions has by far the lowest concentration of dissolved ions and, except for Mg, all are of continental origin. This clearly indicates that dust forms the condensation nuclei on which moisture is deposited when the dust-laden air circulating around a Coastal Low passes over the South Atlantic Ocean and then condenses into fog when advected over the cold Benguela-Upwelling region (Olivier and Stockton, 1989).

Table 6.6: Sea salt fraction of water originating from various directions at Lamberts Bay.

	SSF Ca^{2+}	SSF Mg^{2+}	SSF K^{+}	SSF Cl^{-}
Ave S	34.15	168.46	41.01	280.26
Ave N	45.34	183.31	47.51	66.89
Ave WSW	37.20	172.27	37.70	63.84
Ave WNW	57.01	183.89	48.10	94.35
ENE	23.06	159.78	45.25	52.18
Highlighted values are predominantly of marine origin (i.e.>50%).				

Table 6.7: Summary of trace elements associated with wind directions at Lamberts Bay

Element	N ave	S ave	WNW ave	ENE	WSW ave	Element	N ave	S ave	WNW ave	ENE	WSW ave
Li	7.43	7.82	7.48	1.26	4.39	Te	0.01	0.04	0.00	0.00	0.01
Be	0.02	0.02	0.03	0.01	0.05	Cs	0.00	0.00	0.01	0.01	0.03
Ti	3.87	5.42	2.94	0.28	18.64	Ba	17.41	16.71	20.17	11.66	15.14
V	9.10	10.31	6.30	0.96	3.95	W	0.67	1.06	0.61	0.15	0.49
Cr	1.40	2.40	1.19	0.67	1.67	Pt	0.03	0.04	0.03	0.00	0.04
Mn	144.12	87.15	136.14	0.55	163.13	Hg	1.43	2.49	0.91	0.14	0.81
Co	0.92	0.78	0.89	0.02	0.80	Tl	0.05	0.16	0.04	0.02	0.04
Ni	4.22	4.32	4.26	0.39	5.11	Pb	0.49	0.55	0.75	0.13	1.81
Cu	117.58	227.60	80.04	41.76	88.67	Bi	0.01	0.01	0.01	0.02	0.01
Zn	842.50	161.80	396.45	85.48	1179.33	U	0.07	0.07	0.05	0.01	0.07
As	4.61	6.78	5.06	0.48	1.96	Br	2868.67	4393.00	4597.50		1033.00
Se	14.90	21.03	17.26	2.18	5.85	B	33.59	37.95	33.30		19.92
Rb	3.71	4.94	5.69	0.59	3.25	La	0.09	0.11	0.07		0.07
Sr	209.27	194.25	28.64	56.68	138.75	I	82.36	67.54	94.87		18.35
Mo	1.30	1.65	0.86	0.29	0.77	Fe mg/l	0.04	0.06	0.02		0.01
Cd	0.44	0.24	0.87	0.08	0.35	NH4	1.71	4.67	0.17		0.05
Sn	0.16	5.42	0.05	0.31	0.05	Si	0.77	0.52	0.52		0.48
Sb	0.46	0.56	0.38	0.08	0.51	Al	0.14	0.10	0.11		0.11
						sum Li-U	1386.19	763.63	717.12	204.22	1635.67
						sum Li-Al	4373.55	5267.55	9641.11		2707.66

	Pearsons Correlation Coeff.	t-test
N vs S	0.97	0.60
N vs WNW	0.98	0.56
N vs ENE	0.89	0.14
N vs WSW	0.83	0.38
S vs WNW	0.99	0.66
S vs ENE	0.62	0.03
S vs WSW	0.67	0.47
WNW vs ENE	0.80	0.14
WNW vs WSW	0.70	0.46
ENE vs WSW	0.83	0.20

There appears to be little difference in the composition of trace elements in water originating from the north, south and west-north-west, while west-north-west water is most similar in composition to that associated with southerly and east-north-easterly winds. The mineral load in water associated with northerly, southerly and west-north-westerly winds is apparently due to the heavy load of Br and I (Table 6.7). Both occur in high concentrations in sea water, and this result, once again, reflects the influence of the sea on the chemical composition of water at Lamberts Bay. The largest concentration of trace elements in water associated with west-south-westerly winds, are Zn and Ti. The origin of these is not known since the anthropogenic activities do not differ in different the areas surrounding the site. The relatively low trace element load in waters originating from the east-north-east (and associated with Coastal Lows) corresponds to that for macro-elements, and contrary to expectations, makes this water the least contaminated – despite the assumed dust-based condensation nuclei forming the core of the fog droplets. Since rain does not originate from the east-north-east at Lamberts Bay, it appears that fog water may be less contaminated than rainwater. However, considerable more detailed research is required to confirm this finding.

CHAPTER 7: POTENTIAL IMPACT OF FOG WATER COLLECTION SYSTEMS ON THE ENVIRONMENT

7.1 POTENTIAL IMPACTS

The research discussed in this chapter was conducted on the triangular FWCS at Avontuur during 2013 and 2014. The Avontuur experimental site is located on the saddle linking the Zondachsberg with the Tsitsikamma Mountains at 33.7436°S, 23.1808°E and altitude: 1 040 m AMSL. Details of the design and structure of the system can be found in Chapter 2 (Figure 2.4).

The potential impacts on the environment, discussed in this chapter, refer to those typically contained in an environmental impact report and thus comprise a description and assessment of the significance of any environmental impacts, including cumulative impacts that may occur as a result of the undertaking of the activity or identified alternatives or as a result of any construction, erection or decommissioning associated with the undertaking of the activity.

A number of activities conducted during the erection and maintenance of the FWCS at Avontuur might have an impact on the environment. These are illustrated and described in great detail in Chapter 2 and include site preparation, erection of the system and maintenance of the completed system. The most important of these that may have relevance to and Environmental Impact Assessment (EIA) are mentioned here.

- After selection of the site, all Renosterbos was cut and removed from the area to be occupied by the FWCS. This was to facilitate access to the site and as protection against fire.
- Anchor and pole holes were dug using a backacter, then squared and cleared by hand.
- Where necessary, anchors fittings were chemically fixed to the rock
- Manual labour was used to slip the poles into the holes and to steady the poles while raising them to an upright position. A ladder section was used to keep the pole at the required angle to provide stability and as a safety measure. With the pole halfway into the hole and at a safe angle the pole to pole top cable was clamped to a tractor. A pole was lifted by moving it a few centimetres at a time with the tractor. This entire process was repeated until the poles were vertical in the holes.
- The panels were fitted so as to allow cattle and other animals to pass underneath the nets.

- Water from each net was channelled through the low flow meter to the 5 000 litre water storage tank.

The possible impacts of different stages of the project are shown in Tables 7.1 and 7.2.

Table 7.1: Identification and assessment of cumulative and indirect environmental impacts, as well as interactions, at the Avontuur experimental site.

	Soils and Geology	Surface and groundwater	Air and climate	Flora or fauna	Planned land use	Building / structure	Land-scape/ Aesthetics	Cultural/ Heritage	Health/ smell noise vibration	Quality of life / recreation	Economic life and employment	Use of natural resources
Preparation												
Transport	+	-	+	+	-	-	-	-	+	-	-	-
Clearing of site	-	-	-	+	+	-	-	-	-	-	-	-
Digging holes	+	-	-	+	-	-	-	-	-	-	-	-
Fix anchors	-	-	-	-	-	-	-	-	+	-	-	-
Construction												
Transport	-	-	+	+	-	-	-	-	-	-	-	-
Erection of nets	-	-	-	+	-	-	-	-	+accident risk	-	-	-
Install Jo-jo tanks	-	-	-	+	-	-	+	-	-	-	-	-
Dig trench fog nets to tanks	-	-	-	+	-	-	-	-	-	-	-	-
Surface structure	-	-	+	+	-	-	+	-	-	-	-	-
Operation/maintenance												
Transport	+	-	-	-	-	-	-	-	-	-	-	-
FWH IMPACT	**H**	**L**	**H**	**H**	**L**	**L**	**M**	**L**	**H (temporary)**	**L**	**L**	**L**

In Table 7.1, (+) indicates aspects in the project assumed to have an impact on the environment, while (-) indicates that a significant environmental impact is not likely to arise. At the bottom of Table 7.1, High impact: H ≥3(+) per column; Medium impact: M=2(+) per column; Low impact L ≤1(+) per column.

Table 7.2: Checklist for identifying activities and possible further environmental impact of FWHSs at the Avontuur experimental site after construction and establishment of the structures and equipment.

	Soils and Geology	Surface and groundwater	Air and climate	Flora or fauna	Planned land use	Building / structure	Land-scape/ Aesthetics	Cultural/ Heritage	Health/ smell noise vibration	Quality of life / recreation	Economic life and employment	Use of natural resources
onstruction												
Transport	-	-	+	+	-	-	-	-	-	-	-	-
Erection of nets	-	-	-	+	-	-	-	-	+ accident risk	-	-	-
Install Jo-jo tanks	-	-	-	+	-	-	+	-	-	-	-	-
Dig trench fog nets to tanks	-	-	-	+	-	-	-	-	-	-	-	-
Surface structure	-	-	+	+	-	-	+	-	-	-	-	-
Operation/ maintenance												
Transport	+	-	-	-	-	-	-	-	-	-	-	-
Fire hazard management	+	-	-	+	-	-	-	-	+ accident risk	-	-	-
FWH IMPACT	**M**	**L**	**M**	**H**	**L**	**L**	**M**	**L**	**M(temporary)**	**L**	**L**	**L**

In Table 7.2, (+) indicates which aspects the project is assumed to impact the environment, while (-) indicates that a significant impact is not likely to arise. At the bottom of Table 7.2, High impact: H ≥3(+) per column; Medium impact: M=2(+) per column; Low impact L ≤1(+) per column.

Environmental aspects that have been identified for being influenced by a fog water collection project, are:

- Land use;
- Bulk water supply: Water collection tanks >250 m^2;
- Micro-climate:
  - Disruption to wind flow patterns;
  - Shadow effect;
- Ecology:
  - Fragmentation of habitat;
  - Flora;
- Noise/ traffic management during construction phase;
- Accident risk;
- Aesthetics.

7.2 ASSESSMENT OF EFFECTS

From the information given above, the following legislations seem to apply:

- National Environmental Management Act (NEMA), 1998 (Act No. 107 of 1998);
- The Mountain Catchment Areas Act, 1970 (Act No. 63 of 1970);
- National Environmental Management: Biodiversity Act (Act No. 10 of 2004);
- Occupational Health and Safety act No. 85 of 1993: Occupational Health and Safety act as amended No. 81 of 1993.

In terms of section 24(2)(a) of the NEMA, the following activities may not commence without an environmental authorisation from a competent authority.

7.2.1 Land use

Probably the most important property of South African mountains is their function as natural drainage areas. Their capacity for rainfall and mist interception, and eventual release of water into rivers, is of great importance to a relatively arid country such as South Africa. Runoff from mountain catchments is the main source of most of the Western Cape's rivers. To yield the maximum quantity of water of the highest possible quality on the most dependable basis without reducing plant cover and the variety of species, optimal management of mountain catchment areas is necessary. The Mountain Catchment Areas Act, 1970 (Act No. 63 of 1970) was promulgated to provide for the conservation, use, management and control of land situated in declared mountain catchment areas (Fuggle and Rabie, 1992).

In terms of the Act any (private) area of which the water yield is of great importance may be declared a mountain catchment area. Mountain catchment areas are managed by means of management guidelines relating to conservation, use and control of land, and vegetation within the area (Fuggle and Rabie, 1992). Two mountain catchment areas have been declared as conservation areas, either entirely or partly, in the Eden District Municipality (DMA), namely (1) the Uniondale / Kammanassie Mountain Catchment Area and (2) the De Rust / Swartberg Mountain Catchment Area.

As indicated in Figure 7.1, the Avontuur experimental fog water harvesting site does not fall within these mountain catchment conservation areas.

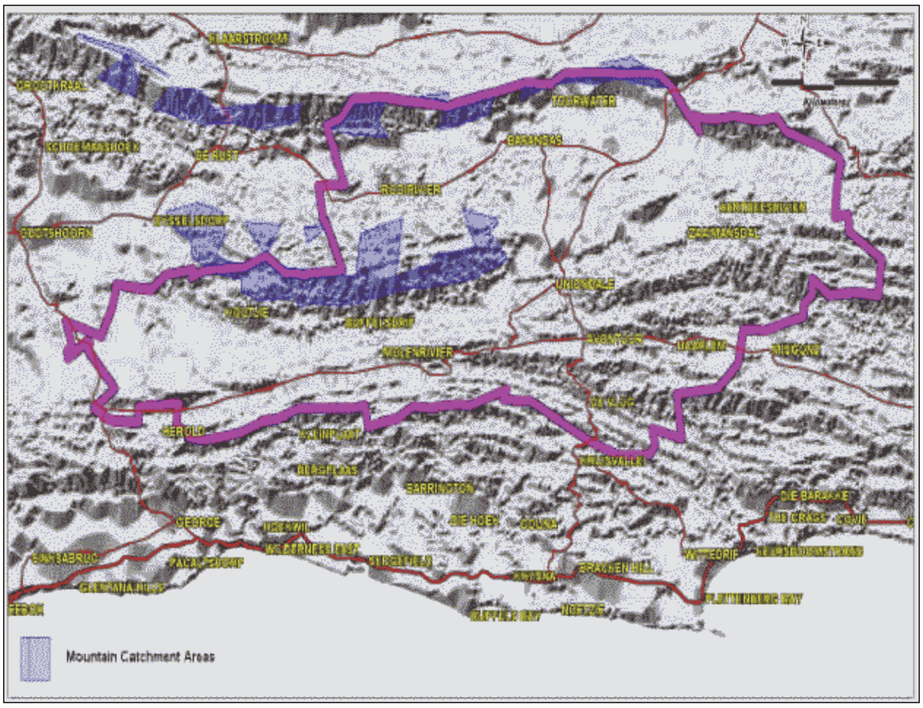

Figure 7.1: *The Mountain Catchment area (Eden District Management Area), indicated by a purple boundary, in which the Avontuur experimental site is located (Source: Eden District Management Area Spatial Development Framework, 2004).*

7.2.2 Bulk water supply

Because of low water yields, the impact on bulk water supply is not applicable. A single triangular FWCS with a surface area of around 90 m^2 delivered, on average, an amount of around 50 ℓ.day^{-1}, which translates to an average amount of 0.56 ℓ.m^{-2}.day^{-1}. Moreover, the capacity of the water storage tank is only 5 000 litres. This is far below the 250 m^3 as stipulated for bulk water flow in the Environmental Impact Assessment Regulations Listing Notice 3 of 2010. However, if a 'fog water farm' is to be established at an ideal site where fog water collection rates reach 10 ℓ.m^{-2}.day^{-1}, water from at least 25 000 m^2 should be stored in order to reach the capacity of 250 m^3. Only then would a comprehensive Environmental Impact Assessment be essential.

7.2.3 Microclimate

The term microclimate referrers to micro-scale (as small as a few m^2) characteristics of the surrounding climate. Contributing factor to microclimate may be the slope and aspect of an mountainous area, temperature, wind speed and direction, relative humidity and solar irradiance.

The changes in the micro-climate may impact on the habitat components and processes, possibly causing shifts in the composition of the animal and plant communities. Such shifts themselves may influence a larger habitat and the function of the ecological system.

7.2.3.1 Micro-scale changes in wind flow patterns

When wind encounters a barrier, air flow patterns are modified. According to Oke (1987), this modification begins before the air reaches the barrier. Immediately above the barrier, the air is displaced up and over the barrier causing acceleration. Downwind of the barrier, the air again diverges and deceleration occurs. A weak high pressure forms on the windward side of an obstacle, while the reverse occurs on the leeward side. The latter cause winds to curl inwards in a clockwise motion in the Southern Hemisphere – in both the horizontal and vertical planes. Downwind disruption in flow patterns may occur up to 10 to 15 times the height of the barrier. As the angle of incident wind deviates from perpendicular, the area of shelter is proportionally reduced until with parallel flow the shelter-effect is negligible. Moreover, wind speeds near the ends of a barrier experience increased wind speeds, and probably greater turbulence. Figure 7.2 shows displacement zones in wind flow patters associated with solid barriers.

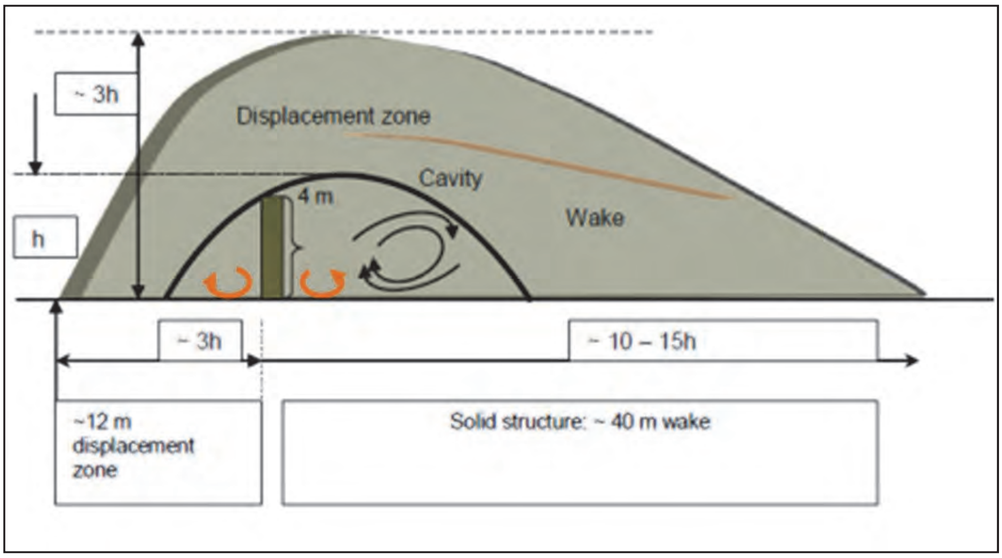

Figure 7.2: *The displacement zone in wind patterns (shaded) as caused by a solid structure of 4 meters in height (modified from Oke 1987, 243).*

However, fog nets are not solid barriers but are permeable and allow wind to move through. Oke (1987) indicates that in such a case, minimal disruption in wind flow patterns take place, with a cushioning effect of wind speeds on the downwind side of the obstacle. Bresci (2001) described the patterns in wind speed upwind, above, below and behind a standard fog water collector in Chile. She found that the presence of the fog collector is felt up to a downwind distance equal to the height of the collector, and that the extent of deceleration is dependent upon the incident wind speed. Low velocity winds are only slightly influenced by the presence of the collector, whereas higher wind speeds are affected to a greater extent.

Field data on wind speed and direction were collected at the Avontuur experimental site during the period 1 Jan 2012 to 31 Dec 2012, using fixed cup anemometers connected to data loggers. These were installed at the positions AWS1 and AWS2, as shown in Figure 2.4. Continuous data were collected for wind speed and direction and logged at hourly intervals. Due to the large amount of data, this report focuses on results for March, June, September and December 2012 in an attempt to elucidate seasonal trends. To determine the type of relationship between undisrupted wind speed coming from outside towards the net (AWS2), and the wind inside the triangular FWCS (AWS1), the best fit was determined for linear, power and logarithmic functions.

Data were divided into different wind speed classes, ranging from 0 to 12 $m.s^{-1}$. Deviations in wind speed (wind speed out – wind speed in), as well as ratios of wind speed-in to wind speed-out were calculated. Negative deviations and ratios of < 1 imply a deceleration in wind speed caused by the fog net. The possible impact of net wetness on wind flow patterns was determined by dividing the data sets into hours without fog or rain (*dry*) (zero on T3 as well as on the rain gauge in Figure 2.4); hours with fog alone (*fog only*) (values on T3 but zero on rain gauge in Figure 2.4); hours with rain and fog (*rain & fog*) (values on both T3 and rain gauge in Figure 2.4); and hours with rain alone (*rain only*) (no values on T3, but rain collected in rain gauge in Figure 2.4). Note that these definitions for distinguishing between rain and fog events were also discussed in Chapter 5.

<u>Relationship between undisturbed and disturbed wind speed patterns</u>

Correlations between wind speed outside the FWCS and wind speeds within the triangular FWCS yielded a Pearson's Linear Correlation Coefficient of $r = 0.809$, $N= 348$ hours, for March 2012. This is highly statistically significant at the $p = 0.005$ level. The total deviation in wind speed (wind speed-out minus wind speed-in) for this period was found to be 0. However, it is possible that the direction of incident wind may affect the extent of deviation inside the structure. It should be kept in mind that wind speed data were only available for the wind speed-out and wind speed-in datasets, and thus the impact of net 1 alone (the south-facing net in Figure 2.4) could be determined. For this reason, the calculations were limited to winds with a southerly component. It was assumed that any disruptions in wind flow due to nets 2 and 3 would be minimal.

Figure 7.3 shows the strongest relationship between wind speed-out and wind speed-in as occurring during *dry, fog only, rain only* and *rain & fog* conditions.

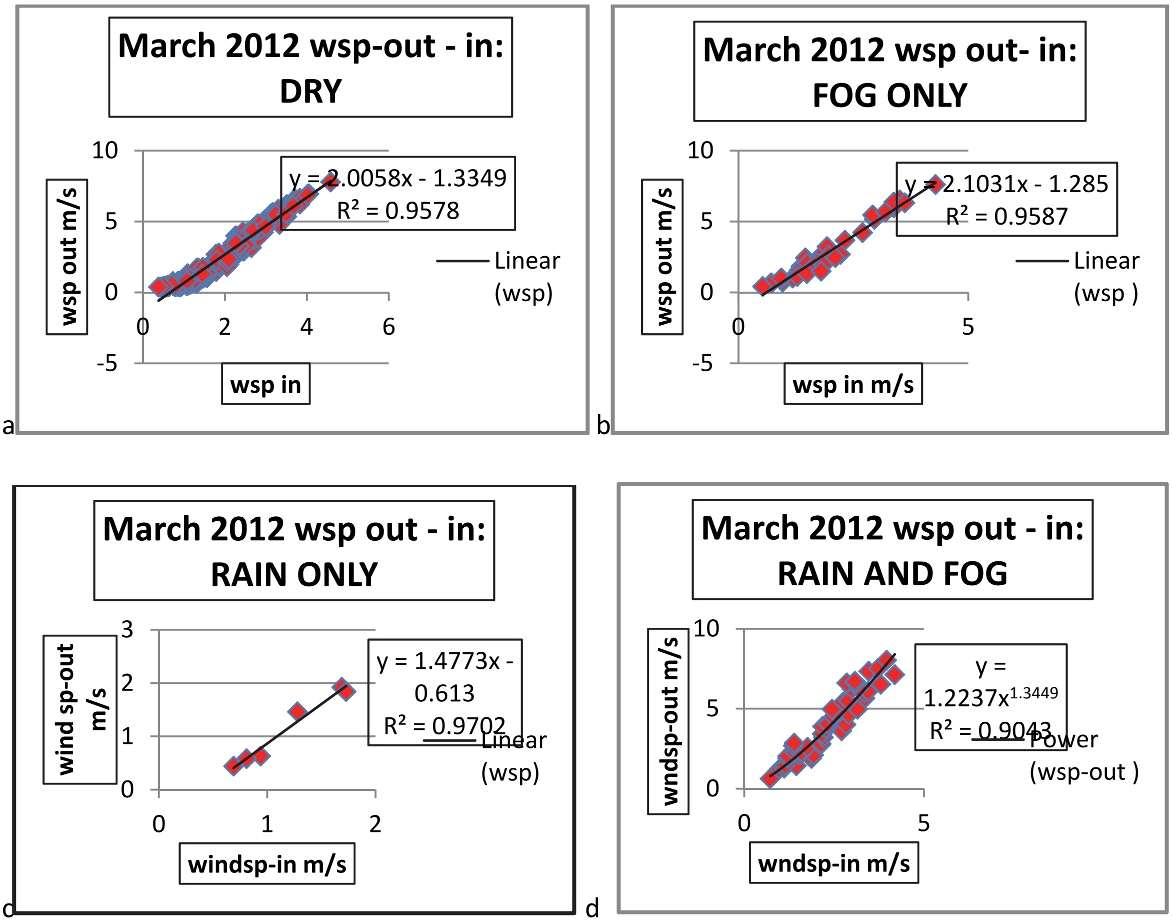

Figure 7.3: *Relationships between wind speed outside and wind speed inside the Fog Water Collection System (FWCS) at the Avontuur experimental site during a) dry; b) fog only; c) rain only and d) rain & fog conditions.*

Pearson's linear correlation coefficient (r) for *dry*, *fog only* and *rain only* conditions was found to be 0.98; 0.98 and 0.99, respectively. Although a power function best describes the relationship between wind speed outside and inside the FWCS during *rain & fog* conditions, Pearson's linear correlation coefficient was found to be 0.95 which is still highly statistically significant.

In Table 7.3, the r-values as well as mean deviations in wind speed between the anemometer outside and inside, for *dry*, *fog only*, *rain & fog* and *rain only* during March, June, September and December 2012, are listed.

Table 7.3: Mean deviation in wind speed and Pearson linear correlation coefficients (r) between winds that appeared outside and inside of the FWHS at the Avontuur experimental site.

Southerly winds only	Conditions	Pearson's correlation coefficient (r)	Sample size: N (hours)	Mean deviation in wind speed (out-in) ($m.s^{-1}$)	Mean monthly deviation in wind speeds ($m.s^{-1}$)
March	*Dry*	0.9786	371	0.50	
	Rain alone	0.9850	5	-0.09	
	Fog alone	0.9791	43	0.82	
	Rain & fog	0.9453	51	1.63	
			N= 470		***0.65***
June	*Dry*	0.9201	83	0.10	
	Rain alone	0.974	7	1.59	
	Fog alone	0.92	16	0.83	
	Rain & fog	0.895	28	1.23	
			N=134		***0.50***
September	*Dry*	0.989	283	1.64	
	Rain alone	0.97	6	1.76	
	Fog alone	0.93	61	1.80	
	Rain & fog	0.95	27	2.06	
			N=377		***1.70***
December	*Dry*	0.9966	328	1.75	
	Rain alone	0.9385	4	0.64	
	Fog alone	0.956	99	1.96	
	Rain & fog	0.85	48	2.59	
			N=479		***1.87***

From Table 7.3 it becomes clear that there is a strong linear relationship between wind speeds outside and within the FWCS throughout the year.

Deviation in wind speeds

In general, it was found that the fog net has a buffering effect on wind speeds. The fog net affects speed of southerly winds by decreasing the wind by an average of around 1.1 $m.s^{-1}$ during the four months considered in the analyses. This varies from month to month, with greatest wind breaking effect of 1.87 $m.s^{-1}$ that appeared during December 2012.

Impact of net wetness

In general, the buffering effect of the net is found to be least during *dry* conditions (0.10 to 1.75 $m.s^{-1}$). When the net has been thoroughly wetted by fog and rain, it has a greater impact on wind speed, reducing it by between 1.23 and 2.59 $m.s^{-1}$. Thus, the wetter the net the greater its buffering impact on wind the speed on the downwind side of the net.

Overall: a *dry* net decreases wind speed by 1.16 $m.s^{-1}$; *rain alone* net by 1.12 $m.s^{-1}$; *fog alone* net by 1.61; and *rain & fog* net by 1.93 $m.s^{-1}$.

Impact of incident wind speed on the extent of acceleration/deceleration

To indicate the impact of wind speed on the buffering effect, the ratio between wind speeds in/out were calculated for the wind speed classes: 0-1.99 $m.s^{-1}$; 2-3.99 $m.s^{-1}$; 4-5.99 $m.s^{-1}$ etc. These are shown in Table 7.4. Ratios of 1 indicate no change in wind speed; a ratio of >1 indicates acceleration inside the FWCS, while values of < 1 indicate a buffering effect with wind speeds inside the system lower than incident wind speeds.

Table 7.4: Wind speed ratio inside the triangular Fog Water Collection System (FWCS) and outside the triangular FWCS (in/out)

MONTH	Conditions	0-1.99 $m.s^{-1}$	2-3.99 $m.s^{-1}$	4- 5.99 $m.s^{-1}$	6-7.99 $m.s^{-1}$	8-9.99 $m.s^{-1}$	10-11.99 $m.s^{-1}$	OVERALL MEAN
Mar	*Dry*	1.34	0.75	0.61	0.58			**1.03**
	Fog only	1	0.72	0.58	0.55			**0.83**
	Fog & rain	0.89	0.68	0.57	0.5			**0.64**
	Rain only	1.19	-	-	-			**1.19**
Jun	*Dry*	1.63	0.84	0.67	0.55	0.59		**1.34**
	Fog only	1.29	0.62	0.67	0.7	-		**0.96**
	Fog & rain	1.46	0.59	0.73	0.68	-	0.54	**0.85**
	Rain only	-	0.95	0.73	-	0.56		**0.74**
Sep	*Dry*	0.51	0.55	0.56	0.58	0.58		**0.55**
	Fog only	0.47	0.47	0.49	0.6	-	-	**0.48**
	Fog & rain	-	0.49	0.52	0.57	-	-	**0.52**
	Rain only	-	0.59	0.59	-	-	-	**0.59**
Dec	*Dry*	0.5	0.51	0.54	0.56	0.58	-	**0.53**
	Fog only	0.42	0.44	0.45	0.5	-	-	**0.44**
	Fog & rain	0.42	0.5	0.41	0.43	-	-	**0.44**
	Rain only	-	-	-	-	-	-	**-**

In general, most ratios in Table 7.4 have a value of < 1, indicating a buffering effect of the wind by the nets. This applies to all the results, except for very weak winds, during January and March. In general, and especially during March and June, values reflect previous findings by Oke (1987) and Bresci (2001) that the influence of the collector increases with speed of incident wind.

7.2.3.2 Micro-climatic effects of fog nets on wind direction

It is expected that, if a small low pressure forms on the leeward side of the nets, winds should break in a cyclonic (clockwise) direction. Hence immediately behind the net, wind direction should deviate to the left. However, the anemometer registering wind direction inside the triangular system was erected at least 2 m behind the nets (in the centre of the triangular space). Here, the wind direction may deviate to the right, hence giving a negative value for the deviation. Figure 7.4 attempts to explain deviation in wind direction at the triangular FWCS.

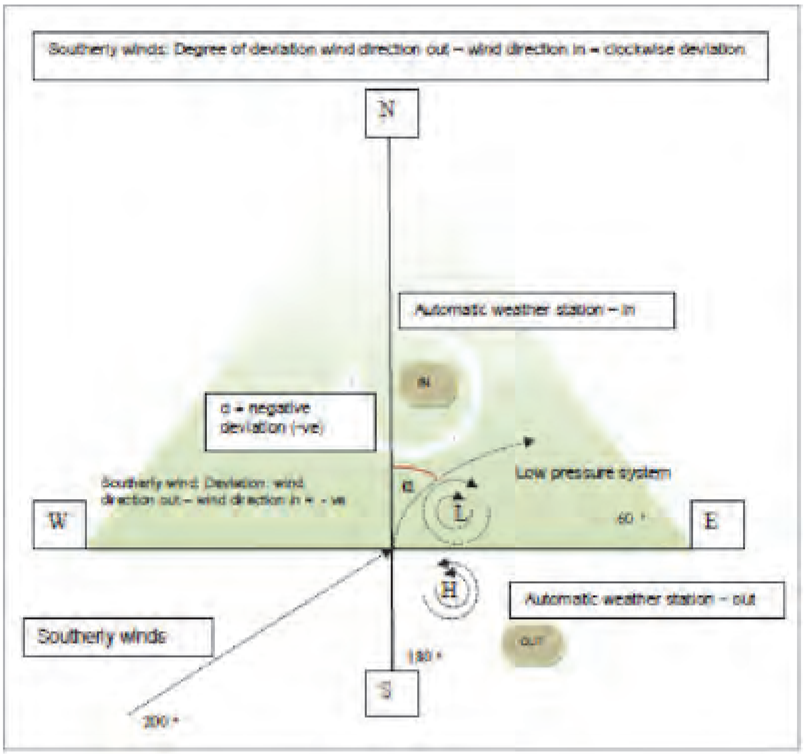

Figure 7.4: *Possible explanation for the deviation in wind direction as recorded at the Avontuur experimental site.*

Table 7.4 reflects the deviation in wind direction (in front of net Net1 in Figure 2.4 minus wind direction inside the Fog Water Collection System (FWCS)) (out-in).

Table 7.5: Monthly mean deviation in wind direction (outside net Net1 in Box 1.7 minus inside the Fog Water Collection System (FWCS)).

	March	June	September	December
Deviation in degrees	-2.43	-2.98	-0.78	-0.15

In general, the direction deviations listed in Table 7.5 are negative, as expected from the discussion above. However, scrutiny of individual hourly deviations shows a number of positive values. It is possible that factors such as the direction of incident winds and net wetness might have affected these deflections.

The results of the analyses for different incident wind directions and net wetness are given in Table 7.6.

Table 7.6: Deviation of wind directions on south facing net (wind-out minus wind-in).

Month	Conditions	Easterly	South-easterly	Southerly	South-westerly	Westerly
March	*Dry*	-6.19	-8.36	-1.64	+3	+2.25
	Fog only	-7.5	-0.67	-1	+4.5	+6
	Fog & rain	-7.0	-	2.58	-0.85	-3
	Rain only	+1	-	-2.50	-	-
June	*Dry*	-58.4	-7	-3.78	+0.88	+3.64
	Fog only	-2	0	-0.8	+6.2	-2.4
	Fog & rain	-	-	-1.6	+1.64	+7.75
	Rain only	-	-	-	+4	+4
September	*Dry*	-1.61	-13.5	-1.14	+3.43	+4.38
	Fog only	-2	-2.75	-2.68	+3	+10
	Fog & rain	-	-2	-1.8	+3.7	+3
	Rain only	+5	-	-	+5.4	-
December	*Dry*	+0.67	-1.84	-2.56	+9.1	+12.67
	Fog only	- 4.2	-3	-3.88	+8	-
	Fog & rain	-6	+1	-0.85	+1.25	+7
	Rain only	-40.2	-	-	-	-

From Table 7.6 it appears that when the winds are predominantly from the east, south-east and south, deflections are negative, as expected. However, south-westerly and westerly winds show a positive deviation in direction. It is possible that the winds from the west are almost parallel to net Net1 in Figure 2.4, but are directly incident upon net Net3. A weak low thus develops just to the inside of net Net3 (see Figure 7.4) and at the point of measurement, appears to originate from a north-easterly to easterly direction. This might explain the positive deviation encountered during winds with a westerly component.

7.2.3.3 The shading effect

It is possible the triangular FWCS might disturb the micro-climate by casting a shadow over the enclosed triangular area (as well as to the east and west of the FWCS). A shadow might affect the temperature, evaporation rate and hence the moisture regime.

Pythagoras theorem was used to determine the length of the shadow to completely 'fill' the triangular inside area of the system. If the net reached the ground, this length was found to be 8.66 m (Figure 7.5, top). The angle of solar radiation required to cast this shadow length was determine by calculating the tangent of this angle. This was found to be 8 degrees (Figure 7.5, bottom). Since the sun 'moves' at 15 degree per hour at equinox, it is estimated that the entire area within the triangle will only be in total shade for approximately 30 minutes after sunrise and 30 minutes before sunset (and assuming that nets are perpendicular to the rising and setting sun)

– assuming that the bottom of the nets touch the ground. This effect would be thus minimal since the duration of the shadow effect is short and the solar radiation intensity is small just after sunrise and before sunset.

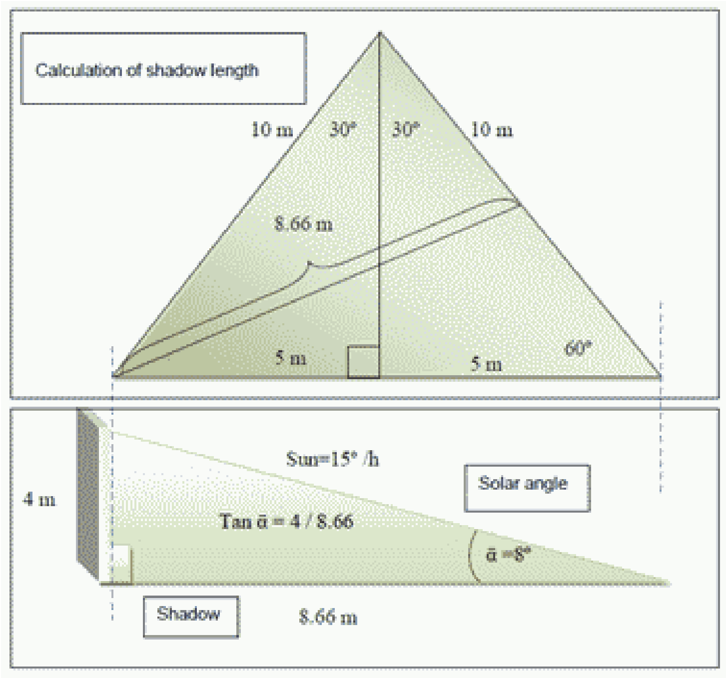

Figure 7.5: *An illustration of the shadowing effect of the triangular Fog Water Collection System (FWCS) which might block out some solar radiation.*

Areas outside the nets are affected even less since they can have a maximum of 30 minutes of shade per day.

7.2.3.4 Possible changes in the wavelength of light

The colour of the net shade cloth may also contribute to the reflection and absorption of specific wavelengths of radiation. Colour netting performs two important functions: (1) transforming direct light into scattered light and (2) selectively filtering different bands of solar radiation. It is assumed that if shading is required, pale colored materials should be used as these uniformly reflect solar radiation. Research at the UF Mid-Florida Research and Education Center (http://gardeningsolutions.ifas.ufl.edu) has shown that red and blue nets cause *Aspidistra* to grow more compactly; blue and grey nets cause *Philodendron* to grow taller and red and grey nets cause *Pittosporum* to have greater growth. It must, therefore, be kept in mind that each plant has its own individual requirements for sunlight and shade under which it flourishes. Fynbos can survive windy, hot, dry summers with low water consumption but many seeds don't germinate when in the shade of established fynbos. However, most fynbos plants can grow very well in a surprising amount of shade. In most cases half a day of direct sunshine, either morning or afternoon, is also adequate. Since sunshine stimulates flower bud production, plants growing in a shade position may not flower as much as in direct sun (http://www.capepoint.com).

Currently, black nets are used on the FWCSs. Research needs to be conducted to assess the impact of colour of netting on the flowering of fynbos, whether pest infestations differ between standard and photo-selective shade cloth and whether the micro-climate vary with different colour or types of shade cloths.

7.2.4 Biodiversity

Habitat fragmentation with concomitant impacts on species diversity and population numbers is frequently caused by humans when native vegetation is cleared for human activities such as agriculture, rural development or urbanization. The term habitat fragmentation includes five discrete phenomena:

- Reduction in the total area of the habitat;
- Decrease of the interior edge ratio;
- Isolation of one habitat fragment from other areas of habitat;
- Breaking up of one patch of habitat into several smaller patches;
- Decrease in the average size of each patch of habitat.

Micro-climatic changes in light, temperature and wind can alter the ecology around the fragment, and in the interior and exterior portions of the fragment. Fires become more likely in the area as humidity drops and temperature and wind levels rise. Pest species may establish themselves easily in such disturbed environments. Also, habitat along the edge of a fragment has a different climate and favors different species from the interior habitat. Small fragments are therefore unfavorable for species which require interior habitat. FWCSs may therefore play a role in fragmentation of habitat.

7.2.4.1 Flora

Veld type in the area (between the Tsitsikamma-, Outeniqua-, Zondagsberg and Kouga Mountains) was predominantly grasslands until the 20th century. It is presumed that overgrazing and possibly adverse rainfall patterns during the 20th century have led to the denudation of these grasslands and the establishment of 'Renosterveld' – a variety of Cape Fynbos over the northern slopes of these mountains extending northwards to the Klein Karoo veld types. Fynbos can be divided broadly into mountain and lowland fynbos, but within this definition there is a high diversity of fynbos communities that vary extensively in their conservation importance. Some communities have been almost entirely destroyed due to agricultural expansion, such as the Renosterveld (Eden District Management Area Spatial Development Framework, 2004).

At the Avontuur experimental site, some of the flora such as the 'Renosterbos', suffered severely during a huge veld fires in 2007. Following this, the area was used for cattle, which further contributes to the demise of the Renosterbos. The Avontuur FWCS area is situated alongside the firebreak established close to this ridge. To establish the FWCS, the site was cleared by cutting the remaining Renosterbos prior to fencing the area (Figures 7.6 and 7.7). This action was required for fire prevention and will need to be continued in future.

Figure 7.6: *Taaitrek bos – found on old lands.*

Figure 7.7: *Renosterveld – south fence of FWCS.*

Figure 7.8: *Rooigras forming 85% of the vegetation at the Avontuur Fog Water Collection System (FWCS) experimental site.*

7.2.4.2 Re-establishment of plants

Rooigras forms about 85% of the vegetation both inside and outside the triangular FWCS (Figure 7.8). Observation of the triangular FWCS from a distance reveals an immediate area within the triangle that appears to be greener. Close inspection revealed that the grass height both inside and outside of the triangular FWCS was found to be about 500 mm in height. The Rooigras outside the FWCS had seeded and the typical reddish color of the Rooigras is striking.

The fynbos show signs of becoming established within the Rooigras (Figure 7.9). The following are beginning to prosper: Botterblom, Sewejaartjie (scarce in the region), Geelaandblom as well as the more common Harpuisbos (a pioneer) and Besembos (Dekriet) (Figure 7.10) (personal communication: Mr Jimmy Zondach, 2013). A variety of these plants are listed in Table 7.7.

Figure 7.9: *Evidence of fynbos re-growth within fenced-off experimental area that was cleared for erecting the Fog Water Collection System (FWCS).*

Figure 7.10: *Sewejaartjies (left) and Besembos (right).*

Table 7.7: Summary of some of the flora that was re-established in the vicinity of the Avontuur Fog Water Collection System (FWCS) experimental area.

Botanical Name	Common name	Family	Conservation status	Ecology
Euryops abrotanifolius	Berg Harpuis bos	Asteraceae	Not Threatened	*Euryops abrotanifolius* is quick to re-establish after a fire, becoming dominant for a few years after a burn and then slowly being replaced by other fynbos plants as the veld recovers. It is also an effective pioneer and is quick to exploit disturbed or open ground (http://www.plantzafrica.com).
Gazania krebsiana	Botterblom	Asteraceae	Not Threatened	*Gazania krebsiana* is pollinated by a number of insects: bees, bee flies, beetles, butterflies and ants (http://www. http://myfolia.com)
Helichrysum appendiculatum	Sewejaartjie/ skaapoorbossie	Asteraceae	Not Threatened	Because of the pappus on the achene or fruit, dispersal is achieved by wind. Insects are known to pollinate *Helichrysum appendiculatum* (http://www.plantzafrica.com).
Rhus Lucida	Besembos*	Acanthaceae	Declared indicators of bush encroachment [Regulation 16.a]	Notice 2485 of 1999: National department of agriculture; Conservation of agricultural resources act, 1983 (act 43 of 1983) Regulations: proposed amendment 15 and 16. - Government Notice No. R. 1048 of 25 May 1984, as amended by Government Gazette Notice No. R. 2687 of 6 December 1985. (http://www.http://www.info.gov.za /gazette/notices/1999/2485.htm)
Oenothera stricta	Geelaandblom, evening primrose, nagblom	Onagraceae	Naturalized exotics not assessed for National Red List	

**16.A(1)Indigenous plants specified are hereby declared indicator plants indicating bush encroachment in the corresponding areas specified: South Africa. The land user of an area in which natural vegetation occurs and contain communities of the plants referred to in sub-regulation (1) shall follow practices to prevent the deterioration of natural resources and where bush encroachment occurs, to combat it. The practices contemplated in sub regulation (2) shall consist of the following measures as are necessary under the circumstances provided that the application of any measure is designed to remove the cause of the deterioration, and to improve and maintain the production potential of the natural pastoral land: The plants concerned shall be treated with a herbicide that is registered in connection therewith, in accordance with the directions for the use of such a herbicide. The application of control measures regarding the utilization and protection of veld in terms of regulation 9. Livestock reduction or removal of animals in terms of the control measures of regulations 10 and 11. Any research-based method or strategy that may be applicable and is specified by the executive officer by means of a direction"*

7.2.5 Aesthetics

Visual, scenic and cultural components of the environment can be seen as a resource, much like any other resource. This resource may have a scarcity value, be easily degraded, and is usually not replaceable. Visual and scenic resources are by their nature difficult to assess or quantify as they often have cultural or symbolic meaning. Current South African environmental legislation governing the Environmental Impact Assessment (EIA) process, which may include consideration of visual impacts if this is identified as a key issue of concern, is the NEMA (Act No. 107 of 1998) and the EIA regulations in terms of the Environment Conservation Act (Act No. 73 of 1989).

The Western Cape Province is richly endowed with scenic resources by virtue of the mountainous landscape, the coastline along two oceans, and the unique flora and fauna. In addition to this natural heritage, there are centuries of human settlement that have created a tapestry of vineyards, orchards, wheat fields, farmsteads, tree shelterbelts and country towns.

The scenic resources of the Western Cape have enormous implications for the economy of the region mainly in the form of tourism, which provides income for the province, and creates jobs for the local population. There has therefore been a growing emphasis on visual and scenic assessments for most major projects in the region, in order to maintain the integrity and value of these natural and cultural landscapes as far as possible (Oberholzer, 2005).

A moderate visual impact is expected from a FWCS.

The areas selected for the erection of the FWHS has some scenic, cultural, historical significance but has already been disturbed by agricultural practices. Fog water harvesting system may be classified as a Category 5 development: e.g. treatment plants, power stations, wind energy farms, power lines etc. (Oberholzer, 2005). Fog water harvesting is a low-key development with more than 75% of the area retained as natural (undisturbed) open space. The areas where FWHS is erected is of low aesthetical value as it is mostly on privately owned land at such a distance that it is barely visible with the eye from any public area.

7.3 SUMMARY OF ENVIRONMENTAL IMPACTS

All impacts (both positive and negative) related to the construction phase of the FWCS at the Avontuur experimental site are considered to be of very low to medium significance. Construction-phase impacts relate to construction and the storage and management of materials, as well as the maintenance of the FWCS is of a temporary nature.

All impacts (both positive and negative) related to the maintenance phase are considered to be of very low to medium significance. The only risk worth mentioning is that of the slashing operation done to lower the fire hazard of the area. Whilst slashing is being performed there will be a low level of fuel emissions and noise. Both risks will be managed as to keep the levels as low as possible as by land owner.

7.4 MONOTORING AND MANAGEMENT

In the management of the Avontuur experimental site in future, environmental impacts can be minimised by the following actions:

- Monitor construction sites and the immediate surrounds of the structures periodically for re-infestation by invasive plants;
- Monitor disturbed areas post-construction for a period of three years to ensure that they do not become re-infested with invasive alien plants or that head-cut and other erosion has developed subsequent to construction;
- Remove alien plants and where appropriate, replant with indigenous pioneer plant species to minimise the degradation of terrestrial vegetation and habitats;
- Preserving or planting corridors of native vegetation habitat to lessen effect of fragmentation. This has the potential to mitigate the problem of isolation but not the loss of interior habitat. Another mitigation measure may be the opening of the triangular system in order to increase the amount of interior habitat;
  - Include Visual Impact Assessments (VIA). Monitoring programmes should include procedures for ensuring that the specified visual management actions are carried out on site as part of an Environmental Management Plan (EMP).

CHAPTER 8: CLIMATE CHANGE AND LOCAL FOG FREQUENCIES

8.1 INTRODUCTION

Being located in the dry sub-tropics of the Southern Hemisphere, the climate of South Africa is influenced by both tropical and mid-latitudinal weather systems (Van Heerden and Hurry, 1987). During austral summer months (December-January-February: DJF) when continental outgoing long-wave radiation is higher in comparison to winter, near-surface atmospheric pressure troughs develop over the southern African continent (Todd and Washington, 1999; Taljaard, 1985) and their cyclonic circulation results in moisture advection from the tropics towards the eastern parts of South Africa where the highest rainfall occurs. At the same time, cold fronts from mid-latitudinal cyclonic systems often sweep from west to east across the most southern part of the African continent (Taljaard, 1995). When a cold front passes, the Atlantic High Pressure system normally ridges from behind along the South African coast line and adjacent ocean, and its anti-cyclonic rotation leads to onshore moisture advection from the ocean across the southern and eastern coastal zones of South Africa towards the continental escarpment (Figure 8.1). During austral winter months (June-July-August: JJA) when subtropical continental circulation is dominated by anticylones, continental troughs appear less frequently with less precipitation over the interior. At the same time, the east-west path of cold front propagation shifts northwards, resulting in cold conditions over the South African interior, with moisture advection and rain along the south-western and southern coastal zones.

These synoptic-scale weather patterns give rise to moisture advection from both the tropics and surrounding oceans towards the normally dry southern African sub-continent, allowing for cloud and advection fog formation and higher annual rainfall amounts over the eastern to south-eastern parts of South Africa, with a decrease in rainfall towards the west. Despite these moisture advection patterns, only 35% of South Africa receives more than 500 mm of rain per annum, with the west coast receiving considerably less than 300 mm per year.

In some favourable conditions, moisture advection from the surrounding oceans towards the South African coastal zone and escarpment results in advection fog and low-cloud formation along the slopes of mountains. For example, Forced Topographic Ascent (FTA) of moist marine air against the slopes of the eastern and south-eastern escarpment of South Africa frequently results in adiabatic cooling and mountain fog formation.

The mountains along the South African escarpment rise to altitudes of more than 2500 m AMSL. Distances to the coast (ocean) are frequently short, traversing foothills of the escarpment and a low altitude coastal zone (Figure 8.1). Onshore winds often allow for moisture advection across the coastal zone towards the escarpment, from where FTA, adiabatic cooling and condensation result in the development of mountain fog clouds. It is therefore obvious that not only onshore moisture advection, but also the frequency of FTA events are important factors in determining the amount of water that could be harvested from mountain fog cloud droplets.

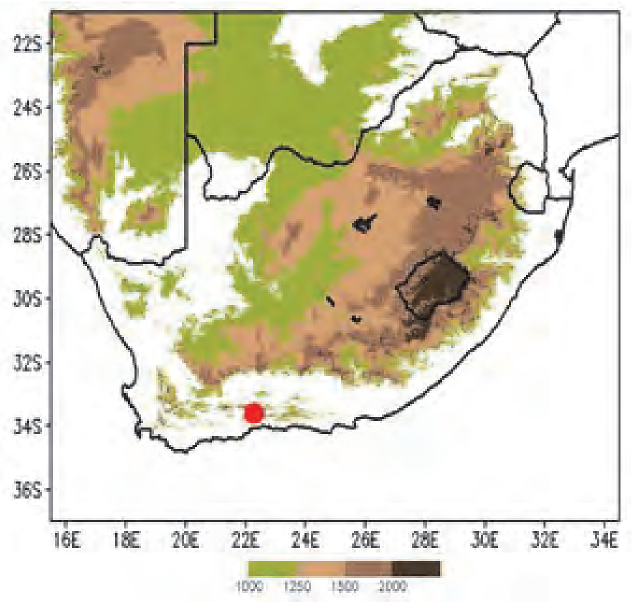

Figure 8.1: *Topographic altitude (shaded in meters Above Mean Sea Level: AMSL) of the South African study domain. Note the escarpment in the east and south with relatively short distances to the coast (ocean) across foothills of the escarpment and a low altitude coastal zone. (Topographic elevation source: GLOBE, 1999). The approximated location of the WRC Avontuur experimental site is indicated by a red circle in the south.*

As outlined in the previous Chapters of this report, the WRC provided funding for the development of a fog water harvesting research site (33º43'58.75'' South; 23º10'13.61'' East; elevation: 880 m AMSL) at the hamlet Avontuur in the mountains of the Western Cape Province of South Africa. The location of this site on the southern South African escarpment makes it ideal for studies of local scale fog distribution, occurrence and characteristics.

With global warming becoming a greater reality, onshore wind direction climates and daily frequencies of FTA might change in future, which might have further implications for both fog water harvesting yields and locations. In its Fifth Assessment Report (AR5), the Inter-governmental Panel on Climate Change (IPCC) (IPCC, 2013) made use of a range of globally coupled Atmosphere-Ocean General Circulation Models (AOGCMs) in efforts to generate future projections of climates under conditions of global warming. These simulations formed part of the Coupled Model Intercomparison Project Phase 5 (CMIP5) (Taylor *et al.*, 2012). However, the relatively coarse spatial resolution of AOGCM grid made it difficult to study local climatic features, especially for impact assessment and adaptation studies.

Recently, the Coordinated Regional-climate Downscaling EXperiment (CORDEX, Giorgi et al., 2009) was initiated with the aim to foster international collaboration in generating an ensemble of high resolution historical and future climate projections at regional scale, by using Regional Climate Models (RCM) forced by the AOGCMs.

In the CORDEX framework, an increasing number of works have investigated the ability of RCMs to simulate the general features of the African climate, especially for precipitation (Nikulin et al., 2012; Endris et al., 2013; Kim et al., 2013; Kalognomou et al., 2013; Panitz et al., 2014; Gbobaniyi et al., 2014). It is shown that in general RCMs simulate the precipitation seasonal mean and annual cycle quite accurately although individual models can exhibit significant biases in some sub-regions and seasons.

The research described in this chapter aims at investigating the seasonal Mean Sea Level Pressure (MSLP) and near-surface onshore wind direction climatology along the South African coast line, as well the daily occurrence (frequency) of local scale FTA events that are assumed to be associated with the potential for mountain fog cloud formation as a result of FTA, adiabatic cooling and condensation. Note that the thermodynamic and physical properties involved during the FTA of moisture bearing air masses did not form part of the study. Historically observed climates and frequencies, as well as anticipated future changes in these climates and frequencies as a result of global warming, are investigated. Results might not only provide more insight on the impact of global warming on the occurrence of mountain advection fog, but also on projected changes in the locations suitable for mountain fog water harvesting in the escarpment mountains of South Africa, like the Avontuur experimental site.

8.2 DATA AND METHODS

Daily data for both observed and model simulations of near-surface winds and MSLP, calculated over a 20-year historical (1986 to 2005) and future (2076 to 2095) period for the four seasons DJF, March-April-May (MAM), JJA and September-October-November (SON), were obtained for the South African domain that extends from 41° to 20° South, and 15° to 35 East°. The same data were used for interpolation in the local scale domain (33,8374° to 33,7238° South, and 23,1326° to 23,2236° East) defined to accommodate the Avontuur experimental site.

8.2.1 Historically observed winds and MSLP

For model verification purposes, daily (average of 00:00 UCT, 06:00 UCT, 12:00 UCT and 18:00 UCT) near-surface wind (10 m above Earth's surface) and MSLP fields for the seasons DJF, MAM, JJA and SON over the 20-year historical period 1986 to 2005 were obtained for the South African domain from the European Centre for Medium-Range Weather Forecasting (ECMWF) Reanalysis (ERA) Interim data site (Dee et al., 2011). ERA Interim fields have a standards grid box resolution of 0.75° x 0.75°.

8.2.2 Model simulated winds and MSLP

Results from four globally coupled AOGCMs, which formed part of the CMIP5 (Taylor et al., 2012), and which were accommodated in the recently released AR5 of the IPCC (IPCC, 2013), were considered as historical and future simulations of global winds. These AOGCMs were: (1) the HadGEM2-ES AOGCM which is a version of the Hadley Centre's "standard" climate model particularly designed to run the major scenarios for the IPCC AR5 (Caesar et al., 2013); (2) the EC-EARTH AOGCM developed by the EC-Earth consortium, gathering 22 national weather departments and universities from currently 10 countries in Europe coordinated by the Royal Netherlands Meteorological Institute (KNMI) (Hazeleger et al., 2012); (3) the CNRM-CM5 AOGCM from the National Centre for Meteorological Research (CNRM) and the Climate Modelling and Global Change team, both from France and with strong links to Meteo France (Voldoire et al., 2011; Alkama et al., 2011); and (4) the MPI-ESM-LR AOGCM, which is developed by the Max-Planck-Institut für Meteorologie (Giorgetta et al., 2013).

Since grid point data from these global AOGCMs were found to be too coarse for the more detailed spatial coverage required for the wind climate and FTA frequency analyses in this paper, it was decided to accommodate a dynamical downscaling approach where data from the four globally coupled AOGCMs were used as lateral boundary input to the COnsortium for Small-scale MOdeling-climate mode (COSMO) (version 4.8) model of the Climate Limited-area Modelling (CLM) community, known as the COSMO-CLM 4.8 or CCLM 4.8 Regional Climate Model (RCM). Downscaled RCM data (ensemble from four globally coupled AOGCMs) for this paper were therefore generated by CCLM 4.8 RCM simulations, as part of the CORDEX initiative. For the purpose of this study, seasonal as well as daily ensemble means were calculated for climatological and diurnal frequency analysis. An evaluation of CCLM's abilities to simulate the African climatology when driven by AOGCMs, can be found in Dosio et al. (2014), including the assessment of the 'added value' of downscaling, which is expected to be found in the fine scales and in the ability of RCM to simulate extreme events.

CCLM simulated data at a 0.44º x 0.44º (approximately 45km x 45km) horizontal grid resolution of daily near-surface winds (2 m above the surface) and MSLP were obtained for the historical (1986 to 2005), as well as for the future period (2076 to 2095). For the future projections, two CO_2 Representative Concentration Pathways (RCPs) associated with atmospheric heat increases of 4.5 $W.m^{-2}$ and 8.5 $W.m^{-2}$ by the year 2100 (RCP 4.5 and RCP 8.5, respectively) were considered (Riahi et al., 2011).

8.2.3 Forced Topographic Ascent (FTA)

As mentioned before, it is accepted that the potential for fog cloud formation could only exist with onshore winds bringing moist air from the ocean, and the subsequent FTA of these moist air masses against the slopes of mountains in the coastal zone or at the South African escarpment. At any topographical elevation point, such FTA could be identified by the following condition:

$$\bar{V} \cdot \bar{\nabla} h = (u\bar{\imath} + v\bar{\jmath}) \cdot (\frac{\partial h}{\partial x}\bar{\imath} + \frac{\partial h}{\partial y}\bar{\jmath}) > 0 \quad (2)$$

where $\bar{V}$ is the horizontal near-surface wind vector in a spherical reference frame with west-to-east ($\bar{\imath}$) and south-to-north ($\bar{\jmath}$) unit vector components u and v, and $\bar{\nabla}$ is the horizontal gradient across the topography elevation point h in the two unit vector directions. Equation 1 was applied as condition for identifying daily FTA frequencies, across each season and at each topography elevation point in the WRC Avontuur site domain. It therefore gave an indication of the proportion of days having the potential for the development of advection fog clouds at each topography elevation point. For this purpose, topographical elevation data for h in Equation 1, at a 1 km x 1 km grid box resolution, were obtained from the Global Land One-kilometre Base Elevation (GLOBE) Digital Elevation Models (GLOBE, 1999) (see Figure 8.1).

8.2.4 Data analyses procedures

For both the South African and Avontuur experimental site domains, historical (1986 to 2005) RCM simulated results for the seasons DJF, MAM, JJA and SON were firstly verified against the associated ERA interim reanalysis data (observations). For the South African domain, observed and RCM simulated seasonal climatology (averaged from daily data) of near-surface winds and MSLP were verified against observed climates (averaged from daily data) (Figure 8.2), while seasonally observed and RCM simulated percentage (%) frequencies of daily FTA events were compared for the Avontuur experimental site domain (Figure 8.3). ERA Interim reanalysis and RCM simulated winds are both given at 10 m above the Earth's surface.

Note that ERA Interim reanalysis and RCM simulated wind and pressure fields in Figure 8.2 are illustrated on 0.75º x 0.75 º and 0.44 º x 0.44 º (only every 2nd grid vector is plotted for the latter) grid box resolutions, respectively, while synoptic-scale winds were interpolated to fit the 1km x 1km topography elevation grid boxes in the FTA % frequency analyses (Figure 8.3) of the Avontuur experimental site domain. It is important to note that the purpose of interpolation was not to downscale the winds to a finer resolution, but rather to obtain the synoptic-scale component of the wind at each 1 km x 1 km topography domain.

A similar approach was followed in the analyses of future projections. For both the South African and Avontuur experimental site domains, results from RCM projections (2076 to 2095) for both the RCP 4.5 and RCP 8.5 scenarios, and for the seasons DJF, MAM, JJA and SON, were firstly compared to historical (1986 to 2005) RCM simulated seasonal climates in order to capture the extent of change (Figure 8.4). This was followed by interpolating the daily data from the RCM projections to 1km x 1km grid boxes covering the Avontuur experimental site, which served as source for the calculation of the projected % frequencies of daily FTA events using Equation 2. These % frequencies were compared to the associated historical % frequencies from where the anticipated magnitude of change in the occurrence of daily FTA events was calculated for the Avontuur experimental site, as well as for each topography elevation grid box (Figure 8.5) in the Avontuur experimental site domain.

8.3 RESULTS

8.3.1 Historically observed and model simulated winds and MSLPs

Historical ERA Interim reanalyses climates (1986 to 2005), also regarded as observed climates for the seasons DJF, MAM, JJA and SON, of near-surface winds ($m.s^{-1}$) and MSLPs are depicted in the left column of Figure 8.2. The associated CCLM 4.8 RCM simulated climates are presented in the right column of Figure 8.2.

For the DJF season (Figure 8.2), RCM simulated climates have similar MSLP patterns if compared to ERA Interim reanalysis fields, with a trough in the west of South Africa and higher pressures towards the east. RCM simulated MSLPs, however, are in the order of 1 hPa to 2 hPa lower than observed over the entire pressure field. RCM simulated and ERA Interim reanalysis near-surface wind fields are also very similar, with strong south-easterly to southerly winds along the west coast, and more moderate south-easterly winds along the southern coast line – RCM simulated winds are stronger over the ocean while observed winds are stronger over the southern coastal zone. Easterly onshore flow along the east coast, which turns south-east towards the northern east coast, is captured in both the observations and simulations.

The weakening of the surface trough in the west and strengthening of higher MSLPs (relative to DJF) over South Africa are captured in both RCM simulated and ERA Interim reanalysis MSLD fields for the MAM season (Figure 8.2).

MSLP magnitudes and spatial patterns are very similar in RCM simulated and ERA Interim reanalysis fields. Near-surface winds along the west coast are predominantly from the south in both fields. While moderate south to south-westerly winds occur along the south coast in the observations, RCM simulated winds are easterly to north-easterly. Over the southern coastal zone RCM simulated winds are from the west, while ERA Interim reanalysis winds are from the north-east and east. Wind direction patterns are better captured along the east coast, where both RCM simulated and ERA Interim reanalysis winds gradually turn from north-east to south-east as one moves northwards along the east coast.

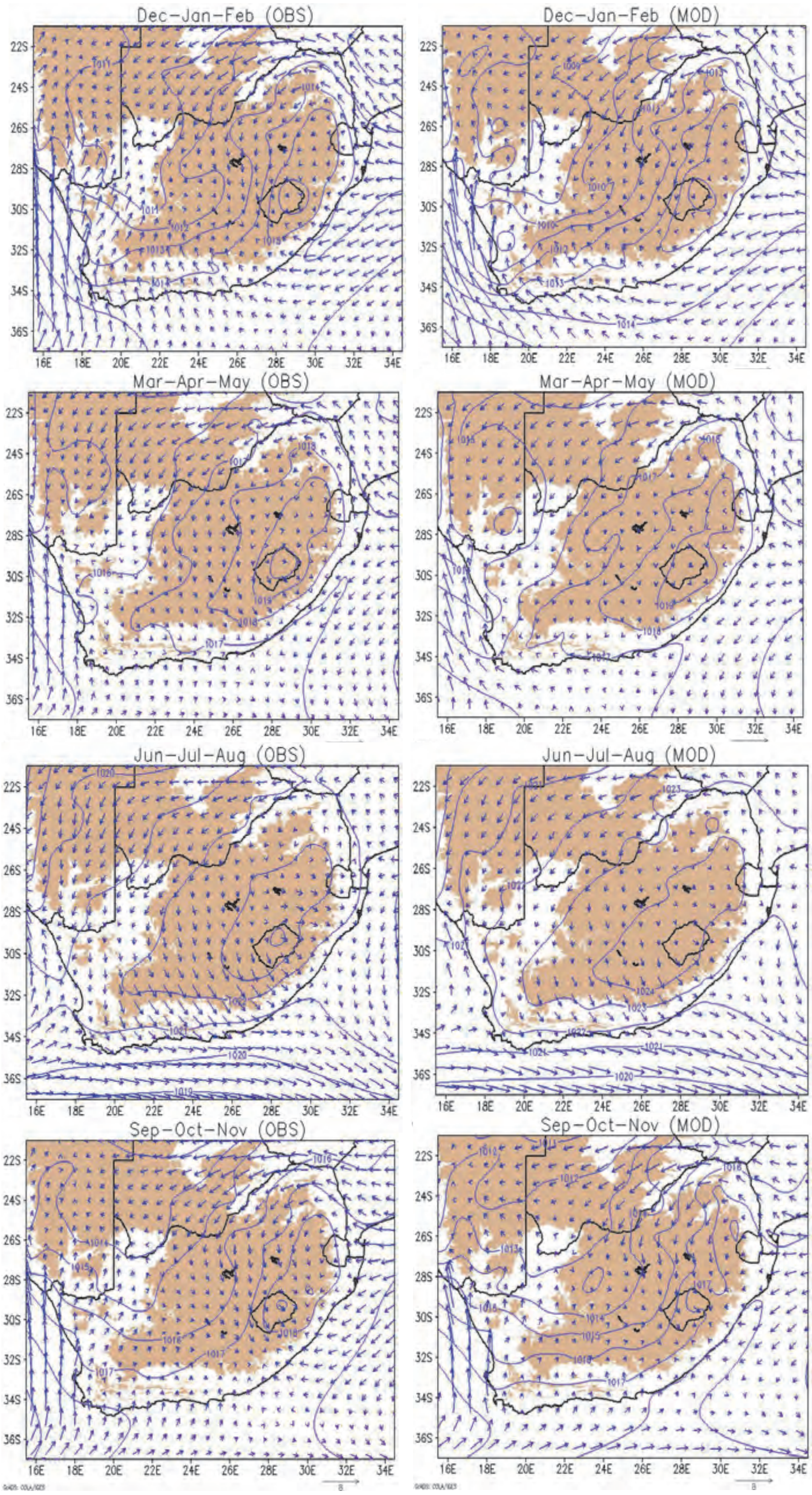

Figure 8.2: *Historically observed (left column) and model simulated (right column) near-surface wind (vectors in $m.s^{-1}$ – at 10 m and 2 m above the surface, respectively) and Mean Sea Level Pressure (MSLP) (contours in hPa) climates for the 20-year period 1986 to 2005 and for the seasons DJF, MAM, JJA and SON. Topographical elevation points > 1000 m Above Mean Sea Level (AMSL) are shaded.*

Typical austral winter MSLP patterns, associated with higher MSLPs over the entire South Africa with a maximum in the east, occur during the JJA season (Figure 8.2) in both RCM simulated and ERA Interim reanalysis fields. However, MSLPs are in general slightly higher (±1 hPa) in the RCM simulations. Although southerly winds still dominate along the west coast, strong north-westerly winds with offshore flow are evident along the south coast. RCM simulated winds along the east coast are again very similar to what have been observed, with easterly winds in the far north that turn southwards towards the south.

With the austral summer approaching during the SON season (Figure 8.2), MSLP patterns exhibit a trough pattern that extends over most of the west of South Africa. This pattern is captured in both the RCM simulated and ERA Interim reanalysis MSLPs. Like for the DJF, SON seasons, MSLPs values are generally lower (±1 hPa) in the RCM simulations. Southerly near-surface winds along the west and southern coastline occur in both ERA Interim reanalysis data and RCM simulations. The easterly to north-easterly flow, from north to south along the east coast, is also well-captured in both the observations and RCM simulated vector fields.

To summarise, apart from some lower than observed RCM simulated MSLPs (≈1hPa to 2 hPa for the DJF season and ≈1hPa for the SON season) and higher than observed RCM simulated MSLPs (≈ 1hPa for the JJA season), general observed synoptic scale troughs and ridges are well-captured in RCM simulations. With the exception of winds along the south coast during MAM, near-surface RCM simulated wind vector climates are also very close to what have been observed along the western, southern and eastern coast lines of South Africa for all seasons.

8.3.2 Historically observed and model simulated percentage frequencies of FTA events

Figure 8.3 depicts historically observed (left column) and RCM simulated (right column) % frequencies of daily FTA events (shaded), as calculated with Equation 2, over the historical 20-year period 1986 to 2005, and for the seasons DJF, MAM, JJA and SON, across the Avontuur experimental site domain. The location of the Avontuur experimental site is indicated by a black circle in Figure 8.3, and topography elevations (in metres AMSL) across the domain are shown as contours. The Avontuur experimental site is located in a mountainous area at an altitude of 1 040 m AMSL, while the elevation of topography points decreases southwards towards the ocean.

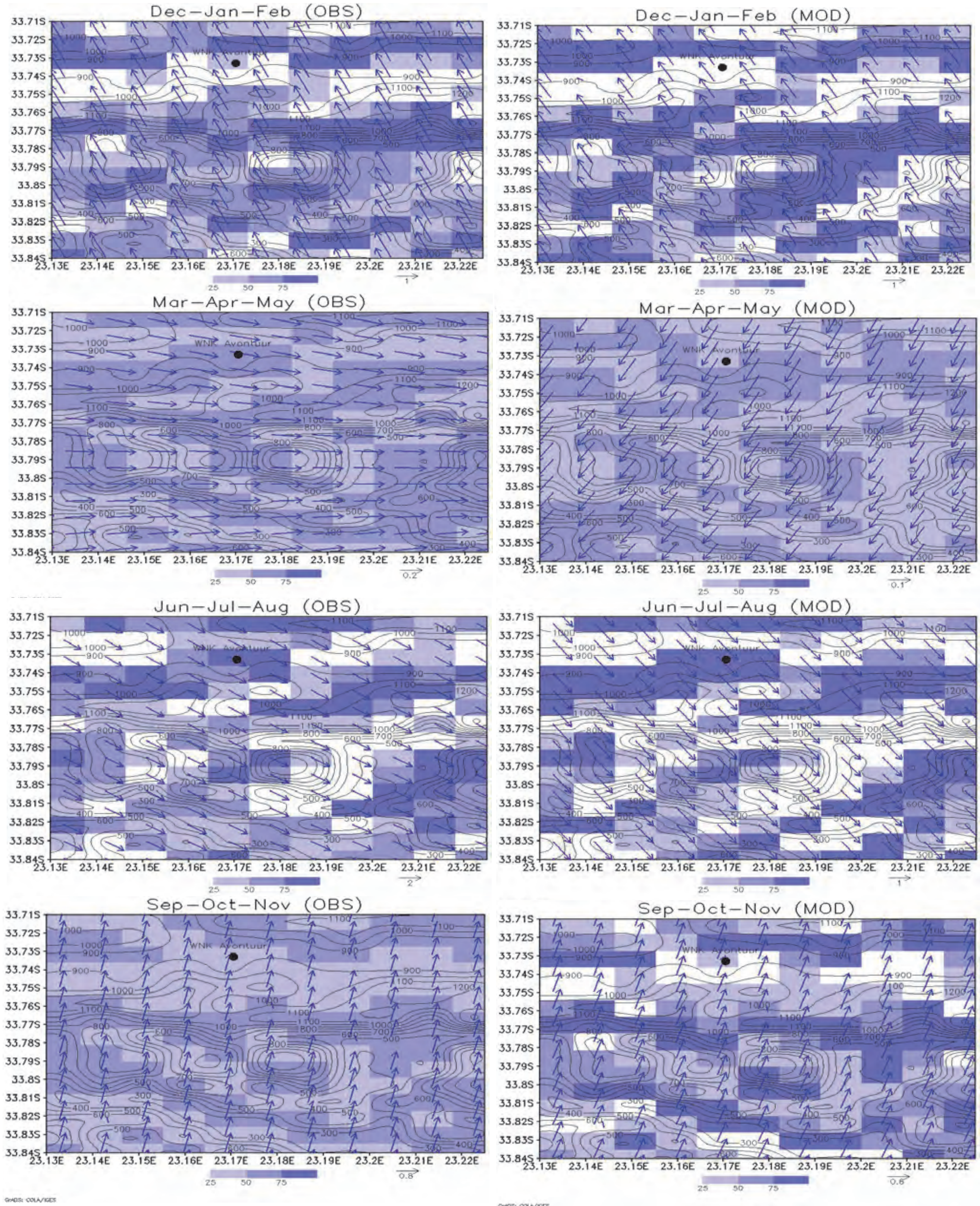

Figure 8.3: *Historically observed (left column) and model simulated (right column) percentage (%) frequency of daily Forced Topographical Ascent (FTA) events (shaded) and near-surface wind climate (vectors) as calculated over the 20-year period 1986 to 2005 and for the seasons DJF, MAM, JJA and SON in the Avontuur experimental site (black circle) domain. Topography elevations (metres Above Mean Sea Level: AMSL) are depicted by contours.*

With south-easterly observed and RCM simulated near-surface winds across the Avontuur experimental site domain (Figure 8.3) during the DJF season, % frequencies of daily FTA events of greater than 75% (implying that FTA occurred on 75% of the days during the season DJF over the 20-year period 1986 to 2005) were calculated for most of the mountain slopes that face southwards (according to the topography elevation contours in Figure 8.3) in the Avontuur experimental site domain. These winds might allow for marine moisture advection across the southern coastal zone towards the escarpment, with mountain fog development against the mountain slopes that face southwards. Note that the % frequency of FTA events was between 50% and 75% for the Avontuur experimental site, meaning that for DJF, between 50% and 75% of the days at the site were associated with FTA events. With south-easterly winds also captured in the RCM simulations for the DJF season (Figure 8.3), % frequencies of FTA events are very similar to what had been observed, with some biases towards maximum and minimum % frequencies in the RCM simulations.

With the transition in season during MAM, observed winds become more westerly over the southern coastal zone (Figure 8.3), allowing for the % frequency of FTA events to become greater than 50% at the western slopes of the topography, while percentage frequencies of < 50% were calculated for the down-slopes facing east. In RCM simulations, winds across the southern coastal zone became north-eastwards (Figure 8.3) which is quite different to what have been observed, allowing for higher % frequencies of FTA events at the slopes that face eastwards. No % frequencies of > 75% or < 50% were calculated for both observed and RCM simulated fields, which is indicative of a higher diurnal variability in near-surface wind direction during the MAM season. Despite of the difference in wind direction, very little mountain fog is anyway expected to develop during the MAM season across the Avontuur experimental site domain as a result of the zonal (observed winds) and continental offshore orientation (RCM simulated winds) of the winds, which create conditions that are not favourable for moisture advection from the ocean to the south, and mountain fog formation.

During the JJA winter season, north-westerly near-surface winds appeared in both observed and RCM simulations across the southern coastal zone of South Africa (Figure 8.3). These north-westerly winds, which approach the WRC Avontuur domain from the dry winter continent, resulted in higher % frequencies of FTA events along topographical slopes that face northwards in both the observed and RCM simulated fields. Percentage frequencies in both observed and RCM simulated fields have very similar spatial patterns, which is indicative of consistency in the number of days associated with FTA events. During JJA the potential for advection mountain fog development against the northern slopes is assumed to be low because of the south-westward advection of dry winter continental air. Note that the Avontuur experimental site (black circle in Figure 8.3) is located at a point with a % frequency of < 25%, meaning that the potential for mountain fog development at the site is regarded as slim.

The SON season, which is a transition between austral winter (JJA) to austral summer (DJF) seasons, is characterised by a climate of south-westerly to southerly flow across the southern coastal zone in both ERA Interim reanalysis data and RCM simulations. Such flow, with its marine environmental origin, creates favourable conditions for moisture advection towards the escarpment and the Avontuur experimental site, with the potential for mountain fog formation. Percentage frequencies of FTA events during the SON season (Figure 8.3), as calculated for both the observations and RCM simulations, are characterised by higher % frequencies of daily FTA events at the mountain slopes that face southwards. The number of days with FTA against the southern slopes are lower (< 75%) in the observed fields than in the RCM simulated fields, meaning that southerly advection is more consistent (percentage of days with FTA against the southern slopes > 75%) in RCM simulated fields. Despite of this, spatial patterns in both observed and simulated fields are still very similar.

In summary, CCLM 4.8 performed well in capturing the observed % frequency of daily FTA events in the Avontuur experimental site domain, for all seasons over the historical period 1986 to 2005 with the exception of the MAM season where wind direction climates differed quite considerably. Although some biases in magnitude occurred, spatial patterns in observed and RCM simulated fields were found to be very similar. It is therefore assumed that the CCLM 4.8 RCM, with its ensembles generated from four globally coupled AOGCMs, is suitable for use in projecting future near-surface winds, and therefore % frequency changes in future daily FTA events as a result of global warming.

8.3.3 Model simulated projections for winds and MSLPs

In Figure 8.4 (left column), historical (1986 to 2005) RCM simulated climates of near-surface winds and MSLP (the same as in Figure 8.2) are given as background against which future simulations could be compared. Also in Figure 5 are RCM results of near-surface winds and MSLP from both the RCP 4.5 and RCP 8.5 scenario RCM simulations, also for the historical 20-year period 2076 to 2095. In Figure 8.4, these climates are all given for the seasons DJF, MAM, JJA and SON.

RCM results from both the RCP 4.5 and RCP 8.5 scenario simulations, for the season DJF (Figure 8.4), are very similar to historical RCM simulations. In both historical and projected RCM simulations, the MSLP trough appears in the western parts of South Africa. However, this trough is slightly deeper in the projection simulations (white shaded areas in Figure 8.4 represent negative MSLP anomalies, and grey shaded areas positive anomalies, relative to the history) if compared to the historical simulations, with a steeper MSLP gradient towards the east of the trough. In both the RCP 4.5 and RCP 8.5 projections, winds are south along the west coast, south-east along the south coast and north-east to south-east from south to north along the east coast, which agree well with historical simulations. In general, near surface-winds appear to be stronger in the projections, especially from the south-east across the southern coastal zone and in the north-east of the country.

During the transition months of MAM from austral summer to winter in Figure 8.4, wind and MSLP results from both the RCP 4.5 and RCP 8.5 scenario RCM simulations appear to be very similar to historical simulations. In RCP 4.5 scenario RCM simulations MSLPs seems to increase slightly in the east (grey shading), while most of the South African domain is characterised with lower MSLPs, relative to the history, in the RCP 8.5 scenario simulation. In all simulations, wind directions are from the south-east to south against the western coastline, while easterly winds occurs along the south coast ocean with easterly to south easterly winds across the southern coastal zone. North-easterly to south-easterly winds were simulated from south to north along the east coast. In some areas projected wind speeds appear to be stronger if compared to historical simulations, especially to the south of the country and in the anti-cyclonic flow in the north-east of the country.

During the JJA season MSLPs are higher over most of South Africa (grey shaded areas in Figure 8.4) in both the RCP 4.5 and RCP 8.5 scenario RCM simulations, with negative anomalies confined to the west of the country. However, according to RCM projections, spatial patterns in winds and MSLPs are not expected to change significantly. In all simulations, southerly winds prevail along the west coast, with strong westerly winds across the ocean to the south and offshore flow across the southern coastal zone, and northerly winds along most of the east coast which turn east in the far north.

For the SON season, spatial patterns in both the RCP 4.5 and RCP 8.5 scenario RCM simulations are very similar to historical simulations (Figure 8.4), although higher pressure anomalies were simulated over most of South Africa in the future projections. All winds are characterised with southerly flow along the west and south coasts, with easterly flow along the east coast.

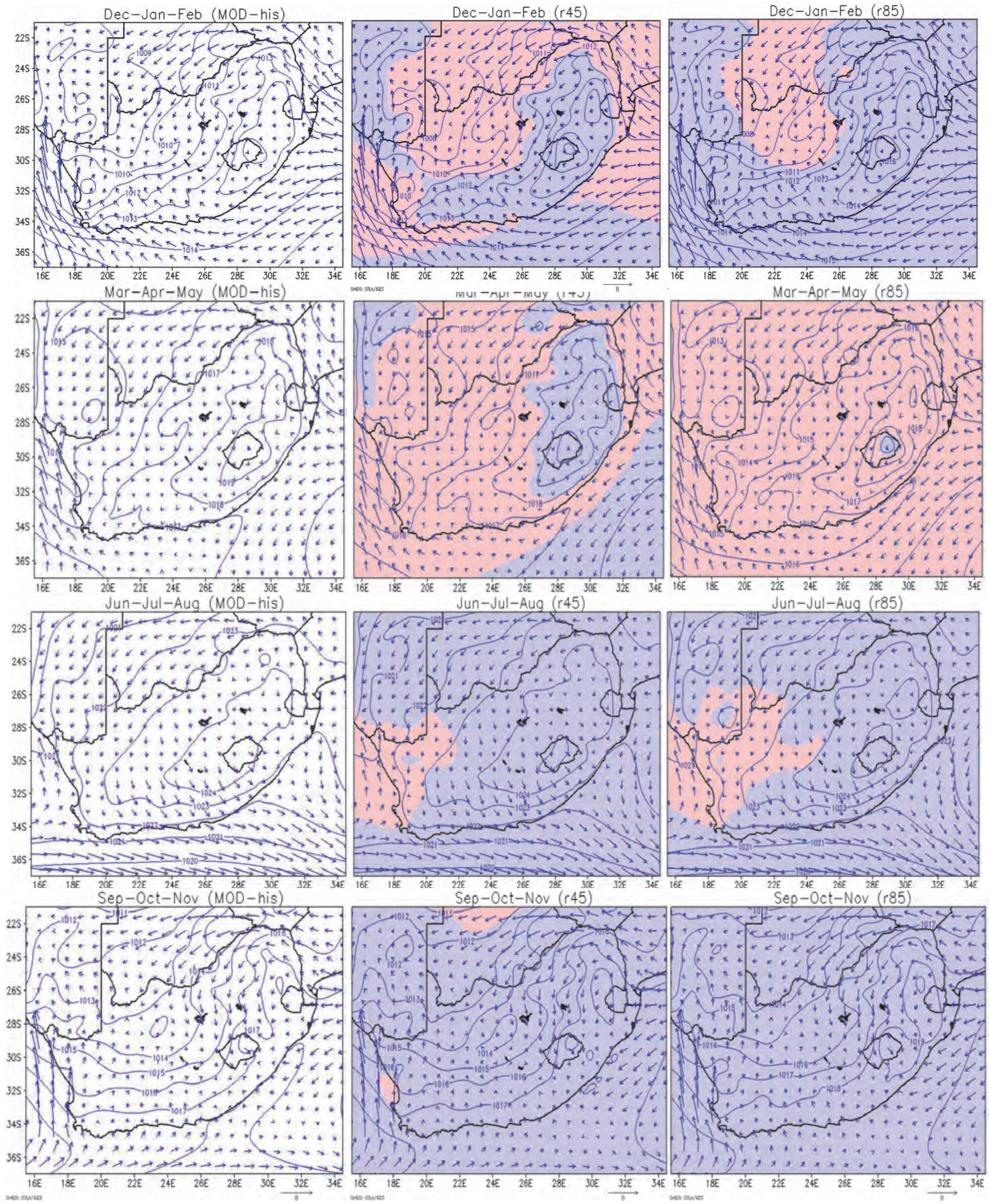

Figure 8.4:

Historically simulated (left column), Representative Concentration Pathway 4.5 (RCP 4.5) simulated (centre column) and RCP 8.5 simulated (right column) near-surface wind (vectors in m.s^{-1} – at 2 m above the surface) and Mean Sea Level Pressure (MSLP) (contours in hPa) climates for the 20-year historical (1986 to 2005: left column) and future projected period (2076 to 2095: centre and right columns) and for the seasons DJF, MAM, JJA and SON. Positive MSLP change anomalies (blue shaded) and negative MSLP change anomalies (red shaded) are relative to the historical simulations.

DJF, MAM, JJA and SON. Positive MSLP change anomalies (blue shaded) and negative MSLP change anomalies (red shaded) are relative to the historical simulations.

8.3.4 Model simulated projections for percentage frequencies of FTA events

Figures 8.5 and 8.6 depicts % frequencies of daily FTA events (left column) across the WRC Avontuur site domain, as projected for the DJF, MAM, JJA and SON seasons by the RCP 4.5 and RCP 8.5 scenario RCM simulations, respectively. The associated % frequency change (anomaly) values, relative to historical simulations (Figure 8.3), for the two scenarios are given at each 1 km x 1 km topographic elevation grid box on the right of each map in the left column of Figures 8.5 and 8.6. It is obvious that % frequency changes in FTA as a result of global warming are a direct function of changes in the near-surface wind speed and direction (see condition for FTA in Equation 2).

In results for the DJF season from the RCP 4.5 scenario simulations, projected winds vectors are, in agreement to historically simulated winds (Figure 8.3), from the south-east (Figure 8.5, left), and changes in the % frequency of FTA events are therefore relatively small (between -3% to +3% in 2076 to 2095: Figure 8.5 right). For the MAM season, projected wind vectors are in the opposite direction (easterly winds) of historical RCM simulated wind vectors (westerly winds). In both MAM historical and projected fields, % frequencies of > 75% and < 25% do occur, which is an indication of high variability in daily wind direction and speed across the Avontuur experimental site domain. The projected changes in % frequencies of FTA for MAM are in the range of -6% to +6%, which is relatively larger than changes for the DJF season. Historically RCM simulated winds for the JJA season are from a north-westerly direction, which is very similar to what have been projected. Relatively small % frequency changes of between -5% to +4% are therefore projected for JJA. In both historical and RCP4.5 simulations, southerly winds appear during SON, with % frequency anomalies of between -5% to +5%.

In RCP 8.5 scenario simulations (Figure 8.6, left), near surface winds for the DJF season are from the south-east, which are very similar to winds from the historical (Figure 8.3) and RCP 4.5 scenario simulations (Figure 8.5, left). Although still small, projected changes in the % frequency of daily FTAs are slightly greater and in the range of -6% to +8%. MAM is again associated with high spatial variability in the occurrence of FTA events, with south-easterly winds projected in the RCP 8.5 scenario simulations (compared to westerly and easterly winds in the historical and RCP 4.5 scenario simulations, respectively).

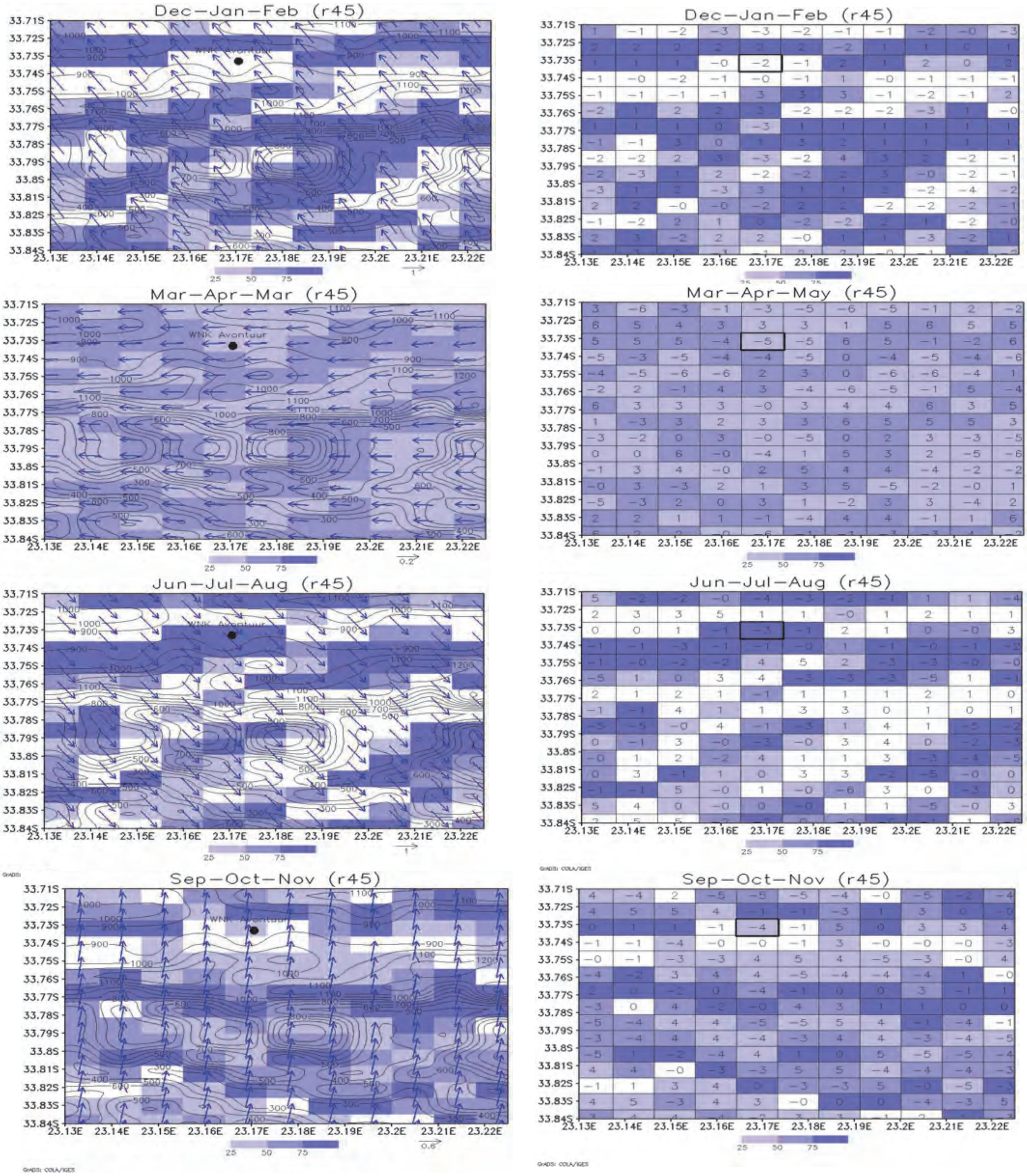

Figure 8.5:

Representative Concentration Pathway 4.5 (RCP 4.5) simulations for the projected percentage (%) frequency of daily Forced Topographical Ascent (FTA) events (shaded in the left and right columns) with wind climates (vectors in left column) and percentage change anomaly values (right column) relative to historical (1986 to 2005) simulations for the 20-year period 2076 to 2095, and for the seasons DJF, MAM ,JJA and SON in the Avontuur experimental site (black circle: left and dark square box: right) domain. Topography elevations (meters Above Mean Sea Level: AMSL) are depicted by contours in the left column.

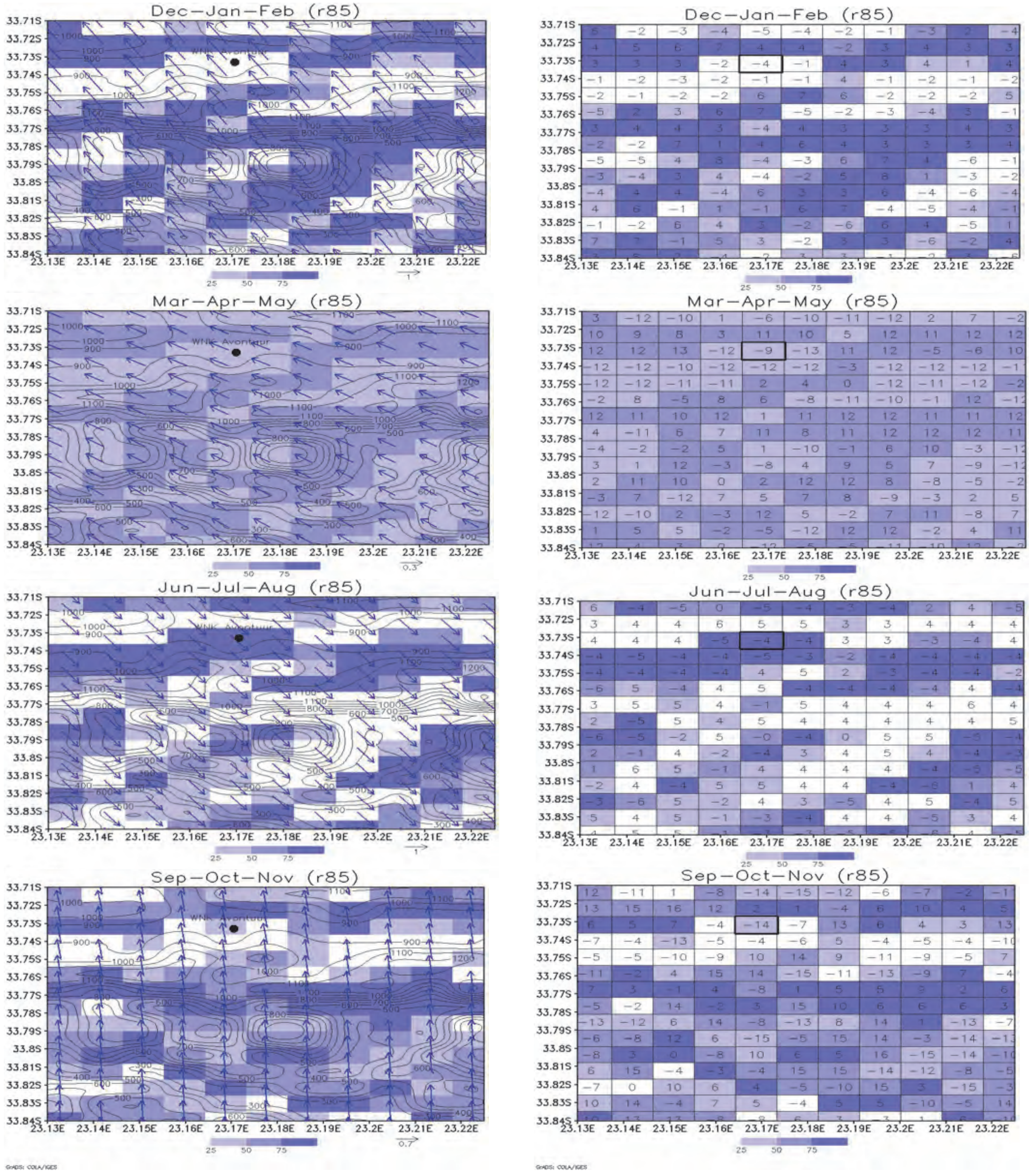

Figure 8.6: *Representative Concentration Pathway 8.5 (RCP 8.5) simulations for the projected percentage (%) frequency of daily Forced Topographical Ascent (FTA) events (shaded in the left and right columns) with wind climates (vectors in left column) and percentage change anomaly values (right column) relative to historical (1986 to 2005) simulations for the 20-year period 2076 to 2095, and for the seasons DJF, MAM, JJA and SON in the Avontuur experimental site (black circle: left and dark square box: right) domain. Topography elevations (meters Above Mean Sea Level: AMSL) are depicted by contours in the left column.*

Percentage frequency changes, which range from -13% to +13%, are therefore larger in comparison to most other simulations. Smaller % frequency changes (-6% to +6%) are projected for the winter season of JJA, where wind directions are consistent to previous findings (north-westerly winds). Previous findings indicated south-westerly orientated winds for the SON season, which turned south-easterly in the RCP 8.5 scenario simulations. With a high spatial consistency in % frequencies of daily FTA which are >75% and <25% in many topographical elevation grid boxes across the Avontuur experimental site domain, relatively small changes in wind direction could had resulted in greater changes in projected % frequencies (-15% to +16%).

In summary, for the DJF and JJA seasons wind directions are relatively consistent from historical to future projections, which resulted in relatively small changes in the % frequencies of FTA. MAM is associated with a higher spatial variability in winds, which is also reflected in the future projections, where relatively larger % changes occurred. SON has been characterised with larger spatial consistency in winds (relative to MAM), and wind direction % frequency changes in the RCP 8.5 simulations were therefore relatively large.

Instead of changes in winds and the % frequencies of FTA events across the Avontuur experimental site domain, the analysis could also be applied to a single grid box (e.g. the Avontuur experimental site – black circle and dark square box in Figures 8.5 and 8.6). However, because of its locality and uncertainties in RCM simulations, it is advisable to also view values and changes in such single grid boxes from the perspective of the larger surrounding patterns.

8.4 SYNTHESIS

The study provides valuable information regarding current and future fog water harvesting yields and site location. Results have indicated that fog frequencies might reduce somewhat (< 10%) in future, but not significantly. The site is would therefore still be suitable for fog water collection, although further improved technologies for optimising fog water yields are required. While the Avontuur experimental site domain was considered for local scale analyses, the methods use could also be applied at other sites along the South African escarpment, which could inform future research in identifying locations for optimal fog water harvesting yields.

Computational resources for the CCLM simulations were made available by the German Climate Computing Centre (DKRZ) through support from the German Federal Ministry of Education and Research (BMBF).

CONCLUSION

CHAPTER 9: CONCLUSIONS AND RECOMMENDATIONS

9.1 SUMMARY

The aim of the project was to optimise fog water harvesting in South Africa. The objectives were three-fold, namely to understand the physical and chemical characteristics of fog, to optimise the fog harvesting process, and from the latter, to develop novel products to measure and capture fog water. Two experimental sites were established, one in the mountains of the south-east coast in the vicinity of Avontuur, and the other near Lamberts Bay on the West Coast. Various structural designs and materials were tested over a period of three years. All large static structures included 3 m by 10 m vertical panels made of a double layer of 40% shade cloth. Water yield and weather data were collected on an hourly basis using Mike Cotton System AWSs and loggers that allowed remote access to data through a GPRS signal.

Comparison of yields collected on similar structures at the Avontuur and Lamberts Bay experimental sites, revealed considerable differences. On the one hand, a total of 53 534 litres of water were collected from the 90 m^2 triangular system Avontuur over a 35 month period, amounting to an average of more than 15 000 litres per month which translates to 0.56 $ℓ.m^{-2}.day^{-1}$. At Lamberts Bay average monthly yields were only 237 litres, i.e. 0.08 $ℓ.m^{-2}.day^{-1}$. Such low water collection rates along the West Coast mitigate against the use of fog water harvesting to supplement exiting water supplies since yields here are just too meagre to justify costs.

Of the designs tested, an open zig-zag FWCS with panels arranged at 60^o to each other was found to be more efficient than a closed triangular system or flat panels facing into the prevailing fog-bearing winds. Yields of 2.7 $ℓ.m^{-2}.day^{-1}$ were obtained from this 60^o system – considerably more than the 1 $ℓ.m^{-2}.day^{-1}$ collected from the triangular FWCS at Avontuur for the corresponding period. Moreover, over a distance of 100 m, the number of open zig-zag 60^o systems (10) would exceed that for the 90^o system (7) and the 120^o system (6). It is thus recommended that the zig-zag FWCS with a 60^o arrangement of panels be implemented in future fog water collection projects. In addition to its strength, this system also takes up less open space than the closed triangular system. An added bonus is that all parts are easily accessible for maintenance. The most efficient water collecting material tested during this project was found to be a 3-dimensional net obtained from Denkendorf in Germany. This is more than twice as effective as the locally produced material used in South Africa. Theoretically, if using the zig-zag design and the more efficient Denkendorf material in a FWCS, around five times more water could be harvested than were obtained from the FWCSs. However, this will still not make fog water collection viable on the West Coast, but will make a considerable difference to the viability of fog water collection in mountainous regions – provided that a suitable site is used.

The most important factors for identifying a suitable fog water collection sites are its altitude, the aspect, the elevation and the absence of topographical obstructions in the vicinity of the site. Altitude influences the rainfall, the liquid water content of the air and the wind speed, and is therefore a good estimator of water yields at levels ranging from 800 m to 2000 m AMSL. It is also crucial that the FWC site be exposed to moisture-bearing winds from the sea to ensure forced topographic uplift. If located on a leeward slope, descending air would heat adiabatically and the fog water droplets would evaporate. A steep slope on the seaward side of the site is also advantageous since this facilitates strong upward motion of moist air advected inland from the ocean, leading to adiabatic cooling and the formation of orographic clouds. Sites located at altitudes where cloud interception occurs can be expected to have highest water collection potential. However, if the site is not accessible or secure, it would be impractical to consider using it for fog water collection. Other factors such as the involvement and cooperation of local communities and land tenure of the site should also be considered when selecting a suitable fog water collection site.

An important output of the project was the development and design of the stronger triangular FWCS (in comparison to previously used horizontal line FWCS), and the refining of construction techniques to facilitate the construction process. Most important was that the design allowed the net panels (10 m by 1.5 m) to be constructed in a controlled environment such as the maintenance shed on the farm Belle-Vue. Using 15 mm polycop pipe through which the net cables ran ensured that the nets could be firmly fixed and further stabilised with vertical cables at net ends. The operational procedure whereby the whole system structure without the nets was first erected and stabilised was similar to procedures followed previously but the use of farm machinery during this phase made the operation both quick and safe. The use of novel brackets with nylon pulleys ensured that hanging of the nets was easy and safe. These brackets also ensured that the very small horizontal movement of the net cables did not cause any damage since most wind stresses on the nets were transferred to the anchors and not the poles. Great care was taken to set anchors in concrete to a depth of at least 1 m and that the soil above this was well compacted. Where significant rock occurred several 12 mm threaded rods were chemical anchor fixed to form a stable anchor position. In this way most (nearly all) of the problems experienced in previous projects were eliminated.

Arguably, one of the major achievements of the project was the development of novel products. To date, there is no instrument available on the market that can effectively measure low and intermittent water flows in isolated remote areas (without electricity). In this project a Low Flow Meter (LFM) was constructed for this purpose, and has proven to be reliable and accurate.

Another innovation was the construction of a rotating fog water collector (the Whirly) that could be used for fog water collection in areas or during periods with low wind speeds. Wind speed determines the amount/volume of fog that can move through a net and hence the volume of water droplets that can be collected. Wind speeds of between 4 and 5 $m.s^{-1}$ were previously found to be optimal for fog water harvesting. For this reason, if fog occurs during windless conditions (as often happens on the West Coast), water collection rates would be low. The Whirly was designed to automatically rotate during foggy periods (RH > 98%) and low wind speeds. The moving panels then sweep through the near-stationary fog, allowing for the collection of fog droplets. Although the Whirly was found to be more efficient than the stationary FWCS at Lamberts Bay, the small panels of the prototype could collect only small amounts of water. Up-scaling and improvement of this novel device needs to receive attention in future research.

In order to facilitate decision making, it was important to investigate how fog frequencies could be influenced by climate change. Since suitable fog water collection locations are often extremely site-specific, a technique using a fine resolution topography field, allowing forced topographic ascent (FTA) at individual topographic points associated with onshore synoptic winds to be determined as the most likely indicator for fog formation, was developed. FTA criteria were applied to projected synoptic wind patterns, and projections of fog frequency changes were obtained for the Avontuur experimental site. It was found that frequencies could decrease by <10% which indicates that fog water collection will still be feasible at Avontuur. The technique developed is not only of value for climate change projections at each topography point in South Africa (or where available), but would also be useful in identifying suitable fog water collection sites along the South African escarpment under current synoptic scale wind conditions.

In general, the aim of the project has been achieved and all the objectives addressed. The results of the project should contribute to the successful employment of fog water harvesting to supplement water supplies in the mountainous regions of the country. Ideally, fog water harvesting should be done in conjunction with roof-rainfall harvesting. While the latter would be suitable for domestic activities and ablution, the high quality water from the fog collectors could be used for drinking and cooking. Indeed, the quality of the water is so good that it could be bottled and sold in a niche market. It is necessary to investigate the feasibility of such a venture that could result in job creation and rural economic development.

9.2 SIGNIFICANCE OF THE RESEARCH

The significance of the research and outcomes can be measured in terms of the degree of compliance to WRC requirements.

9.2.1 Research outputs

Knowledge generated by the project can be measured against research outputs, such as the deliverables that were completed, the articles that were published and the papers that were presented at conferences.

The original project plan included 18 deliverables, in addition to this report which represents the 19th deliverable (these deliverables are listed in Appendix D). A total of eight papers were presented at national and international conferences. A further three articles have been published in accredited journals, and a further two more have been submitted and are in the review stage.

A list of articles and conference papers is presented below:

- KLEMM O, SCHEMENAUER RS, LUMMERICH A, CERECEDA P, MARZOL V, CORELL D, VAN HEERDEN J, REINHARD D, GHEREZGHIHER T, OLIVIER J, OSSES P, SARSOUR J, FROST E, ROTH-NEBELSICK A,ESTRELA M, VALIENTE J, FESSEHAYE GM, EBNER M, MIRANDA T, ANKER K. 2012: Fog as freshwater resource: Overview and perspectives. *Ambio,* (DOI) 10.1007/s13280-012-0247-8.
- OLIVIER J, VAN HEERDEN J, RAUTENBACH CJDEW, JONKER CJ 2012: Fog as an Alternative Water Source. Submitted Proceedings: SANCIAHS National Hydrology Symposium, Pretoria, 1-3 October 2012.
- PRETORIUS I & RAUTENBACH CJdeW 2013: Dynamic downscaling of prevailing synoptic-scale winds over the complex terrain of Mariepskop, South Africa. *Clean Air Journal*, 23 (1), 36-39.
- OLIVIER J, VAN HEERDEN J, RAUTENBACH CJDEW & JONKER CZ: Characteristics of fog events at Lambert's Bay on the west coast of South Africa. Submitted *Water SA,* January, 2014.
- RAUTENBACH CJDeW, DOSIO A, PANITZ HJ, SHONGWE M, OLIVIER J & VAN HEERDEN J: Projected influence of global warming on synoptic winds associated with the potential for mountain fog formation in South Africa. Submitted *Journal of Applied Climatology,* 2015.

CONFERENCES:

- GELDENHUYS M & VAN HEERDEN J, 2013: Estimating fog water yield potential on the Southern Cape Mountains of South Africa. South African Society for Atmospheric Science (SASAS), 26-27 September, 2013. Durban.
- PRETORIUS I and RAUTENBACH CJdeW, 2013: A CDF model of flow over the complex terrain of Mariepskop, South Africa. 29th Annual Conference, South African Society for Atmospheric Sciences (SASAS), 26-27 September, 2013, Durban.
- OLIVIER J, RAUTENBACH CJdeW, VAN HEERDEN J, MEINTJIES S & JONKER, CZ 2013: Optimising water from fog on the West Coast. Water Research Commission Symposium, Pretoria, September 2013.
- RAUTENBACH CJDeW, OLIVIER J & VAN HEERDEN J, 2014: Projected influence of global warming on synoptic winds associated with the potential for mountain fog formation in South Africa. FogLife colloquium, Gobabeb, Namibia, 2014.
- OLIVIER J, VAN HEERDEN J, RAUTENBACH CJDeW & JONKER CZ, 2014: The fog water collection project: Environmental Impact Assessment. FogLife colloquium, Gobabeb, Namibia, 2014.
- RAUTENBACH CJDeW, OLIVIER J & VAN HEERDEN J, 2014: Fog water harvesting in peri-urban environments. Peri-Urban conference, Sydney, Australia, July 2014.
- RAUTENBACH CJDeW, OLIVIER J & VAN HEERDEN J, 2012: Characteristics of fog water harvesting in mountainous terrains in South Africa. Mountain climate conference, Salzburg, Austria, 2012.
- RAUTENBACH CJDeW, OLIVIER J & VAN HEERDEN J, 2013: Modelling of winds and fog incidence at Mariepskop, Mpumalanga, South Africa. JAMSTEC-JST research conference, Yokohama, Japan.
- Other outputs include a data archive that can be accessed on www.avitrack.co.za/aws/showmodels.php.

9.2.2 Human Capital Development

The project was, to a great extent, interdisciplinary of nature in that the largest part of the project involved the actual development and construction of devices/FWCSs, development of scale models for testing in wind tunnels in engineering laboratories, the chemical analysis of water quality, GIS analyses and climate change projections. Most of these activities were associated with innovation. Five post-graduate students were directly involved in this project of whom all barring one have completed their degrees. Table 9.1 provides information on the degrees and topics.

Table 9.1: Summary of student capacity building

Name	ID	University	Degree for which enrolled	Student number	Title	Status
Albert Moloto	7412065560088	UP	MSc Meteorology	23463792	The occurrence and nature of fog at ORTIA	In progress
Markus Geldenhuys	910517 5252089	UP	BSc Hons Meteorology	10088904	Estimating fog water yield potential on the Southern Cape Mountains of South Africa.	Completed
Jody Mallinson	8808120064082	UP	BSc Civil Engineering	28391242	Investigating structural orientations of fog water harvesting systems	Completed
Ilse Pretorius	8612040194080	UP	MSc (Meteorology)	25050797	Dynamic downscaling of prevailing synoptic-scale winds over the complex terrain of Mariepskop, South Africa.	Completed
Christo Swanepoel	9101075056082	UP	BSc Civil Engineering	10177508	Optimisation of a structure for capturing water from fog	Completed

The post graduate students comprised one black male, two white males and two white females. Dr Liesl Dyson (white female) initiated and coordinated post graduate student participation in the fog project at the Tshanowa School while Mr Robert Maisha (black male) was responsible for the erection of the new triangular FWCS at the School. Dr Mxolisi Shongwe (black male) assisted with the climate change projections. The team members were all white males, with the exception of Prof Olivier who is a white female. The project thus fulfils requirement concerning transformation and redress.

In addition to the team members and students directly involved in the project, capacity building, through direct and indirect participation in the project or knowledge of the project, took place over a wide spectrum of sectors. Farmers and farm workers have also been closely involved with the fog projects at both experimental sites. A number of these workers have gained sufficient knowledge of the systems to understand their importance as a source of water and could, with additional training, be in a position to erect similar systems elsewhere. Information passed on by word of mouth has spread throughout neighbouring communities and the villages/hamlets, adding to capacity building in these rural areas.

The fog water harvesting projects have generated a considerable amount of interest in the media. The program *Shoreline* that was aired on national TV during September 2013 included an interview with Prof van Heerden at the Lamberts Bay site. Inserts on fog water harvesting had also been presented as part of the SABC1 and 2 news broadcasts during earlier years. A number of radio interviews, including 'Ecoforum' on Radio Sonder Grense (RSG), Radio Pretoria and Cape Radio, a newspaper article in the Sunday Times and others in *Water Wheel* and *Landbou Nuus,* have served to inform the broader public of the projects. This has elicited interest in the educational sector resulting in numerous small-scale mock-ups of fog water collectors being entered at science festivals over the last few years.

Organisations with interest in fog water harvesting projects include South African Breweries (SAB) and the South African Weather Service (SAWS). These two organisations were involved in replacing the old FWCS with a new triangular FWCS at the Tshanowa School during 2014. Mr. Robert Maisha, ably assisted by Meteorology and Civil Engineering students as well as Mr. Raymond Magaela (a SAWS staff member from the Thohoyandou office) completed this task in March 2013. Government Departments that have taken note of this WRC project thus includes the Department of Environmental Affairs as well as the Department of Land Reform and Rural Development.

9.2.3 Inform policy and decision making

- It is vital that the concept of fog water collection be recognized and included in the government's water provision strategies (e.g. the National Water Resources Management Strategy) and general resource development plans;
- In view of the environment benefits and potential (albeit limited) for job creation and rural development, the Department of Land Reform and Rural Development as well as municipalities should be encouraged to take note of this alternative source of water, and implement the technology and knowledge gained from the project, in suitable areas;
- Incentives in the form of funding should be allocated to further fog-related research. This is already happening to some extent with new mountain research by the South African Environmental Observation Network (SAEON) which is a National Research Foundation (NRF) facility. Research on investigating the most suitable material for fog water collection could contribute significantly to improving fog water yields. Encouraging is that the NRF has approved a fog water collection material science project to the University of Pretoria's

Department of Chemical Engineering as part of their competitive funding to rated researchers that will start in 2015. This project was inspired by the WRC research team;

- It is important that a comprehensive water analysis (for all minerals mentioned in the DWAF Guidelines for Domestic Use) should be a prerequisite to comply with before fog water is consumed or bottled in future.

9.2.4 New products and services for economic development

The project succeeded in making a major contribution in the development of new products and services for economic development. Novel devices, such as the LFM, the Whirly and the variable direction fog catcher (triangular FWCS) have been developed. A technique aimed at identifying suitable fog water collection sites by looking at onshore winds and FTA was developed and applied in climate change research.

9.2.5 Sustainable development solutions and empowerment of communities

The eventual outcome of this project is provision of water to water-poor communities living in the mountainous regions of the South Africa. Accessibility to good quality water would empower communities, and possibly lead to improvement in health, education, motivation (improvement in the quality of life) and subsequently, economic development. Innovations from the project resulted in the erection of a new triangular FWCS at the Tshanowa School, which made a huge difference in the provision of water to the school (and in some cases, to community members). The Tshanowa development is well-known in most government structures in the Limpopo Province, and beyond.

A new project proposal, aimed at the implementation of research output from this project in the development of a farm worker housing project in the vicinity of Avontuur, was submitted to the WRC in 2014. Sustainable development of the resource and empowerment of the community formed the main focus of this new project proposal. Unfortunately, it was deemed to be lacking in the research component relative to the developmental component. It is hoped that other organisations (e.g. Provincial Government) might consider funding this project since it would form a flagship model for similar developments in other parts of the country.

In the project most emphasis was placed on applying the research output to optimise water resource use. If fog water collection could be implemented successfully in communities, the outcome from this project can contribute, albeit in a small way, to the problem of water shortages in South Africa.

9.3 RECOMMENDATIONS

Despite the number of 'successes' as indicated above, the research also had some short-comings which could be addressed as opportunities in future. These included:

- More research is required on the development of a simple but reliable technique for measuring liquid water content of fog-bearing air.
- A scaled-up version of the Whirly showed serious flaws. A stronger and more robust model needs to be developed, based on the experience gained in this project;
- Some of the rain gauges became blocked and did not function effectively, which led to some data loss.

It is thus recommended that:

- More research – especially on materials and techniques to quantify fog droplet sizes and liquid water content – is required;
- A 60° zig-zag system stretching some 200 m might provide the opportunity to truly test the structural and yield properties of an operational size system. Such a system could be erected at Avontuur where infrastructure exists and where the water could be piped to the proposed housing development for farm workers;
- The Avontuur region (slopes of the Zondachsberg) might be ideal for testing the fog water yield / elevation relationship as measurements can extend from below 800 m to the top of the mountain with an altitude of 1300 m. Studies could also extend to the leeward side;
- The role of the Klein Karoo heat low in sucking maritime air up the mountain slopes, providing abundant upslope fog, during the very dry summer months could be investigated in more detail;
- The results of the research should be disseminated to farmers, government officials and local municipalities;
- Research should be conducted on identifying suitable sites prior to any development;
- The database must be kept up to date with new data;
- Both altitude and FTA could serve as good indicators for the potential for fog formation. However, further research, preferably with atmospheric modelling involved, is required to combine these indicators in order to develop optimum fog formation potential maps for South Africa.
- South Africa needs to become part of the global trend in use of alternative resources.

REFERENCES

ABYALHAMAYAL HI & GANDHIDASAN P (2010) Design and testing of large fog collectors for water harvesting in Asir region, Kingdom of Saudi Arabia. In: 5th International Conference on Fog, Fog Collection and Dew, 25-30 July, 2010, Munster, Germany, 116-119.

AHMED AFM, SINGH RP & ELMUBARAK AH (1990) Chemistry of atmospheric precipitation at Western Arabian Gulf Coast. *Atmospheric Environment,* 24(12), 2927-2934.

ALKAMA R, BELAMARI S, BRAUN A, COQUART L & CHAUVIN F (2011) The CNRM-CM5.1 global climate model: description and basic evaluation. *Clim. Dyn*., 40, 2091-2121.

APIGIAN JH (2005) A critical look at the development of fog water collection in Nepal. Report prepared for the Nepal Community Development Foundation and Nepal Water for Health. Kathmandu, March 2005. 128pp.

AZORIN C, CORRELL D, ESTRELA MJ & VALIENTE JA (2010) Fog water collection under sea breeze conditions in the western Mediterranean basin (Valencia Region, Spain). In: 5th International Conference on Fog, Fog Collection and Dew, 25-30 July, 2010, Munster, Germany, 65-68.

BAYGI MM (2008) The implementation of fog water collection systems in northeast of Iran. *International Journal of Pure and Applied Physics,* 4, 13-21.

BRESCI E (2001) Fog collector influence on the wind velocity field. 2nd International Conference on Fog and Fog Collection, St John's, Newfoundland, Canada. 15-20 July 2001, 219-222.

CAESAR J, PALIN E, LIDDICOAT S, LOWE J, BURKE E, PARDAENS A, SANDERSON M & KAHANA R (2013) Response of the HadGEM2 Earth System Model to Future Greenhouse Gas Emissions Pathways to the Year 2300. *J. Climate,* 26, 3275-3284.

CERECEDA P & SCHEMENAUER RS (1988) The role of topography and windflow in high elevation fog water collection. In: Third International Conference in Southern Hemisphere Meteorology and Oceanography, Buenos Aires, Brazil.

CERECEDA P & SCHEMENAUER RS (1993) High elevation fog as a water supply for developing countries. In: 6th International Conference on Rainwater Catchment Systems, Nairobi, Kenya.

DEE D P, UPPALA SM, SIMMONS AJ, BERRISFORD P, POLI P, KOBAYASHI S, ANDRAE U, BALMASEDA MA, BALSAMO G, BAUER P, BECHTOLD P, BELJAARS ACM, VAN DE BERG L, BIDLOT J, BORMANN N, DELSOL C, DRAGANI R, FUENTES M, GEER AJ, HAIMBERGER L, HEALY SB, HERSBACH H, HÓLM EV, ISAKSEN L, KÅLLBERG P, KÖHLER M, MATRICARDI M, MCNALLY AP, MONGE-SANZ BM, MORCRETTE J-J, PARK B-K, PEUBEY C, DE ROSNAY P, TAVOLATO C, THÉPAUT J-N & VITART F (2011) The ERA-Interim reanalysis: configuration and performance of the data assimilation system. *Q.J.R. Meteorol. Soc*., 137, 553-597. DOI: 10.1002/qj.828.

DEPARTMENT OF ENVIRONMENTAL AFFAIRS AND TOURISM (2000) Environmental Potential Atlas for South Africa. DEAT, Pretoria. Department of Water Affairs (1986) Management of the Water Resources of the Republic of South Africa. Government Printer, Pretoria.

DEPARTMENT OF WATER AFFAIRS (1986) Management of the Water Resources of the Republic of South Africa. Government Printer, Pretoria. 56pp.

DEPARTMENT OF WATER AFFAIRS AND FORESTRY (DWAF) (1996) *South African Water Quality Guidelines for Domestic Use* (2nd edn.), Pretoria.

DORATHY A, STEWART O & ESSENWANGER M (1982) A survey of fog and related optical propagation characteristics. *Reviews of Geophysics,* 20(3), 481.

DOSIO A, PANITZ H-J, SCHUBERT-FRISIUS M, LUETHI D (2014) Dynamically downscaling of CMPI5 CGMs over CORDEX-Africa with COSMO-CLM: analysis of the added value over the present climate, *Clim. Dyn., submitted*

ECKARDT FD & SCHEMENAUER RS (1998) Fog water chemistry in the Namib desert, Namibia. *Atmospheric Environment*, 32(14/15), 2595-2599.

EDEN DISTRICT MANAGEMENT AREA SPATIAL DEVELOPMENT FRAMEWORK, 2004.

EMA M & MIYAWAKI E (2001). Effects of monobutyl phthalate on reproductive function in pregnant and pseudopregnant rats. *Reprod.Toxicol.,* 15**,** 261-267.

ENDRIS HS, OMONDI P, JAIN S, LENNARD C, HEWITSON B, CHANG'A L, AWANGE JL, DOSIO A, KETIEM P, NIKULIN G, PANITZ H-J, BÜCHNER M, STORDAL F, TAZALIKA L (2013) Assessment of the performance of CORDEX regional climate models in simulating East African rainfall. *J.Clim.,* 26 (21), pp. 8453-8475. DOI: 10.1175/JCLI-D-12-00708.1

ESCOBAR CM, LOPEZ A, ARISTIZABAL HF & MOLINA WM (2010) Operational fog collection and its role in environmental education and social reintegration: A case study in Colombia. In: 5th International Conference on Fog, Fog Collection and Dew, 25- 30 July, 2010, Munster, Germany, 133.

ESFANDIAMAJAD A, AHANGAR R, KAMALIAN UR & SANGCHOULI T (2010) Feasibility studies for water harvesting from fog and atmospheric moisture in Horm ozgan coastal zone (south of Iran). In: 5th International Conference on Fog, Fog Collection and Dew, 25- 30 July, 2010, Munster, Germany, 2-6.

ESTIE KE (1984) Forecasting the formation and movement of coastal lows. Paper presented at the Coastal Low Workshop, Simonstown, March 1984, 17-27.

FUENZALIDA H (1988) Meteorological aspects of water collection from stratocumuli in northern Chile. Paper presented at the 3rd International Conference on Southern Hemisphere Meteorology, Brazil, 156-161.

FUGGLE RF AND RABIE MA (1992) *Environmental management in South Africa.* Juta & C. Ltd.: Cape Town.

FUZZI S, GAZZI M, PESCI C & VICENTINI V (1980) A linear impactor for fog droplet sampling. *Atmospheric Environment,* 14(7), 797-801.

GARLAND JA (1971) Some fog droplet size distributions obtained by an impaction method, *Quarterly Journal of the Royal Meteorological Society,* 97(414), 483-494.

GBOBANIYI E, SARR A, SYLLA MB, DIALLO I, LENNARD C, DOSIO A, DHIÉDIOU A, KAMGA A, KLUTSE NAB, HEWITSON B, NIKULIN G, LAMPTEY B (2014) Climatology, Annual Cycle and Interannual Variability of Precipitation and Temperature in CORDEX Regional Climate Models Simulation over West Africa, *Int. J. Climatol.,* DOI: 10.1002/joc.3834.

GHEREZGHIHER T (2010) Fog collection pilot project (FCPP) in the Eastern Escarpments of Eritrea. In: 5th International Conference on Fog, Fog Collection and Dew, 25- 30 July, 2010, Munster, Germany, 252.

GIORGETTA MA, JUNGCLAUS JH, REICK CH, LEGUTKE S, BROVKIN V, CRUEGER T, ESCH M, FIEG K, GLUSHAK K, GAYLER V, HAAK H, HOLLWEG H-D, ILYINA T, KINNE S, KORNBLUEH L, MATEI D, MAURITSEN T, MIKOLAJEWICZ U, MUELLER WA, NOTZ D, RADDATZ T, RAST S, REDLER R, ROECKNER E, SCHMIDT H, SCHNUR R, SEGSCHNEIDER J, SIX K, STOCKHAUSE M, WEGNER J, WIDMANN H, WIENERS K-H, CLAUSSEN M, MAROTZKE J, & STEVENS B (2013) Climate and carbon cycle changes from 1850 to 2100 in MPI-ESM simulations for the coupled model inter-comparison project phase 5. *Journal of Advances in Modeling Earth Systems,* 5(3), 572-597.

GIORGI F, JONES C & ASRAR G (2009) *Addressing climate information needs at the regional level: the CORDEX framework.* World Meteorological Organization (WMO) Bulletin 58(July), 175-183.

GLOBE TASK TEAN AND OTHERS (HASTINGS DA, DUNBAR PK, ELPHINGSTONE GM, BOOTZ M, MURAKAMI H, MARUYAMA H, HOLLAND P, PAYNE j, BRYANT NA, LOGAN TL, MULLER J-P, SCHREIER G & MACDONALD JS), EDS. (1999*) The Global Land One-kilometer Base Elevation (GLOBE) Digital Elevation Model, Version 1.0, National Oceanic and Atmospheric Administration (NOAA), National Geophysical Data Center, 325 Broadway, Colorado 80305-3328, U.S.A. (http://www.ngdc.noaa.gov/mgg/topo/globe.html)*

HAZELEGER W, WANG X, SEVERIJNS C, STEFANESCU S, BINTANJA R, STERL A, WYSER K, SEMMLER T, YANG S, VAN DEN HURK B, VAN NOIJE T, VAN DER LINDEN E & VAND DER WIEL K (2012) EC-Earth V2: description and validation of a new seamless Earth system prediction model. *Clim. Dyn.,* 39(11), 2611-2629.

http://en.wikipedia.org/wiki/Habitat_fragmentation [accessed 4 Feb 2013.]

http://gardeningsolutions.ifas.ufl.edu

http://myfolia.com

http://www.http://www.info.gov.za/gazette/notices/1999/2485.htm

http://www.plantzafrica.com

IPCC (2013) Climate Change 2013: *The Physical Science Basis. Contribution of Working Group I to the Fifth Assessment Report of the Intergovernmental Panel on Climate Change [Stocker, T.F., D. Qin, G.-K. Plattner, M. Tignor, S.K. Allen, J. Boschung, A. Nauels, Y Xia, V. Bex and P.M. Midgley (eds.)]. Cambridge University Press, Cambridge, United Kingdom and New York, NY, USA, 1535pp.*

JUVIK JO & PERREIRA DJ (1974) Fog Interception on Mauna Loa, Hawaii. *Association of American Geographers,* 6, 22-25.

KALOGNOMOU E-A, LENNARD C, SHONGWE M, PINTO I, FAVRE A, KENT M, HEWITSON B, DOSIO A, NIKULIN G, PANITZ H-J & BÜCHNER M (2013) A diagnostic evaluation of precipitation in CORDEX models over southern Africa. *Journal of Climate*, 26, 9477-9506.

KENNISH MJ (1989) *Practical handbook of marine sciences*. Boca Raton: CRC Press,

KIM J, WALISER DE, MATTMANN CA, GOODALE CE, HART AF, ZIMDARS P, CRICHTON DJ, JONES C, NIKULIN G, HEWITSON B, JACK C, LENNARD C, FAVRE A (2013) Evaluation of the CORDEX-Africa multi-RCM hindcast: systematic model errors. Climate Dynamics DOI 10.1007/s00382-013-1751-7.

KUMAI M (1973) Arctic Fog Droplet Size Distribution and Its Effect on Light Attenuation. *J. Atmos. Sci.*, 30, 635-643

LATINI G, VERROTTI A AND DE FELICE C (2004). Di-2-ethylhexyl phthalate and endocrine disruption: a review. *Curr. Drug Targets Immune Endocr. Metabol. Disor.,* 4(1)**,** 37-40.

LEKOUCH I, MUSELLI M, KABBACHI B, OUAZZANI J, MELNYTCHOUK-MILIMOUK I & BEYSENS D (2011) Dew, fog and rain as supplementary sources of water in south-western Morocco. *Energy,* 36, 2257-2265.

LOVEKAMP-SWAN T AND DAVIS BJ (2003). Mechanisms of phthalate ester toxicity in the female reproductive system. *Environ. Health Perspect.,* 111, 139-146.

MACQUARRIE KIA, POKHREL A, SHRESTHA Y, OSSES P, SCHEMENAUER RS, VITEZ F, KOWALCHUK K & TAYLOR R (2001) Results from high elevation fog water supply project in Nepal. In: 2nd International Conference on Fog and fog Collection, St Johns, Canada, 15-20 July 2001, 227-229.

MALLET J (2014) Personal Communication, 15 January 2014. Mr Jack Malett, 3 Janus Lalandi Street, Lamberts Bay 8130.

MARLOTH R (1904) Results of experiments on Table Mountain for ascertaining the amount of moisture deposited from SE clouds. *Transactions of the SA Philosophical Society*, 14, 403-408.

MARLOTH R (1907) Results of further experiments on Table Mountain for ascertaining the amount of moisture deposited from SE clouds. *Transactions of the SA Philosophical Society*, 16, 97-105.

MARZOL V, SÁNCHEZ JL & YANES A (2011) Meteorological patterns and fog water collection in Morocco and the Canary Islands. *Erdkunde*, 65(3), 291-303.

NAGEL JF (1956) Fog precipitation on Table Mountain. *Quarterly Journal of the Royal Meteorological Society,* 82, 452-460.

NAGEL JF (1959) The measurement of fog precipitation. South African Weather Bureau News Letter No. 125, 1-9.

NEL W & SUMNER PD (2005) First rainfall data from the KZN Drakensberg escarpment edge (2002 and 2003). *Water SA*, 31, 399-402.

NEL W, REYNHARDT DA & SUMNER PD (2010) Effect of altitude on erosive characteristics of concurrent rainfall events in the northern KwaZulu-Natal Drakensberg. *Water SA,* 36(4), 509-512.

NIKULIN G, JONES C, GIORGI F, ASRAR G, BUECHNER M, CEREZO-MOTA R, CHRISTENSEN OBS, DEQUE' M, FERNANDEZ J, HANSLER A, VAN MEIJGAARD E, SAMUELSSON P, SYLLA MB & SUSHAMA L (2012) Precipitation Climatology in an Ensemble of CORDEXAfrica Regional Climate Simulations. Journal of Climate 25(18):6057-6078. DOI 10.1175/JCLI-D-11-00375.1.

NERIN C, CACHO J AND GANCEDO P (1993). Plasticisers from printing inks in a selection of food packagings and their migration to food. *Food Additives and Contaminants, 10,* 453-460.

OBERHOLZER B (2005) Guideline for involving visual & aesthetic specialists in EIA processes: Edition 1. CSIR Report No ENV-S-C 2005 053 F. Republic of South Africa, Provincial Government of the Western Cape, Department of Environmental Affairs & Development Planning, Cape Town.

OKE TR (1987) *Boundary Layer Climates* 2nd *edition*. Cambridge: University press.

OLIVIER J (1999) A Review of Research in South African Meteorology and Atmospheric Sciences: 1995-1998. *South African Journal of Science*, 95, 288-306.

OLIVIER J (2001) A prototype fog water collection system in the Northern Province of South Africa. In: 2nd International Conference on Fog and Fog Collection. St John's, Newfoundland, Canada, 15-20 July 2001, 239-242.

OLIVIER J (2002) Fog water harvesting along the West Coast of South Africa: A feasibility study. *Water SA*, 28(4), 349-360.

OLIVIER J (2004) Fog Harvesting: An alternative source of water on the west coast of South Africa. *GeoJournal,* 61, 203-214.

OLIVIER J & RAUTENBACH CJdeW (2002) Implementation of fog water collection systems in South Africa. *Atmospheric Research,* 64, 227-238.

OLIVIER J & STOCKTON PL (1989) The influence of upwelling extent on fog incidence at Luderitz, southern Africa. *International Journal of Climatology,* 9, 69-75.

OLIVIER J & VAN HEERDEN J (1999) *The South African Fog Water Collection Project*. Water Research Commission Report No. 671/1/99. 159pp.

OLIVIER J & VAN HEERDEN (2002) Implementation of an operational prototype fog water collection system. Water Research Commission Report No. 902/1/02. 91pp.

PANITZ H-J, DOSIO A, BUECHNER M, LUETHI D & KEULER K (2014) COSMO-CLM (CCLM) climate simulations over CORDEX Africa domain: Analysis of the ERA-Interim driven simulations at 0.44 and 0.22 deg. resolution, *Clim. Dyn*, DOI: 10.1007/s00382-013-1834-5.

PARKS LG, OSTBY JS AND LAMBRIGHT CR (2000). The plasticizer diethylhexyl phthalate induces malformations by decreasing fetal testosterone synthesis during sexual differentiation in the male rat. *Toxicol. Sci*., 58**,** 339-349.

RAUTENBACH CJdeW & OLIVIER J (2001) An operational " Water from Fog" initiative at Lepelfontein along the West Coast of South Africa. In: 2nd International Conference on Fog and Fog Collection St John's, Newfoundland, Canada, 15-20 July 2001, 243-245.

RIAHI K, ROA S, KREY V, CHO C, CHIRKOV V, FISHER G, KINDERMANN G, NAKICENOVIC N & RAFAJ P (2011) RCP 8.5 – A scenario of comparatively high greenhouse gas emissions. *Climate Change, 109, 33-57.*

SCHEMENAUER RS & CERECEDA P (1991) Fog water collection in arid coastal locations. *Ambio,* 20, 303-308.

SCHEMANAUER RS & CERECEDA P (1992) Water from fog-covered mountains. *Waterlines*, 10(4), 275-290.

SCHEMANAUER RS & CERECEDA P (1993) Meteorological conditions at a coastal fog collection site in Peru. *Atmosfera*, 6, 175-188.

SCHEMANAUER RS & CERECEDA P (1994) Fog collection's role in water planning for developing countries. *Natural Resources Forum*, 18(2), 91-100.

SCHEMENAUER RS & JOE PI (1989) The collection efficiency of a massive fog collector. *Atmospheric Research,* 24, 53-69.

SCHEMANAUER RS, CERECEDA P & CARVAJAL N (1987) Measurements of fog water deposition and their relationships to terrain features. *Journal of Climate and Applied Meteorology,* 26, 1285-1291.

SCHEMENAUER RS, FUENZALIDA H & CERECEDA P (1988) A neglected water resource: The Camanchaca of South America. *Bulletin of the American Meteorological Society,* 69, 138-147.

SCHEMENAUER RS, OSSES P, LARA F, ZYWINA C & CERECEDA P (2001) Fog collection in the Dominican Republic. In: 2nd International Conference on Fog and fog Collection, St Johns, Canada, 15-20 July 2001, 235-238.

SHARPE RM AND IRVINE DS (2004). How strong is the evidence of a link between environmental chemicals and adverse effects on human reproductive health? *BMJ*, 328, 447-451.

SCHULZE RE (1979) Hydrology and water resources of the Drakensberg. Natal Town and Regional Planning Commission, Pietermaritzburg. 179pp.

SCHUTTE JM (1971) Die onttrekking van water uit die lae op Mariepskop. Technical Note no. 20. Division of Hydrological Research, Department of Water Affairs, Pretoria.

SOUTH AFRICAN NATIONAL STANDARDS (SANS) (2011) Drinking water standards (SANS 241:2005, 2011), South African Bureau of Standards, Pretoria.

SOUTH AFRICAN WEATHER BUREAU (SAWB) (1986) *The Climate of South Africa: Climate statistics up to 1984 WB40 .* Department of Environmental Affairs, Pretoria.

STRUTHERS MJ (1997) *Water from Fog Study on the Cape West Coast December 1995 to May 1997*. Progress report, CSIR Report no ENV/S- 1 97018.

SUAU C (2010) Fog collection and sustainable architecture in Atacama coast. In:, 5th International Conference on Fog, Fog Collection and Dew, 25- 30 July, 2010, Munster, Germany, 179-188.

TALJAARD JJ (1985) Cut-off lows in the South African Region, Technical Paper no. 14, South African Weather Bureau (SAWB), Department of Transport, Pretoria, South Africa, 153pp.

TALJAARD JJ (1995) Atmospheric Circulation Systems, Synoptic Climatology and Weather Phenomena of South Africa, Part 4: Rainfall in South Africa, Technical Paper no. 30, South African Weather Bureau (SAWB), Department of Environmental Affairs and Tourism, Pretoria, South Africa, 42pp.

TAYLOR KE, STOUFFER RJ & MEEHL GA (2012) An Overview of CMIP5 and the experimental design. *Bull. Amer. Meteor. Soc.,* 93, 485-498.

THOMPSON C (2008). Build it. Share it. Profit. Can open source hardware work. *Wired Magazine*, 16(11), 16-11.

TODD MC & WASHINGTON R (1999) Circulation anomalies associated with tropical tropical-temperate troughs over southern Africa and the south-west Indian Ocean. *Climate Dynamics*, 15, 937-951.

TSUTSUMI T, ICHIHARA T, KAWABE M, YOSHINO H, ASAMOTO M, SUZUKI S AND SHIRAI T (2004). Renal toxicity induced by folic acid is associated with the enhancement of male reproductive toxicity of di(n-butyl)phthalate in rats. *Reprod. Toxicol.,* 18 (1):35-42.

TYSON PD, PRESTON-WHYTE RA & SCHULZE RE (1976) The climate of the Drakensberg. Natal Town and Regional Planning Commission, Pietermaritzburg. 82pp

VAN HEERDEN J & HURRY L (1987). Southern Africa's weather patterns: an introductory guide. Acacia Publishers (ISBN: 0-86817-045-3), Pretoria, South Africa. 95pp.

VAN HEERDEN J, OLIVIER J & VAN SCHALKWYK L (2010) Fog water systems in South Africa: An update. Conference book: 5th International conference on fog, fog collection and dew, Munich, Germany, 25-30 July, 2010, 160.

VOLDOIRE A, SANCHEZ-GOMEZ E, SALAS Y MÉLIA D, DECHARME B, CASSOU C, SÉNÉSI S, VALCKE S, BEAU I, ALIAS A, CHEVALLIER M, DÉQUÉ M, DESHAYES J, DOUVILLE H, FERNANDEZ E, MADEC G, MAISONNAVE E, MOINE M-P, PLANTON S, SAINT-MARTIN D, SZOPA S, TYTECA S, ALKAMA R, BELAMARI S, BRAUN A, COQUART L & CHAUVIN F (2011) The CNRM-CM5.1 global climate model: description and basic evaluation, *Clim. Dyn*., 40, 2091-2121.

WILSON VS, LAMBRIGHT C AND FURR J (2004). Phthalate ester-induced gubernacular lesions are associated with reduced insl3 gene expression in the fetal rat testis, *Toxicol. Lett*. 146, 207-215.

WORLD HEALTH ORGANISATION (WHO) (2011) Guidelines for drinking-water quality. 4th Ben-hua, Y. U. A. N.(2012) Design of the Temperature Measurement System Based on Arduino Board [J]. *Journal of Anhui Agricultural Sciences* 8, WHO Geneva.

ZAGHLOUL MS (2014) GSM-GPRS Arduino Shield (GS-001) with SIM 900 chip module in wireless data transmission system for data acquisition and control of power induction furnace.

APPENDIX A

ADDENDUM 8.1 PHYSICAL COMPOSITIO AND MACRO-ELEMENTS IN WATER AT LAMBERTS BAY AND AVONTUUR

	pH	pHs	SAR	EC (mS/m)	F	NO_2	NO3	Cl	SO_4	PO_4	CO_3	HCO_3	Na_2CO_3	$NaHCO_3$	alk	Temp Hard	Perm Hard	Na	K	Ca	Mg	B	TDS
LB																							
S 24.6.14	6.45	7.83	15.98	552	0.43	25.17	20.51	313.12	77.77	1.18	0	68.93	0	0	56.5	56.5	707.54	1014.1	53.15	80.29	136.39	0.18	1756.54
S 23.8.14	8.04	9.26	3.33	41	0.13	0	29.17	133.71	17.03	1.77	0	17.08	0	0	14	14	47.67	59.89	4.47	10.69	8.33	0.05	273.46
ave S	***7.25***	***8.55***	***9.66***	***296.50***	***0.28***	***12.59***	***24.84***	***223.42***	***47.40***	***1.48***	***0.00***	***43.01***	***0.00***	***0.00***	***35.25***	***35.25***	***377.61***	***537.00***	***28.81***	***45.49***	***72.36***	***0.12***	***1015.00***
N 24.6.14	6.48	8.81	8.46	157	0.19	15.15	29.32	363.13	69.24	5.06	0	21.35	0	0	17.5	17.5	197.07	283.91	15.74	26.88	35.47	0.11	854.33
N 13.5.14	6.13	7.85	14.14	468	0.79	59.63	32.98	1200.16	237.21	0	0	59.78	0	0	49	49	614.38	835.73	35.91	88.77	106.62	0.22	2627.11
N 31.7.14	6.21	8.79	9.52	245	0	0	37.14	747.84	109.11	0	0	18.3	0	0	15	15	251.76	356.86	16.18	32.85	44.6	0.09	1352.85
N 23.8.14	7.09	8.7	10.08	252	0.52	0	67.1	924.23	115.2	0.87	0	20.74	0	0	17	17	251.91	379.52	18.12	36.15	43.15	0.08	1594.63
Ave N	***6.48***	***8.54***	***10.55***	***280.50***	***0.38***	***18.70***	***41.64***	***808.84***	***132.69***	***1.48***	***0.00***	***30.04***	***0.00***	***0.00***	***24.63***	***24.63***	***328.78***	***464.01***	***21.49***	***46.16***	***57.46***	***0.13***	***1607.23***
WSW 24.6.14	6.53	8.5	7.67	147	0.52	0	29.52	309.57	69.72	1.93	0	38.43	0	0	31.5	31.5	171.34	250.27	18.51	30.1	30.59	0.13	759.79
WSW 23.8.14	6.9	8.98	8.24	214	0	0.47	89.62	714.83	89.73	0	0	10.98	0	0	9	9	260.49	310.57	14.22	36.12	43.31	0.08	1303.51
Ave WSW	***6.72***	***8.74***	***7.96***	***180.50***	***0.26***	***0.24***	***59.57***	***512.20***	***79.73***	***0.97***	***0.00***	***24.71***	***0.00***	***0.00***	***20.25***	***20.25***	***215.92***	***280.42***	***16.37***	***33.11***	***36.95***	***0.11***	***1031.65***
WNW 24.6.14	5.8	8.4	14.23	411	0.52	0	34.27	1046.96	181.19	0	0	26.23	0	0	21.5	21.5	519.22	759.73	32.14	56.61	96.68	0.12	2220.89
WNW 13.5.14	6.23	8.05	15.04	518	1.48	35.48	22.63	451.2	103.73	0	0	40.87	0	0	33.5	33.5	702.62	936.63	45.2	82.43	128.13	0.23	1827.57
WNW 31.7.14	7.18	8.92	10.6	221	1.59	0	16.34	739	90.72	0	0	17.08	0	0	14	14	209.76	363.61	14.52	26.35	38.06	0.1	1298.46
WNW 23.8.14	8.02	7.88	13.35	334	0.27	3.42	20.41	1045.61	179.83	2	0	112.24	0	0	92	92	286.95	596.4	29.63	43.98	65.05	0.11	2041.88
Ave WNW	***6.81***	***8.31***	***13.31***	***371.00***	***0.97***	***9.73***	***23.41***	***820.69***	***138.87***	***0.50***	***0.00***	***49.11***	***0.00***	***0.00***	***40.25***	***40.25***	***429.64***	***664.09***	***30.37***	***52.34***	***81.98***	***0.14***	***1847.20***
ENE 31.7.14	***7.48***	***8.76***	***4.18***	***68***	***0.2***	***0.82***	***17.23***	***218.77***	***25.08***	***0***	***0***	***31.72***	***0***	***0***	***26***	***26***	***78.59***	***97.91***	***4.76***	***18.68***	***13.91***	***0.05***	***413.14***
fog1 LB 1.3.13	6.18	9.5	0.71	7	0.27	0	1.16	14.8	1.93	0.06	0	18.91	0	0	15.5	15.5	5.73	7.34	1.68	4.62	2.17	0.06	42.56
LB 21.11.13	***7.59***	***8.68***	***0.54***	***24***	***0.21***	***0***	***0.16***	***49.79***	***3.98***	***4.41***	***0***	***49.41***	***0***	***0***	***40.5***	***40.5***	***16.19***	***9.28***	***2.72***	***12.75***	***5.9***	***0.04***	***113.3***
Av 21.5.12	6.69	9.99	3.84	32	0.04	0.2	18.27	107.48	17.69	0	0	8.54	0	0	7	7	28.55	50.96	2.08	3.81	5.79	0.16	210.73
Av 13.01.10	6.03	9.75	1.75	23	0.06	0	6.73	20.49	8.63	0	0	15.86	0	0	13	13	6.26	17.69	0.41	3.18	2.75	0	67.07
Av dec 2009	7.09	10.11	0.95	6	0	0	2.12	7.74	4.02	0.36	0	12.2	0	1.52	10	9.09	0	6.51	0.81	1.69	1.15	0.01	29.9
Ave Avontuur	***6.60***	***9.95***	***2.18***	***20.33***	***0.03***	***0.07***	***9.04***	***45.24***	***10.11***	***0.12***	***0.00***	***12.20***	***0.00***	***0.51***	***10.00***	***9.70***	***11.60***	***25.05***	***1.10***	***2.89***	***3.23***	***0.06***	***102.57***

APPENDIX B

ADDENDUM 8.2 TRACE ELEMENT COMPOSITION OF WATER AT LAMBERTS BAY AND AVONTUUR

		31/7/14 LAM N	23/8/14 LAM N	N 10/6/14	N 24/6/14	N 13/5/14	N ave		23/8/14 LAM S	S 10/6/14	S 24/6/14	S ave		23/8/14 LAM WNW	31/7/14 LAM WNW	WNW 24/6/4	WNW 13/5/14	WNW ave		31/7/14 LAM ONO	ONO 24/6/14		23/8/14 LAM WSW	WSW 24/6/14	WSW ave		LB 21/11/13	LB 1/3/13	LB tot		Avontuur 29/5/12	Avontuur dec 2009	Avont tot
		W885	W888		W505	W509			W889		W504			W890	W886	W507	W510			W887	W508		W891	w506									
Elements	Units																																
7 Li	ppb	4.17	5.51	11.56	3.80	12.11	7.43		1.30	10.08	12.08	7.82		5.94	4.48	8.09	11.42	7.48		1.26	11.55		4.78	4.00	4.39		1.25		1.25		0.61		0.61
9 Be	ppb	0.03	0.03	0.00	0.02	0.04	0.02		0.01	0.00	0.04	0.02		0.02	0.03	0.03	0.03	0.03		0.01	0.03		0.07	0.03	0.05		0.01		0.01		0.00		0.00
Ti	ppb	2.08	1.89	3.76	7.33	4.29	3.87		1.17	9.51	5.59	5.42		1.93	4.01	2.38	3.43	2.94		0.28	2.06		33.43	3.853	18.64		1.601		1.601		0		0
V	ppb	0.85	1.49	20.39	5.30	17.48	9.10		0.70	18.66	11.57	10.31		1.68	0.85	9.11	13.57	6.30		0.96	10.98		2.52	5.379	3.95		6.203		6.203		4.289		4.289
Cr	ppb	0.81	0.85	2.12	0.96	2.24	1.40		0.71	4.10	2.41	2.40		1.01	0.82	1.41	1.53	1.19		0.67	2.33		1.96	1.375	1.67		24.27		24.27		0.468		0.468
Mn	ppb	46.17	84.38	223.10	56.77	310.20	144.12		3.06	148.40	110.00	87.15		181.13	27.86	96.48	239.10	136.14		0.55	5.08		315.48	10.78	163.13		0		0		44.87		44.87
Co	ppb	0.64	0.96	1.47	0.35	1.20	0.92		0.01	1.43	0.88	0.78		0.95	0.51	0.99	1.10	0.89		0.02	0.46		1.34	0.263	0.80		0		0		0.335		0.335
Ni	ppb	2.29	3.77	6.02	2.55	6.46	4.22		0.12	7.86	4.99	4.32		3.68	3.11	3.87	6.40	4.26		0.39	4.97		7.96	2.267	5.11		0		0		0		0
Cu	ppb	56.60	45.00	198.90	101.50	185.90	117.58		34.89	274.50	373.40	227.60		77.42	23.93	72.29	146.50	80.04		41.76	351.90		75.93	101.4	88.67		4.051		4.051		0.105		0.105
Zn	ppb	2463.06	740.26	170.70	653.60	184.90	842.50		98.09	178.90	208.40	161.80		450.10	432.78	516.80	186.10	396.45		85.48	285.90		2207.46	151.2	1179.33		10.48		10.48		627.5		627.5
As	ppb	0.86	1.49	7.66	2.64	10.43	4.61		0.27	10.13	9.94	6.78		1.56	0.92	7.41	10.36	5.06		0.48	8.11		1.20	2.7	1.96		1.2		1.2		0.0		0.0
Se	ppb	5.73	7.25	23.91	8.27	29.36	14.90		2.08	30.30	30.72	21.03		9.24	2.98	23.90	32.93	17.26		2.18	22.14		4.59	7.106	5.85		1.914		1.914		1.631		1.631
Rb	ppb	2.11	2.64		3.54	6.54	3.71		0.63		9.25	4.94		4.27	1.78	7.57	9.14	5.69		0.59	7.67		2.94	3.558	3.25		1.214		1.214		0.865		0.865
Sr	ppb	30.10	30.80	714.80	241.30	29.36	209.27		2.30	555.10	25.35	194.25		40.90	23.70	20.85	29.12	28.64		56.68	20.38		31.60	245.9	138.75		46.01		46.01		44.63		44.63
Mo	ppb	0.73	0.78	1.59	1.28	2.14	1.30		0.29	1.97	2.68	1.65		0.95	0.38	0.00	2.13	0.86		0.29	0.00		0.54	1.008	0.77		0.23		0.23		0		0
Cd	ppb	0.38	0.26	0.64	0.30	0.60	0.44		0.04	0.24	0.43	0.24		0.38	0.28	0.59	2.23	0.87		0.08	0.25		0.54	0.2	0.35		0.0		0.0		0.0		0.0
Sn	ppb	0.30	0.48	0.00	0.00	0.00	0.16		0.17	16.10	0.00	5.42		0.14	<0.03	0.00	0.00	0.05		0.31	0.00		0.11	0	0.05		0		0		0		0
Sb	ppb	0.19	0.13	0.74	0.35	0.90	0.46		0.13	0.90	0.67	0.56		0.19	0.11	0.32	0.91	0.38		0.08	1.23		0.43	0.589	0.51		0.058		0.058		0.098		0.098
Te	ppb	0.00	0.03	0.00	0.00	0.00	0.01		0.09	0.01	0.03	0.04		0.00	0.00	0.00	0.00	0.00		0.00	0.01		0.00	0.012	0.01		0		0		0.173		0.173
Cs	ppb	0.01	0.01	0.00	0.00	0.00	0.00		<0.01	0.00	0.00	0.00		0.02	0.02	0.00	0.00	0.01		0.01	0.00		0.07	0	0.03		0		0		0		0
Ba	ppb	8.12	9.74	15.03	10.92	43.22	17.41		<0.12	11.81	21.61	16.71		16.27	6.59	22.28	35.56	20.17		11.66	22.43		19.88	10.39	15.14		0.758		0.758		5.914		5.914
W	ppb	0.21	0.17	1.08	0.99	0.89	0.67		0.18	1.73	1.26	1.06		0.25	0.12	0.87	1.18	0.61		0.15	1.63		0.16	0.82	0.49		0.161		0.161		0		0
Pt	ppb	0.00	0.01	0.01	0.09	0.07	0.03		0.01	0.04	0.08	0.04		0.01	0.00	0.06	0.05	0.03		0.00	0.05		0.01	0.07	0.04		0		0		0		0
Hg	ppb	0.31	<0.05	1.81	1.82	1.79	1.43		0.09	4.73	2.64	2.49		0.28	0.47	1.51	1.39	0.91		0.14	1.19		0.51	1.111	0.81		0		0		0		0
Tl	ppb	0.04	0.03	0.08	0.05	0.06	0.05		0.02	0.19	0.28	0.16		0.03	0.02	0.06	0.07	0.04		0.02	0.06		0.03	0.047	0.04		0		0		0		0
Pb	ppb	0.65	0.18	0.00	0.92	0.67	0.49		0.16	0.09	1.40	0.55		0.16	0.55	1.31	0.99	0.75		0.13	0.27		2.67	0.956	1.81		0.771		0.771		0		0
Bi	ppb	0.03	0.03	0.00	0.00	0.00	0.01		0.02	0.00	0.00	0.01		0.01	0.02	0.00	0.00	0.01		0.02	0.00		0.02	0	0.01		0		0		0		0
U	ppb	0.02	0.01	0.11	0.07	0.16	0.07		0.01	0.06	0.14	0.07		0.02	0.01	0.05	0.13	0.05		0.01	0.09		0.06	0.084	0.07		0.032		0.032		0		0
Br				3052	1292	4262	2868.67			3837	4949	4393.00				3965	5230	4597.50			3334			1033	1033.00		40.09		40.09		40.82		40.82
B				38.6	20.77	41.41	33.59			44.73	31.16	37.95				23.34	43.26	33.30			36.57			19.92	19.92		8.506		8.506		0		0
La				0.008	0.174	0.089	0.09			0.097	0.12	0.11				0.094	0.051	0.07			0.049			0.072	0.07		0.079		0.079		0		0
I				49.83	20.45	176.8	82.36			60.16	74.91	67.54				29.94	159.8	94.87			83.65			18.35	18.35		6.813		6.813		6.938		6.938
Fe mg/l				0.01	0.08	0.02	0.04			0.05	0.06	0.06				0.02	0.01	0.02			0			0.01	0.01		0.06	0.154	0.06		0.05	0.01	0.05
NH4				5	0.06	0.06	1.71			9.25	0.09	4.67				0.18	0.16	0.17			0.07			0.05	0.05		14.37		14.37				
Si				0.62	0.57	1.12	0.77			0.51	0.53	0.52				0.31	0.72	0.52			0.77			0.48	0.48		0.42		0.42				
Al				0.08	0.24	0.09	0.14			0.19	0	0.10				0.17	0.04	0.11			0			0.11	0.11		0.08	0.68	0.08		0.07		0.07
S																												1.252			7.2		7.2
E coli																											neg		neg		neg		neg
Coliform																											0		0		0		0
Tot bact																											640		640		>3000		>3000

APPENDIX C

THE ANALYSIS OF A FOG WATER SAMPLE FOR ESTROGENIC ACTIVITY USING THE RECOMBINANT YEAST ESTROGEN SCREEN (YES) AND THE T47D-KBLUC REPORTER GENE ASSAY

FINAL REPORT

Analysis and report by: Mrs MC van Zijl and Dr NH Aneck-Hahn

EDC Laboratory

University of Pretoria

Tel: +27 (0)12 354 1676

Fax: +27 (0)12 354 2500

E-mail: naneckha@medic.up.ac.za

Report no: 018/052012

Date: May 2012

1. Introduction

A fog water sample was delivered to the EDC laboratory for the analysis of estrogenic activity using the recombinant yeast estrogen screen (YES) and the T47D-KBluc reporter gene assay.

The recombinant yeast estrogen screen (YES)

A recombinant yeast strain was developed in the Genetics Department at Glaxo for use in a test to identify compounds that can interact with the human estrogen receptor alpha (ER_) (Routledge and Sumpter, 1996). Yeast cells were transfected with the ER_ gene, together with expression plasmids, containing oestrogen-responsive elements and the lac-Z reporter gene encoding the enzyme _-galactosidase. The yeast cells are incubated in a medium containing the test substance, vehicle control and 17_-estradiol (E2) positive control respectively, together with the chromogenic substrate, chlorophenol red-_-d-galactopyranoside (CPRG). Active ligands, which bind to the receptor, induce _-galactosidase (_-gal) expression and that causes the CPRG (yellow) to change into a red product that can be measured by absorbance (Routledge and Sumpter, 1996).

The T47D-KBluc reporter gene assay

The US EPA developed an estrogen-dependent stable cell line, which contain both endogenous ER_ and ERß. T47D human breast cancer cells were transfected with an estrogen-responsive element (ERE) luciferase reporter gene construct. This provides an *in vitro* system that can be used to evaluate the ability of chemicals to modulate the activity of estrogen-dependent gene transcription (Wilson et al., 2004). In principle, compounds enter the cell; estrogen receptor ligands bind to the ER; two ligand-bound receptors dimerize and bind coactivators; then the dimer binds to the ERE on the reporter gene construct and activates the luciferase reporter gene. The presence of the luciferase enzyme can then be assayed by measuring the light produced when the enzyme substrate, luciferin, and appropriate cofactors are added. The amount of light produced is relative to the degree of estrogenic activity of the test sample. When testing with the T47D-KBluc cells, an estrogen is defined as a sample that induced dose dependent luciferase activity, which could be specifically inhibited by the anti-estrogen ICI. Agonists stimulate luciferase expression and are compared to the vehicle control (media plus ethanol) or to the relative response of their respective E2 control. Anti-estrogens block the E2-induced luciferase expression, which is compared to the

E2 control (Wilson et al., 2004).

2. Experimental procedures

2.1 Sample collection and storage

A fog water sample was collected in a glass bottle and was delivered to the EDC laboratory. The pH of the water sample was adjusted to approximately 3 and was stored at 4°C until extraction. The extracted sample was kept at -20°C.

2.2 Extraction procedure

Prior to extraction, the water sample was passed through a glass wool filter and through a 0.22 micron, 47 mm sterile filter to remove particulates. For extraction and enrichment of potential estrogen-like compounds, the sample and an extraction control were extracted onto a preconditioned Chromabond C18 ec, SPE cartridge (Macherey-Nagel), according to the protocol described in Bornman et al. (2007). The sample residue was reconstituted with 1m_ ethanol and placed into a sterile amber glass bottle, and stored at –20°C prior to analysis (Aneck-Hahn, 2003; Aneck-Hahn et al., 2008; Bornman et al., 2007).

2.3 Assay procedures

2.3.1 YES assay

The yeast was obtained from Prof. J.P. Sumpter's laboratory, in the Department of Biology and Biochemistry, Brunel University, Uxbridge, Middlesex in the United Kingdom. The YES was performed according to the method described by Routledge and Sumpter (1996) with minor adjustments (Aneck-Hahn 2003; Aneck-Hahn et al., 2005; 2008; Bornman et al., 2007). The stock cultures and growth medium were prepared using medium components described in Routledge and Sumpter (1996). Short term stock cultures were used to prepare the assay medium for the experimental procedure (Aneck-Hahn, 2003; Routledge and Sumpter, 1996). The growth medium was inoculated with 125µ_ of the 10x concentrated yeast stock and incubated at 28°C in a rotating water bath at 150-155upm until turbid (Aneck-Hahn, 2003; Aneck-Hahn et al., 2005; 2008; Bornman et al., 2007). Serial dilutions of the sample extract and controls were made in ethanol (solvent), in 96 well microtiter plates. 10µ_ Aliquots were then transferred to a second plate and allowed to evaporate to dryness. Aliquots (200µ_) of the assay medium containing the yeast and chromogenic substrate (CPRG) were then dispensed into each sample well. Each plate contained at least one row of blanks (assay medium and solvent ethanol) and a standard curve for 17ß-estradiol, ranging from 1x10-8M (2.724µg/_) to 1.19x10- 15M (3.24x10-13g/_). The plates were sealed with parafilm and placed in a naturally ventilated incubator at 32°C for 3 to 5 days. After 3 days incubation the colour development of the medium was checked for 3 days (day 3 to 5) at an absorbance (abs) of 540nm for colour change and 620nm for turbidity of the yeast culture. The absorbance was measured on a Multiskan Spectrum v1.2 spectrophotometer to obtain data with the best contrast. After incubation the control wells appeared light orange in colour, due to background expression of ß-galactosidase and turbid due to the growth of the yeast. Positive wells were indicated by a deep red colour accompanied by yeast growth. Clear wells, containing no growth indicated lysis of the cells and colour varied. All experiments were performed in triplicate. The following equation was applied to correct for turbidity: Corrected value = test abs (540nm) – [test abs (620nm) – median blank abs (620nm)]. The 17 _-estradiol standard curve was fitted (sigmoidal function, variable slope) using Graphpad Prism (version 4), which calculated the minimum, maximum, slope, EC50 value and 95% confidence limits. The detection limit of the yeast assay was calculated as absorbance elicited by the solvent control (blank) plus three times the standard deviation. The Estradiol Equivalents (EEq) of the sample was interpolated from the

estradiol standard curve and corrected with the appropriate dilution factor.

2.3.2 The T47D-KBluc reporter gene assay

The extract was processed according to the chemical protocol described in Wilson et al. (2004).

T47D-KBluc cells were maintained in RPMI growth media supplemented with 2.5g/_glucose, 10mM HEPES, 1mM sodium pyruvate, 1.5g/_ NaHCO3, 10% fetal bovine serum (FBS), 100µg/m_ penicillin, 100U/m_ streptomycin and 0.25µg/m_amphotericin B. One week prior to the assay, cells were placed in growth media modified by replacement of 10% FBS with 10% dextran-charcoal treated FBS excluding antibiotic supplements (Wilson et al. 2004).

Cells were seeded at 5 x 104 cells per well in 96-well luminometer plates and allowed to attach overnight. Dosing dilutions were prepared in growth media containing 5% dextran-charcoal treated FBS and vehicle (ethanol) did not exceed 0.2%. Each plate contained agonist positive control (E2), negative control (solvent only), antagonist control (E2 plus ICI) and background control (solvent plus ICI). Each sample was tested alone as well as in the presence of 0.1nM E2 or ICI. Cells were incubated 24h with 100µ_/well dosing solution at 37oC, with 5% CO2. After the incubation period, cells were washed with phosphate buffered saline at room temperature and lysed with 25µ_ lysis buffer. Luciferase activity was determined using a microtiter plate luminometer and quantified as relative light units. Each well received 25µ_ reaction buffer (25mM glycylglycine, 15mM MgCl2, 5mM ATP, 0.1mg/m_ BSA, pH 7.8), followed by 25µ_ 1mM D-luciferin 5s later. Relative light units were converted to a fold induction above the vehicle control value. The 17 _-estradiol standard curve was fitted (sigmoidal function, variable slope) using Graphpad Prism (version 4), which calculated the minimum, maximum, slope, EC50 value and 95% confidence limits. The estradiol equivalents (EEq) of extracts with greater than a twofold induction above the vehicle control were interpolated from the estradiol standard curve and corrected with the appropriate dilution factor for each sample.

3. Results and discussion

No estrogenic activity was detected in the sample using the YES assay. Slight cytotoxicity was observed in ten times and higher concentrations of the sample. It is important to note that cytotoxicity could mask estrogenic activity if it is present in the sample. No estrogenic or anti-estrogenic activity was observed in the T47D-KBluc assay.

Although no estrogenic activity was observed in the assays, it should be kept in mind that a water sample consists of a complex mixture of chemicals with possible (anti)-androgenic and (anti)-estrogenic activity, as well as other chemicals not measured, that could affect the outcome of the assay. The complexity of the sample, pH, extraction procedure and the nature of the assay (i.e. a biological system) might all have an influence on the results and may possibly lead to an under-estimation of the results or even to false negatives. Additional samples are required before any conclusions can be made regarding the estrogenic activity present in fog water from the selected area.

FOG REFERENCES ENDOCRINE DISRUPTORS:

AHMED AFM, SINGH RP and ELMUBARAK AH (1990) Chemistry of atmospheric precipitation at Western Arabian Gulf Coast. *Atmospheric Environment,* 24(12) 2927-2934.

ECKARDT FD and SCHEMENAUER RS (1998)Fog water chemistry in the Namib desert, Namibia. *Atmospheric Environment,* **32**(14/15), 2595-2599.

Ema M and Miyawaki E (2001). Effects of monobutyl phthalate on reproductive function in pregnant and pseudopregnant rats. *Reprod Toxicol.,* **15**, 261-267.

KENNISH MJ (1989) *Practical handbook of marine sciences*. Boca Raton: CRC Press.

Latini G, Verrotti A and De Felice C (2004). Di-2-ethylhexyl phthalate and endocrine disruption: a review. *Curr Drug Targets Immune Endocr Metabol Disor.,* **4(1)**, 37-40.

LEKOUCH I, MUSELLI M, KABBACHI B, OUAZZANI J, MELNYTCHOUK-MILIMOUK I and BEYSENS D (2011) Dew, fog and rain as supplementary sources of water in south-western Morocco. *Energy,* 36, 2257-2265.

Lovekamp-Swan T and Davis BJ (2003). Mechanisms of phthalate ester toxicity in the female reproductive system. *Environ Health Perspect,* **111**, 139-146.

Nerin C, Cacho J and Gancedo P (1993). Plasticisers from printing inks in a selection of food packagings and their migration to food. *Food Additives and Contaminants, 10,* 453-460.

OLIVIER J and STOCKTON PL (1989) The influence of upwelling extent on fog incidence at Luderitz, southern Africa. *International Journal of Climatology,* 9, 69-75.

Parks LG, Ostby JS and Lambright CR (2000). The plasticizer diethylhexyl phthalate induces malformations by decreasing fetal testosterone synthesis during sexual differentiation in the male rat. *Toxicol. Sci*., **58**, 339-349.

SOUTH AFRICAN NATIONAL STANDARDS (SANS) (2011) Drinking water standards (SANS 241:2005, 2011), South African Bureau of Standards, Pretoria.

Sharpe, R.M. and Irvine, D.S (2004). How strong is the evidence of a link between environmental chemicals and adverse effects on human reproductive health? *BMJ*, **328** 447-451.

Tsutsumi, T., Ichihara, T., Kawabe, M., Yoshino, H., Asamoto, M., Suzuki, S and Shirai, T (2004). Renal toxicity induced by folic acid is associated with the enhancement of male reproductive toxicity of di(n-butyl)phthalate in rats. *Reprod. Toxicol.,* 18 (1):35-42.

Wilson, V.S., Lambright, C and Furr, J (2004). Phthalate ester-induced gubernacular lesions are associated with reduced insl3 gene expression in the fetal rat testis, *Toxicol. Lett*. **146**, 207-215.

APPENDIX D: LIST OF DELIVERABLES

DELIVERABLE	TARGET DATE	PROGRESS
1 Prototype low flow water meter	31/5/2011	Completed
2 GIS fog water potential map	30/6/2011	Completed
3 System on E Coast	31/7/2011	Completed
4 Design of fog water collector for windless conditions	30/8/2011	Completed
5 Annual report	3/2/2012	Completed
6 System on West Coast	31/05/2012	Completed
7 Proposal for M student	30/06/2012	Completed
8 Report on EIA	30/11/2012	Completed
9 Report on climate change and fog	31/12/2012	Completed
10 Annual report	28/02/2013	Completed
11 Expanded and new FWCS design	30/06/2013	Completed
12 Presentation on East and West Coast fogs	30/11/2013	Completed (2 presentations – one by Geldenhuys, one by Olivier
13 Publication: Characteristics of west coast fogs	30/11/2013	Late – but completed. Submitted to WATER SA
14 WRC annual progress report	28/02/2014	Completed
15 Publication: Rautenbach C.J.deW., Dosio A., Panitz, H.-J., Shongwe, M., Olivier J. and Van Heerden J. (2015) Projected influence of global warming on near-surface winds associated with the potential for mountain fog formation in South Africa.	30/06/ 2014	Completed Submitted: Journal of Applied Climatology
16 Prototype for small users	31/10/2014	Completed – erected at Lamberts Bay August 2014
17 Presentation of FWHS on the environment	31/12/2014	Completed (presentation at FogLife colloquium, Gobabeb Namibia, Nov 2014)
18 Dissertation	31/12/2014	Completed. Two B Eng student research reports 12/11/2014
19 FINAL WRC REPORT	31/03/2015	